Title

Scoping study to expedite development of a field deployable and portable instrument for UF6 enrichment assay

Authors

Chan, CYG
Valentine, JD
Russo, RE

Publication Date

2017-09-14

Peer reviewed

BERKELEY LAB
LAWRENCE BERKELEY NATIONAL LABORATORY
U.S. DEPARTMENT OF ENERGY

LBNL-2001050

Scoping study to expedite development of a field deployable and portable instrument for UF_6 enrichment assay

Final Report
July 2017

George Chan
John Valentine
Richard Russo

Lawrence Berkeley National Laboratory

Final Report:

Scoping study to expedite development of a field deployable and portable instrument for UF_6 enrichment assay

George Chan, John Valentine, and Richard Russo

Lawrence Berkeley National Laboratory

This work was performed under the auspices of the U.S. Department of Energy by Lawrence Berkeley National Laboratory under Contract DE-AC02-05CH11231. The project was funded by the Safeguards Technology Development Program in the U.S. Department of Energy/National Nuclear Security Administration's (DOE/NNSA's) Office of Nonproliferation and Arms Control (NPAC).

Executive Summary

The primary objective of the present study is to identity the most promising, viable technologies that are likely to culminate in an expedited development of the next-generation, field-deployable instrument for providing rapid, accurate, and precise enrichment assay of uranium hexafluoride (UF_6). UF_6 is typically involved, and is arguably the most important uranium compound, in uranium enrichment processes. As the first line of defense against proliferation, accurate analytical techniques to determine the uranium isotopic distribution in UF_6 are critical for materials verification, accounting, and safeguards at enrichment plants. As nuclear fuel cycle technology becomes more prevalent around the world, international nuclear safeguards and interest in UF_6 enrichment assay has been growing.

At present, laboratory-based mass spectrometry (MS), which offers the highest attainable analytical accuracy and precision, is the technique of choice for the analysis of stable and long-lived isotopes. Currently, the International Atomic Energy Agency (IAEA) monitors the production of enriched UF_6 at declared facilities by collecting a small amount (between 1 to 10 g) of gaseous UF_6 into a sample bottle, which is then shipped under chain of custody to a central laboratory (IAEA's Nuclear Materials Analysis Laboratory) for high-precision isotopic assay by MS. The logistics are cumbersome and new shipping regulations are making it more difficult to transport UF_6. Furthermore, the analysis is costly, and results are not available for some time after sample collection. Hence, the IAEA is challenged to develop effective safeguards approaches at enrichment plants. In-field isotopic analysis of UF_6 has the potential to substantially reduce the time, logistics and expense of sample handling. However, current laboratory-based MS techniques require too much infrastructure and operator expertise for field deployment and operation. As outlined in the IAEA Department of Safeguards Long-Term R&D Plan, 2012–2023, one of the IAEA long-term R&D needs is to "develop tools and techniques to enable timely, potentially real-time, detection of HEU (Highly Enriched Uranium) production in LEU (Lowly Enriched Uranium) enrichment facilities" (Milestone 5.2).

Because it is common that the next generation of analytical instruments is driven by technologies that are either currently available or just now emerging, one reasonable and practical approach to project the next generation of chemical instrumentation is to track the recent trends and to extrapolate them. This study adopted a similar approach, and an extensive literature review on existing and emerging technologies for UF_6 enrichment assay was performed. The competitive advantages and current limitations of different analytical techniques for in-field UF_6 enrichment assay were then compared, and the main gaps between needs and capabilities for their field use were examined. Subsequently, based on these results, technologies for the next-generation field-deployable instrument for UF_6 enrichment assay were recommended.

The study was organized in a way that a suite of assessment metric was first identified. Criteria used in this evaluation are presented in Section 1 of this report, and the most important ones are described briefly in the next few paragraphs. Because one driving force for in-field UF_6 enrichment assay is related to the demanding transportation regulation for gaseous UF_6, Section 2 contains a review of solid sorbents that convert and immobilized gaseous UF_6 to a solid state, which is regarded as more transportation friendly and is less regulated. Furthermore, candidate solid sorbents, which show promise in mating with existing and emerging assay technologies, also factor into technology recommendations. Extensive literature reviews on existing and emerging technologies for UF_6 enrichment assay, covering their scientific principles, instrument options, and current limitations are detailed in Sections 3 and 4, respectively. In Section 5, the technological gaps as well as start-of-the-art and commercial off-the-shelf components that can be adopted to expedite the development of a fieldable or portable UF_6 enrichment-assay instrument are identified and discussed. Finally, based on the results of the review, requirements and recommendations for developing the next-generation field-deployable instrument for UF_6 enrichment assay are presented in Section 6.

An ideal instrument for UF_6 isotopic assay should be the one that excels in five areas: fast temporal response, accuracy, precision, sensitivity, and field-deployability or portability. Accordingly, all reviewed candidate technologies were evaluated based on a suite of seven metrics: meeting predefined target of analytical accuracy and precision (two separate criteria), meeting relaxed target of accuracy and precision (two criteria), simultaneous ^{235}U and ^{238}U measurement, measurement time, and overall ease of operation. For analytical accuracy and precision, one of the very important comparison benchmarks is the International Target Values (ITVs) published by the IAEA [1]. The ITVs are considered to be achievable values in routine measurements, and are the uncertainties to be considered in judging the reliability of analytical techniques applied to the analyses of nuclear materials. Because the main goal of the present study is to search for techniques that potentially can replace laboratory-based MS, the ITVs of thermal ionization MS (TIMS) and multi-collector inductively coupled plasma MS (MC-ICP-MS) are used as baselines for comparisons of analytical accuracy and precision for all evaluated techniques. Because the IAEA ITVs are intended for more established techniques, to better gauge the potential of emerging technologies that are still under active development, an additional set of performance criteria is set by relaxing the target values by a factor of 10 under the assumption that over time these techniques have the potential to achieve the ITVs. Furthermore, nearly achieving the ITVs may provide a useful benefit of facilitating in-field analysis, thereby allowing a more-limited, 'informed' choice of samples to be sent to a central laboratory for more definitive analysis by standard techniques.

Simultaneous measurements of the ^{235}U and ^{238}U signals are very important in the compensation of correlated noise, and are crucial in defining the accuracy and precision of isotope-ratio measurements. So far, no technique is capable of *directly* measuring the $^{235}U/^{238}U$ ratio. Instead,

all current methods for U-enrichment assay consist of measuring and taking the ratio of two individual quantities – the ^{235}U and the ^{238}U signals, measured either simultaneously or sequentially. Although all measurements unavoidably contain noise, noise reduction is possible if the noise is correlated and the signals are simultaneously measured, as has been repeatedly reported in the literature. Examples of noise that are correlated in nature include: flickering of the measurement system; variations in the sample introduction system; fluctuations in atomization, ionization or excitation efficiencies for optical and mass spectrometric sources; and interference noise from a power supply. In contrast, signal-noise correlation typically and substantially degrades for sequential measurements [i.e., when two (or more) signals are measured successively, one at a time]. Consequently, one criterion for evaluating a candidate analytical technique is its capability to perform truly simultaneous measurements for ^{235}U and ^{238}U.

Measurement time is based on the typical time required for one measurement, and are categorized into one of three pre-defined grades: within 10 minutes, within an hour, or more than one hour. The metric "overall ease of operation" reflects the overall complexity of the measurement procedures (including sample-preparation procedures) and instrument operation (e.g., push-button *versus* numerous complicated steps requiring a subject matter expert), as well as general robustness of the instrument and the technique.

All reviewed techniques are ranked based on their performance in the aforementioned seven evaluation metrics. In addition, the potential of the technique to be further developed into field-deployable instrumentation is also taken into account. Finally, the techniques are classified into one of the three categories – recommended, promising, and not recommended – as the next generation field-deployable instrument for UF_6 enrichment assay. A prerequisite for a technique to be labeled as "recommended" or "promising" is that the technique must have the potential to be developed into a field-deployable instrument.

It should be noted that the evaluations are based solely on results that can be found in the open literature, for example: journal articles, conference proceedings, publicly accessible reports, traceable presentations in scientific meetings or conferences, and IAEA or NNSA factsheets. In cases where the emerging technique is so new that experimental data are not yet available specifically for uranium, projected or extrapolated values from very similar techniques sharing the same scientific working principle are used. Because active research is still on-going on many emerging techniques, the most updated performance of a technique could be better than what was published in the open literature and available to us. Furthermore, it is appropriate to stress that each technique is evaluated solely for its suitability to provide on-site enrichment assay specifically for UF_6. Accordingly, a technique labeled as "not recommended" (for UF_6 in-field enrichment assay) should not be viewed in a completely negative light because it is possible that the candidate technique could be promising for other applications (e.g., for other types of U samples, as an in-laboratory analytical method, or in its ability to perform quick screening

measurements that do not require the stated high accuracy or precision of the ITVs to which it was compared).

The list presented below summarizes the outcome of the present study, and groups all reviewed techniques into "recommended", "promising", or "not recommended"; the "benchmark" techniques are also included and labeled as such. The list is presented in a highly abridged way such that only the final recommendations are given. The performance of a technique in the seven evaluation metrics and its ranking are summarized in Table 6.1, whereas short discussion and comments on the recommendation can be found in Section 6.2 of this report. Furthermore, comprehensive and in-depth reviews on the scientific principle of each technique, its instrument option, its limitations and main gaps between needs and capabilities for their field use are detailed in Sections 3 and 4 of this report, respectively, for established and emerging technologies. A very concise description for each technique is offered in the list below only for quick referencing, and readers should refer to Sections 3 and 4 for more detailed descriptions on scientific principle, performance and limitation.

- **Benchmark techniques:**
  - Gas source mass spectrometry (GSMS)
    - Mass spectrometric principle; offers direct measurement of gaseous UF_6 with precision even better than thermal ionization mass spectrometry, but requires long (hours) measurement time.
  - Thermal ionization mass spectrometry (TIMS)
    - Mass spectrometric principle; offers high measurement precision and usually regarded as the gold standard for isotopic analysis, but requires long (hours) measurement time and is non-field deployable.
  - Multi-collector inductively coupled plasma mass spectrometry (MC-ICP-MS)
    - Mass spectrometric principle; offers high measurement precision comparable to TIMS in many cases and with faster (within 1 hour) measurement time; non-field deployable due to instrument size and argon consumption rate of the ICP.
  - COMbined Procedure for Uranium Concentration and Enrichment Assay (COMPUCEA)
    - Radiometric and X-ray principles; currently the only on-site destructive-analysis technique for U-enrichment assay and is capable to offer accuracy and precision within a factor of 3 compared to laboratory-based MS techniques; requires extensive on-site sample preparation by a subject matter expert (chemist).
- **Recommended techniques:**
  - Liquid sampling-atmospheric pressure glow discharge mass spectrometry (LS-APGD-MS)
    - Mass spectrometric principle; micro-plasma based ionization source for MS; currently the most promising, in terms of published analytical capabilities (e.g., meeting precision ITVs of MC-ICP-MS and TIMS), in all the emerging techniques reviewed.
  - Atmospheric-pressure solution-cathode glow-discharge mass spectrometry (AP-SCGD-MS)
    - Mass spectrometric principle; micro-plasma based ionization source for MS with a different design and plasma-generation mechanism than LS-APGD; already demonstrated its potential for elemental analysis.

- Laser ablation absorbance ratio spectrometry (LAARS)
  - Optical spectrometric principle; promising accuracy (within a factor of 2) and precision (within 3× to 6×) from ITVs as a replacement for laboratory-based MS; offers simultaneous isotopic measurements on the same ablation plume but requires the operation of three (or more) lasers.
- Laser ablation – diode laser – atomic absorption spectrometry (AAS)
  - Optical spectrometric principle; predecessor to LAARS with slightly degraded analytical performance; like LAARS, it requires the operation of three lasers but the angle-offset approach for the two laser probe beams completely eliminates the need for an optical spectrometer or grating.
- Laser induced spectrochemical assay for uranium enrichment (LISA-UE)
  - Optical spectrometric principle; a development still in its very early stage through extension of well-established laser induced breakdown spectroscopy (LIBS) to on-site UF_6 enrichment assay; directly measure gaseous UF_6, and is intended to be applicable for both on-line and off-line measurements.

- **Promising techniques:**
  - Atmospheric pressure surface-enhanced laser desorption and ionization (AP-SELDI)
    - Mass spectrometric principle; an extension of the well-known matrix-assisted laser desorption/ionization (MALDI) technique for uranium enrichment assay; still in its relatively early stage of development and is currently undergoing an NA-24-funded test campaign, in which more information on their analytical performance is expected to be available.
  - Molecular MS w/ fieldable mass spectrometer
    - Mass spectrometric principle; can be viewed as a miniaturized version of GSMS; compared to full-scale laboratory-based GSMS, degradation in analytical performance is > 10×, but measurement time is reduced to minutes; a field-deployable prototype equipped with automated sampling manifold already has been built.
  - Laser ablation ionization mass spectrometry (LAI-MS)
    - Mass spectrometric principle; probes the ions directly generated from laser ablation; still in its relatively early stage of development and is currently undergoing an NA-24-funded test campaign, in which more information on their analytical performance is expected to be available.
  - Tunable laser infrared (IR) absorption
    - Optical spectrometric principle; non-destructive and highly fieldable technique, but measurements for ^{235}U and ^{238}U are sequential in nature; reported analytical performance is > 30× that from laboratory-based MS techniques.
  - High performance infrared (HPIR) spectroscopy
    - Optical spectrometric principle; non-destructive and highly fieldable technique, but measurements for ^{235}U and ^{238}U are sequential in nature; consider as an upgraded version of tunable laser IR absorption with the use of quantum cascade laser.

- **Not recommended techniques:**
  - ICP-Array (Mattauch-Herzog)-MS
    - Mass spectrometric principle; the latest technological development in commercial ICP-MS instruments, and offers isotopic precisions approach that of MC-ICP-MS; not field deployable due to argon consumption rate of the ICP.

- Atomic emission with ICP
  - Optical spectrometric principle; a proven technique with long history (decades), and promising recent results (within 10× ITVs as a replacement for laboratory-based MS); operation is relatively simple compared to ICP-MS, but similar to ICP-Array-MS, the technique is not field deployable due to argon consumption rate of the ICP.
- Laser ablation – diode laser – atomic fluorescence spectrometry (AFS)
  - Optical spectrometric principle; highly fieldable technique but measurements for ^{235}U and ^{238}U are sequential, and need to account for temporal dependence or pulse-to-pulse fluctuations of U atomic population in laser plume.
- Multi-photon ionization time-of-flight (TOF)-MS
  - Mass spectrometric principle; directly analyze gaseous UF_6 after dilution with a buffer gas (e.g., argon); pulsed laser causes photolysis of UF_6 molecule and ionization; a technique first reported in 1996 but quantitative details on analytical accuracy and precision are not yet available.
- Atomic beam tunable diode laser absorption
  - Optical spectrometric principle; highly fieldable technique but measurements for ^{235}U and ^{238}U are sequential; narrow absorption linewidth due to directional motion of atomic beam (i.e., low Doppler temperature) which exhibits high immunity to spectral interference; current analytical performance is inadequate (> 30× above the requirement) as a replacement for laboratory-based MS for UF_6 enrichment assay.
- Glow discharge optogalvanic spectroscopy (GD-OGS)
  - Optical spectrometric principle; highly fieldable technique but measurements for ^{235}U and ^{238}U are sequential, with somewhat complicated in-field sample preparation (transformation to solid sample and mixing with metallic binder to form electrically conducting hollow cathodes).

To summarize, under the support from DOE NNSA NA-241 (Safeguards Technology Development Program, Office of Nonproliferation and Arms Control), a comprehensive and in-depth review was conducted on existing state-of-the-art and emerging technologies for field enrichment analysis of UF_6. All techniques were assessed for their potential to serve as an alternative for laboratory-based mass spectrometry and are classified into one of the three categories – recommended, promising, and not recommended. Loosely speaking, the classification also ties to the years of further development likely needed to implement the technology for in-field UF_6 enrichment assay. In short, a total of five techniques are recommended – two belong to mass spectrometric and three operate with optical spectrometric principles. Although all technologies that we were aware of (through literature research and word of mouth from funding agencies) were included in this study, there is always a possibility that other technologies are being developed and may prove to be superior to those included here.

Table of Content

List of Acronyms and Abbreviations

ABACC	Brazilian–Argentine Agency for Accounting and Control of Nuclear Materials
Al_2O_3	aluminum oxide (also known as alumina)
AP	atmospheric pressure
APGD	atmospheric pressure glow discharge
AP-SCGD-MS	atmospheric pressure-solution cathode glow discharge-mass spectrometry
CCD	charged coupled device
CID	collision-induced dissociation
CMOS	complementary metal–oxide–semiconductor
COMPUCEA	COMbined Procedure for Uranium Concentration and Enrichment Assay
COTS	commercial off-the-shelf
DA	destructive analysis
DL	diode laser
DU	depleted uranium
EC	European Commission
EMCCD	electron multiplying CCD (charged coupled device)
FWHM	full width at half maximum
GD	glow discharge
GSMS	gas source mass spectrometry
HCWG	hollow core wave-guide
HEU	highly enriched uranium
HPIR	high performance infrared
IAEA	International Atomic Energy Agency
IATA	International Air Transport Association
ICCD	intensified–CCD (charged coupled device)
ICP	inductively coupled plasma
ICP-MS	inductively coupled plasma mass spectrometry
IFREMER	Institut Français de Recherche pour l'Exploitation de la Mer
IPEN	Instituto de Pesquisas Energéticas e Nucleares
IR	infrared
IRMM	Institute for Reference Materials and Measurements
ITU	Institute for Transuranium Elements
ITV	international target value
JPL	Jet Propulsion Laboratory
JRC	Joint Research Centre
LA	laser ablation
LAARS	laser ablation absorbance ratio spectrometry
LAI	laser ablation ionization
LAMIS	laser ablation molecular isotopic spectrometry
LANL	Los Alamos National Laboratory
LBNL	Lawrence Berkeley National Laboratory

LEU	lowly enriched uranium
LIBS	laser induced breakdown spectroscopy
LIF	laser induced fluorescence
LISA-UE	laser induced spectrochemical assay for uranium enrichment
LS-APGD-MS	liquid sampling-atmospheric pressure glow discharge mass spectrometry
MALDI	matrix-assisted laser desorption/ionization
MC	multi-collector
MC-ICP-MS	multi collector-inductively coupled plasma mass spectrometry
MEMS	micro-electro-mechanical systems
MPI	multi-photon ionization
MS	mass spectrometry or mass spectrometer
N/A	not applicable
NaF	sodium fluoride
NASA	National Aeronautics and Space Administration
Nd:YAG	neodymium-doped yttrium aluminium garnet
NDA	non-destructive analysis
NIST	National Institute of Standards and Technology
NMAL	Nuclear Materials Analysis Laboratory
NNSA	National Nuclear Security Administration
NU	natural uranium
OES	optical emission spectrometry
OGS	optogalvanic spectroscopy
ORNL	Oak Ridge National Laboratory
PNNL	Pacific Northwest National Laboratory
Q	quadrupole
QCL	quantum cascade laser
RIMS	resonance ionization mass spectrometry
RSD	relative standard deviation
SCGD	solution cathode glow discharge
SELDI	surface-enhanced laser desorption and ionization
SIMS	secondary ion mass spectrometry
SOA	state-of-the-art
SRNL	Savannah River National Laboratory
TIMS	thermal ionization mass spectrometry
TOF	time-of-flight
$u(r)$	random uncertainty
$u(s)$	systematic uncertainty
UF_6	uranium hexafluoride
UO_2F_2	uranyl fluoride

1. Introduction, objective and methodology of this study

1.1 Introduction to uranium hexafluoride (UF_6) enrichment assay

Uranium hexafluoride (UF_6) is arguably the most important uranium compound in the nuclear fuel cycle, particularly for uranium isotope enrichment. The enrichment of the ^{235}U isotope in UF_6 is a necessary major step in the production of fuel for most nuclear power plants. As nuclear fuel cycle technology becomes more prevalent around the world, international nuclear safeguards and interest in UF_6 enrichment assay has been growing. As the first line of defense against proliferation, accurate analytical techniques to determine the uranium isotopic distribution in UF_6 are critical for materials verification, accounting, and safeguards at enrichment plants.

Currently, the International Atomic Energy Agency (IAEA) monitors the production of enriched UF_6 at declared facilities by collecting between 1–10 g of gaseous UF_6 into a sample bottle, which is then transferred and tamper-sealed in an approved shipping container. The sample is shipped under chain of custody to a central laboratory [e.g., IAEA's Nuclear Materials Analysis Laboratory (NMAL) in Seibersdorf, Austria] for high-precision isotopic assay by mass spectrometry (MS) [2, 3]. The logistics are cumbersome and the analysis is costly, and results are not available for some time after sample collection. In addition, new shipping regulations are making it more difficult to transport UF_6 [3]. The IAEA is challenged to develop effective safeguards approaches at enrichment plants while working within budgetary constraints [4].

There is one on-site enrichment-assay technique, termed COMbined Procedure for Uranium Concentration and Enrichment Assay (COMPUCEA), which offers exceptional analytical capabilities with typical combined (systematic and random) measurement uncertainty around 0.25% relative [5, 6]. COMPUCEA combines energy-dispersive X-ray absorption edge spectrometry and gamma-ray spectrometry to measure uranium elemental content and ^{235}U enrichment, respectively. The method is already in use in inventory verification campaigns at European lowly enriched uranium (LEU) fuel fabrication plants [5]. Currently, the method is utilized only for solid samples and is not yet applied to UF_6 enrichment assay. IAEA is exploring extending the COMPUCEA system to in-field UF_6 enrichment determination [7]. Major shortcomings of the method are its comparatively complicated sample preparation, and its hours-long measurement time for each sample.

For off-site U-enrichment measurements, MS is currently the most sensitive analytical technique; however, current MS techniques require too much infrastructure and operator expertise for field deployment and operation. In-field UF_6 enrichment assay has the potential to substantially

reduce the time, logistics and expense of bulk sample handling by allowing for an 'informed' choice of samples to be sent to NMAL for definitive analysis by standard laboratory techniques.

The objective of the present study is to identify the potential, viable technologies that are likely to culminate in an expedited development of the next generation of field deployable instrumentation for rapidly determining UF_6 enrichment. One common approach to project the next generation of chemical instrumentation is to track the current trends and to extrapolate them [8]. This approach, albeit somewhat conservative, has been demonstrated with a fair degree of reliability in the fields of analytical science and chemical instrumentation [8]. Therefore, an extensive literature review on existing and emerging technologies for UF_6 enrichment assay is performed, and the competitive advantages and current limitations of different analytical techniques are compared. Based on the results of the review, requirements and recommendations for development of the next-generation field-deployable instrument for UF_6 enrichment assay are addressed.

1.2 Methodology

In this study, a comprehensive list of UF_6 enrichment-assay methods is reviewed and evaluated. COMPUCEA [5, 6] is a radiometric technique and serves as a benchmark for on-site U enrichment assay. Evaluated mass spectrometric techniques include: gas source mass spectrometry (GSMS) [9], thermal ionization mass spectrometry (TIMS) [10], inductively coupled plasma mass spectrometry (ICP-MS) [10, 11], multi-photon ionization mass spectrometry [12, 13], UF_6 molecular mass spectrometry with portable mass spectrometer [14], laser ionization mass spectrometry [15], surface-enhanced laser desorption and ionization (SELDI) [3], liquid sampling-atmospheric pressure glow discharge mass spectrometry (LS-APGD-MS) [16-18], and atmospheric-pressure solution-cathode glow-discharge mass spectrometry (AP-SCGD-MS) [19]. Techniques based on optical spectrometric principles include: optical atomic emission with argon afterglow discharge or ICP [20-22], glow discharge optogalvanic spectroscopy (GD-OGS) [23], laser ablation-diode laser-laser induced fluorescence (LA-DL-LIF) [24], laser ablation absorbance ratio spectrometry (LAARS) [25, 26], atomic beam tunable diode laser (DL) absorption [27], tunable laser infrared (IR) absorption [28, 29] and its high performance version with quantum cascade laser [30], and laser induced spectrochemical assay for uranium enrichment (LISA-UE).

GSMS, TIMS and ICP-MS are included to enable comparison with laboratory techniques. Otherwise, all other techniques should be directly compared with COMPUCEA for their potential to serve as an alternative field-based enrichment assay technique. Each technique is evaluated against a suite of criteria, discussed below.

1.3 Evaluation criteria

In this study, all the reviewed analytical techniques are assessed for their suitability to operate for in-field UF_6 enrichment assay. The evaluation will be based on a set of broad performance metrics in three categories: analytical performance, operation details, and ease of operation. The evaluations are summarized in Tables 3.1 and 4.1, to be presented and discussed in Sections 3 and 4, respectively. Each entry in the table is color coded in green, yellow or red. Overall, a "green" rating indicates meeting the criteria, a "yellow" rating represents not meeting the criteria but fails only marginally, and a "red" rating denotes not meeting the criteria. However, the meaning of "marginal fail" (i.e., yellow rating) depends on the exact context. For example, in the metric "portable or field-deployable instruments", "green" rating indicates a portable instrument system, "yellow" indicates field-deployable instrument, and "red" indicates non-fieldable. The definitions and details of the performance criteria are discussed in the various subsections below.

1.3.1 Criteria on analytical performance

To evaluate the analytical accuracy and precision of a candidate analytical technique, reported analytical figures of merit are compared to the international target values (ITVs) of TIMS and multi collector (MC)-ICP-MS [1], which serve as comparison references. The IAEA published ITVs [1] for a wide variety of measurement techniques for nuclear material accountancy and safeguards verification. The ITVs are considered to be achievable values in routine measurements and are uncertainties to be considered in judging the reliability of analytical techniques applied to the analyses of nuclear materials [1]. GSMS, TIMS and MC-ICP-MS are the only three MS systems listed under destructive analysis (DA) techniques [1]. Although more techniques (five) are listed under the category of non-destructive analysis (NDA), it is notable that measurement uncertainties from NDA techniques are much larger – typically more than an order of magnitude larger – than the three MS-based DA techniques [1]. As the interest of IAEA is to find alternatives for laboratory-based mass spectrometry, the *u(s)* and *u(r)* (i.e., systematic and random uncertainties, respectively) ITVs specifically for TIMS and MC-ICP-MS [1] are used here as comparison benchmarks. Table 1.1 lists the target *u(s)* and *u(r)* in the present evaluation. As the IAEA ITVs define the strict target for analytical accuracy and precision and are intended for more established techniques, to better judge the second-tier analytical techniques and to gauge the potential of emerging techniques that are still under active development, an additional set of performance criteria is set by relaxing the target values by 10× (i.e., increases *u(s)* and *u(r)* from 0.5% to 5% relative for depleted U, see Table 1.1).

Table 1.1 Comparison benchmarks, adopted from IAEA ITVs for TIMS and MC-ICP-MS [1], for evaluation of a candidate technique on its analytical accuracy and precision.

^{235}U Enrichment	ITV Target		10× ITV Target	
	u(s), relative **Systematic uncertainty (Accuracy/Bias)**	*u(r)*, relative **Random uncertainty (Precision/Repeatibility)**	*u(s)*, relative **Systematic uncertainty (Accuracy/Bias)**	*u(r)*, relative **Random uncertainty (Precision/Repeatibility)**
Depleted U (DU) ^{235}U < 0.3%	0.5%	0.5%	5%	5%
Natural U (NU) 0.3% < ^{235}U < 1%	0.2%	0.2%	2%	2%
Lowly Enriched U (LEU) 1% < ^{235}U < 20%	0.1%	0.1%	1%	1%
Highly Enriched U (HEU) ^{235}U > 20%	0.05%	0.05%	0.5%	0.5%

In this study, analytical accuracy and precision are separately evaluated and are two different criteria. If the candidate technique offers analytical accuracy or precision meeting the target, a "green" rating is awarded and noted in the performance evaluation table. A "yellow" rating represents not meeting the criteria but within 3× the target value (i.e., marginally fail), and a "red" rating denotes not meeting the criteria even if the target value is relaxed by a factor of 3.

Other evaluation falling onto the analytical performance category include: metrics "direct measurements on both ^{235}U and ^{238}U", "simultaneous measurements on ^{235}U and ^{238}U", "portable or field-deployable instrumentation", and "measurement time".

The metric "direct measurements on both ^{235}U and ^{238}U", which summarizes whether both ^{235}U and ^{238}U are directly measured (denoted by green), or at least one of them is indirectly measured (denoted by red). The metric "simultaneous measurements on ^{235}U and ^{238}U" evaluates if the measurements for ^{235}U and ^{238}U are performed in a truly simultaneous fashion. The importance of simultaneous measurements for isotopic-ratio determination will be discussed in Section 1.4. Techniques labelled "green" indicates truly simultaneous measurements, "yellow" depicts quasi-simultaneous measurements, and "red" represents sequential measurements.

The metric "portable or field-deployable instrumentation" indicates the footprint and weight of the instrument system. Instruments that can be hand-held with a weight limit of 40 pounds are marked "green". Field-deployable instrument is marked in "yellow" and is defined as an instrument that weighs less than 400 pounds [31] and can be mounted on a cart rack. Instruments that are heavier than 400 pounds are marked "red".

The metric "measurement time" refers to typical measurement time for one sample. Techniques rated "green" are fast and typically require less than 10 minutes for one measurement. Techniques that typically require more than 10 minutes but less than one hour per sample are rated "yellow", and those requiring more than one hour are rated "red".

1.3.2 Criteria on operation details

Each candidate technique is evaluated against a list of factors related to operation details, like "non-destructive assay (NDA) or destructive assay (DA)", "direct measurement on gaseous UF_6", "no physical UF_6 sampling needed", "relative ease to implement as an in-line technique", "comparatively free from memory effect", "no repetitive on-site calibration required", and "no consumables or chemicals needed". Similar to evaluation on analytical performance, ratings "green", "yellow" and "red" indicate that the techniques pass, marginally fail and fail the listed criteria, respectively.

Non-destructive assay is defined as a measurement without producing significant physical or chemical changes in the sample, whereas destructive assay is defined as a measurement normally involves destruction of the physical form of the sample [32]. As such, a candidate technique is classified as NDA if the measured sample still exists in the form of UF_6 after measurement and as DA if the measured sample no longer exists in the form of UF_6. Techniques that involve breaking the chemical bonds of UF_6 are thus classified as DA, regardless of the amount of sample consumed. For all atomic (either optical or mass) spectrometric methods, because the UF_6 sample needs to undergo atomization (i.e., bond cleavage) to give U atoms, these methods are inherently destructive in nature. In contrast, for techniques that directly probe UF_6 as intact molecules with no change (including ionization) in its chemical form (e.g., infrared spectroscopy), the technique is then classified as NDA.

For techniques that do not require physical UF_6 sampling, they are evaluated with an additional criterion "signal independent of cylinder parameter". This metric indicates whether the measurement is representative and independent of cylinder-related parameters. For techniques that require physical UF_6 sampling, this criterion becomes not applicable (N/A).

For techniques that require calibration standards, they are further evaluated on the "frequency of recalibration". Techniques that require infrequent recalibration (less than once per day) are rated "green", some recalibration (once or twice per day) are rated "yellow", and frequent recalibration (recalibrate after one or a few sample measurements, e.g., standard-to-sample bracketing) are rated "red".

The metric "relative ease to implement as an in-line technique" evaluates the complexity or practical feasibility to implement the technique for in-line UF_6 enrichment assay measurements. A "green" rating indicates that the technique can, in principle, be readily transformed to an in-line technique and is usually associated with those techniques that can directly measure gaseous UF_6. A "yellow" rating indicates, although some chemical transformation is likely needed for measurement, an automated system to perform the transformation process is readily available. A "red" rating refers to technique that requires chemical transformation before analysis can be performed, which complicates in-line coupling.

1.3.3 Criteria on ease of operation

The candidate technique is also assessed on its relative ease of operation. The overall complexity of the system and its operation details, which includes "overall maturity level of commercial instrument", "level of automation on instrument operation", "level of automation on data processing for isotopic analysis", "mechanical robustness of the instrument", "electrical requirement", "sample preparation", and "overall complexity of the system", are all evaluated. The first three criteria assess the maturity as a commercial instrument or its components (if a commercial system is not available) and level of automation in instrument control, data acquisition and data processing. The criterion on mechanical robustness is particularly targeted to a field-deployable instrument, in which frequent instrument vibration and imperfect environment control (e.g., temperature control and stability) are likely. Similarly, electrical requirements need to be considered for a field-deployable instrument, and systems that require high or special (e.g., three phase) power supplies are at a disadvantage.

"Sample preparation" evaluates the complexity of the sample-preparation procedures. A "green" rating indicates that the technique accepts gaseous UF_6 samples directly, and hence, no sample preparation is needed. A "yellow" rating represents some simple (two steps or less) preparation is needed (e.g., the two-step conversion from gaseous UF_6 to uranyl nitrate solution, or simple UF_6 chemisorption onto a solid substrate). A "red" rating denotes that sample preparation is comparatively complicated (e.g., a multiple step process, for example, the conversion to a solid powder followed by mixing with other metallic powder in a well-defined ratio for glow discharge-optogalvanic spectroscopy to be discussed in Section 3.4.4).

The last criterion "overall complexity of the system" assesses the overall complexity and ease of operation of the technique. The rating is high (green) if the system is a turn-key system that can be mastered by a technician, and rating is low (red) if it is a complex system which requires regular attentions from an expert with extensive training.

1.4 Importance of simultaneous measurement and signal correlation in isotope-ratio determination

Signal correlation is crucial in defining the accuracy and precision of isotope-ratio measurements, and thus, its importance needs to be stressed. So far, none of the analytical techniques address ***directly*** the $^{235}U/^{238}U$ ratio. Instead, all available techniques indirectly gauge the $^{235}U/^{238}U$ ratio through either sequential or simultaneous, but separate, measurements of the signals from ^{235}U and ^{238}U. All measurements unavoidably contain noise. Noise can be further categorized as uncorrelated and correlated. Examples of uncorrelated noise include shot (also known as Poisson) noise and thermal (also known as Johnson) noise [33, 34]. Shot noise is the result of random arrival of particles (e.g., radioactive decay particles, photons for emission source, or ions for ionization source) onto the detector [34]. Thermal noise is the consequence of random movement of electrons in resistors in electronic devices [33, 34]. Correlated noise is due to flickering of the system, and examples include: variations in the sample introduction system, fluctuations in atomization, ionization or excitation efficiencies for optical and mass spectrometry, and interference noise from power supply [33, 34].

The relative error in the ratio of two signals, x and y, could be larger or smaller than those in the individual signals (i.e., a further degradation or an improvement in measurement precision); the outcome is heavily dependent on the correlation of noise in the two signals. To illustrate the importance of signal correlation, computer simulated signals with both correlated and uncorrelated noise components have been generated and are shown in Figure 1.1 below. The precisions of the two signals, x and y, [relative standard deviation (RSD) ~ 20%] are rather unacceptable for many situations. However, because the two signals are highly correlated – that is, signal dips and peaks occur at the same time for the two signals – the noise is greatly reduced in the ratio x/y (RSD ~ 1.5%). These highly correlated signals are usually achievable only when the two signals are simultaneously acquired, as repeatedly proven in the literature [35-37]. Signal correlation typically greatly degrades for sequential measurements (i.e., when signals x and y are measured one by one, sequentially in time). Therefore, the ability to perform simultaneous measurements for the two isotopes is included in one of the broad set of performance criteria metrics for evaluation of a candidate technique in the present study.

Through the simple error-propagation formula, it can be shown that uncertainty in the ratio (expressed in standard deviation and denoted by $\sigma_{x/y}$) relates to individual measurement uncertainties (denoted by σ_x and σ_y) through this relationship [36, 37]:

$$\left(\frac{\sigma_{x/y}}{x/y}\right)^2 = \left(\frac{\sigma_x}{x}\right)^2 + \left(\frac{\sigma_y}{y}\right)^2 - 2\rho\left(\frac{\sigma_x}{x}\right)\left(\frac{\sigma_y}{y}\right) \tag{1.1}$$

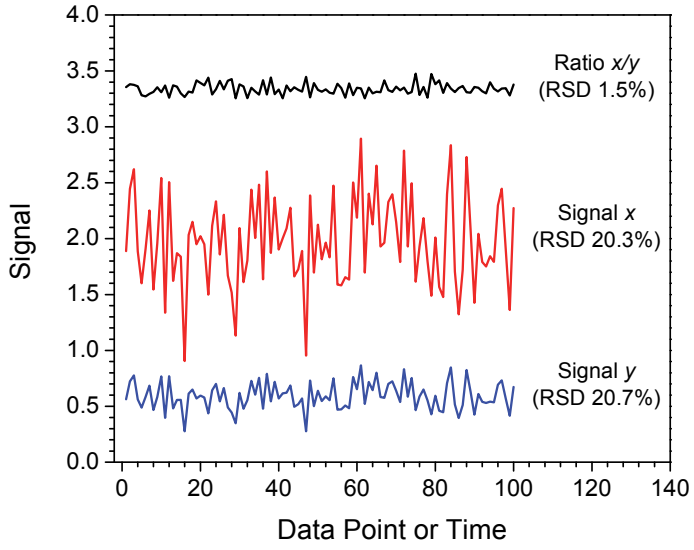

Figure 1.1 **Two simulated signals, *x* and *y*, and the resultant signal ratios (*x*/*y*), demonstrating the importance of correlated noise and simultaneous measurement in improving the signal (isotopic) ratios.**

where ρ is the correlation coefficient between the two signals x and y. For U-enrichment assay, x and y are the ^{235}U and ^{238}U signals. It is clear from this relationship that if the two signals are uncorrelated (i.e., $\rho = 0$), the precision in the ratio is degraded (larger uncertainty) compared to the relative uncertainty in x or y alone. On the other hand, precision improvement is possible if there is some correlation (i.e., $\rho > 0$) between the two signals x and y. If the two signals are highly correlated (i.e., $\rho \approx 1$) and if their relative standard deviations are approximately the same [i.e., $(\sigma_x / x) \approx (\sigma_y / y)$], the two noise components will be largely cancelled. It should be noted that the so-called common-mode noise rejection – a noise reduction technique frequently adopted in the engineering field is based on this principle of noise correlation.

Meija and Mester [36] compared the correlation coefficients between isotopes of three types of mass analyzers (quadrupole, time-of-flight, and multi-collector) coupled to ICP. As a quadrupole mass analyzer is a single-channel detector, it is capable of performing only sequential measurements. A time-of-flight mass analyzer extracts all ions simultaneously but performs measurement of each ion-mass sequentially in time (i.e., not truly simultaneous). A multiple-collector mass analyzer extracts and measures all ions in a truly simultaneous fashion. In line with the expectation from simultaneous measurements, the reported ρ values were 0.066, 0.276 and >0.999 for quadrupole, time-of-flight, and multi-collector ICP-mass spectrometers, respectively [36]. Because of the highly correlated signals from MC-ICP-MS, the reported RSD of the measured isotopic ratio of a test element, hafnium, was only 0.005% [36]. Clearly, the

capability of performing truly simultaneous measurements on the two isotopes is crucial in cancelling any correlated noise that would otherwise degrade the precision of the determined isotopic ratio. Although the above example is from mass-spectrometric measurements, the same argument is equally valid for measurements based on other principles [37, 38].

It should be noted that not all noise sources are correlated in nature. From the foregoing discussion, one well-known source of uncorrelated noise, which is particularly relevant to isotopic analysis, is counting statistics (also known as Poisson noise). In an ideal case in which all other noise sources are eliminated, precision of isotopic analysis is governed by counting statistics. Because radiometric techniques usually do not have other noise sources, their precisions are largely limited by counting statistics. For a truly simultaneous ICP mass spectrometer, it has been shown that isotopic-ratio precision close to the counting-statistics limit is achievable [39]. Accordingly, a candidate analytical technique will be evaluated on its capability to perform truly simultaneous measurements for ^{235}U and ^{238}U.

2 Review of solid sorbents for UF_6 enrichment assay

2.1 Introduction to review of solid sorbents for UF_6

Destructive analysis (DA) for UF_6 enrichment assay provides the highest level of analytical accuracy and precision. However, in the current workflow, the UF_6 sample is shipped off-site for MS analysis. Not only the shipping is cumbersome and costly, but new shipping regulations complicate the transport of UF_6. Although only a gram-sized quantity of UF_6 in specialized container is shipped for DA and air transport of gram-sized UF_6 is approved by the International Air Transport Association (IATA), a full ban on Type A transports of UF_6 is under discussion in various national regulatory air transport venues [7]. Clearly, transporting a hazardous material such as UF_6 is becoming more difficult, where it is allowed at all. A way to deal with that is to convert gas-phase UF_6 to a solid state (e.g., solid uranyl fluoride, UO_2F_2), which is regarded as more transportation friendly and is less regulated.

Furthermore, as some of the analytical techniques (e.g., LAARS to be discussed in Section 4.2.1) require the transformation of gaseous UF_6 onto a solid sorbent before measurements can be performed, the materials and chemistries that are currently employed for such transformation are reviewed and summarized below. Sorbents that are designed to adsorb gaseous UF_6 include: sodium fluoride (NaF) [40], alumina (Al_2O_3) [41, 42], activated carbon [43, 44], and synthetic zeolite nanoparticles [25]. Sodium fluoride and alumina are the two sorbents that are widely used, and detailed comparisons of their adsorption characteristics have already been documented in the report by Schultz and co-workers [45].

2.2 Sodium Fluoride

Sodium fluoride has been studied and used for decades as a solid sorbent for gaseous UF_6 [46, 47]. The reaction proceeds through formation of an addition complex and is reversible:

$$UF_{6\,(g)} + 2\ NaF_{\,(s)} \leftrightarrow UF_6 \bullet 2\ NaF_{\,(s)}$$

At temperatures < 200°C, the reaction proceeds forward and favors the formation of the solid $UF_6 \bullet 2$ NaF complex [40]. However, at higher temperatures (> 300°C), the complex decomposes and coverts back to gaseous UF_6 [40, 44]. A virtually complete recovery of gaseous UF_6 is possible [45]. At temperature below 100°C, decomposition of the complex can be safely ignored [47]. NaF is the only sorbent reviewed in this study that exhibits reversibility in UF_6 sorption; all other reviewed sorbents (alumina, carbon or zeolite) are based on irreversible

chemical reactions. Depending on the specific application and purpose, this reversibility can be regarded as an advantage or disadvantage. From the viewpoint of transportation safety, a reversible reaction is undesirable. On the other hand, for material trapping, a reversible reaction could be desirable as one can readily recover UF_6 in the same chemical form.

Compared to alumina, which will be reviewed in the next section, another advantage of NaF is its faster reaction rate. It was reported that with comparable UF_6 pressure < 50 torr, the NaF pellets attained a 40% weight increase due to UF_6 adsorption within 1 hour of reaction time, whereas alumina took 50 hours to reach this same level [45]. For a reaction time of 20 minutes, an ~18% weight increase was reported for NaF sorbent [45]. Loading capacity of NaF is slightly higher that of alumina [45], although the two values are quite comparable. Loading capacity, defined as the ratio of the mass of UF_6 that can be adsorbed per unit mass of adsorbent used, ranges from 0.6 to 0.8 for NaF and 0.6 to 0.7 for alumina [45].

One drawback of NaF sorbent is that NaF reacts with HF to form bifluoride through a similar complex-forming reaction:

$$HF_{(g)} + NaF_{(s)} \leftrightarrow HF \bullet NaF_{(s)}$$

In fact, NaF has a higher affinity for HF than UF_6 at low temperature (< ~ 100°C). Thus, in the presence of excess HF at room temperature, NaF preferentially adsorbs HF. The decomposition of the HF • NaF complex occurs at a lower temperature, and the bifluoride formation can be generally avoided if the operating temperature is maintained above 100°C [45]

2.3 Alumina (Aluminum Oxide)

Alumina (aluminum oxide, Al_2O_3) is another solid sorbent extensively used for adsorption of gaseous UF_6. It is the sorbent currently used in the ABACC-Cristallini method [41], developed by the ABACC – Brazilian-Argentine Agency for Accounting and Control of Nuclear Materials, for UF_6 sampling. Alumina is hygroscopic (water absorbing); thus, unless alumina undergoes a thermal treatment, a small amount of water is present in its solid lattice. This lattice water is important because the adsorption is initiated through a hydrolysis reaction [45]:

$$UF_{6\,(g)} + 2\ Al_2O_3 \bullet H_2O_{(s)} \rightarrow UO_2F_{2\,(s)} + 4\ HF_{(g)} + 2\ Al_2O_{3\,(s)}$$

The resulting HF further reacts with alumina to produce additional water [45]:

$$6\ HF_{6\,(g)} + Al_2O_{3\,(s)} \rightarrow 2\ AlF_{3\,(s)} + 3\ H_2O$$

The water content in alumina is critical to its adsorbing performance and needs to be well controlled. It is reported that the optimal water content is around 3 to 4 wt% [45]. If the water content is too high (> 7 to 8 wt%), the pellet will be so reactive that the pores leading to the interior of the pellet will be plugged, and uranium loading will be largely limited to the pellet periphery [45].

Some of the adsorption characteristics of alumina have already been discussed and compared with NaF in the previous section. Briefly, the adsorption reaction between UF_6 and alumina is not reversible and is slower than that with NaF. For instance, data showed that for a reaction time of 20 minutes, weight increase for alumina sorbent was < 5% whereas that for NaF sorbent was ~ 18% [45]. It should be noted that, although the adsorption kinetics for alumina are comparatively slow, because sensitivities of many analytical techniques are very high (e.g., ICP-MS), the adsorption does not need to proceed to the full loading capacity. For example, it has been reported that 10 to 30 minutes of contact of UF_6 with alumina pellets retained enough uranium for subsequent isotopic analysis [41].

An advantage of alumina sorbent is that the reaction product uranyl fluoride (UO_2F_2) is very soluble whereas alumina is insoluble. Thus, a uranium sample solution for enrichment assay can be readily prepared by rinsing/washing the pellet with distillated water [41]. In the so-called "Cristallini Method", alumina with controlled water content is made into a pellet shape that can be fitted to a fluorothene P-10 tube, and UF_6 sampling is achieved by adsorption and hydrolysis in the alumina pellets [48]. A recent study [48] conducted by the European Commission (EC) Joint Research Centre (JRC) validated the Cristallini sampling method by comparing the determined $^{235}U/^{238}U$ isotope ratios in UF_6 samples taken by the Cristallini method versus that with the traditional liquid-nitrogen cooled UF_6 sampling tube followed by subsequent distillation and hydrolysis. Overall, results from the two sampling methods were in good agreement, but some statistically significant differences were found [48]. Specifically, albeit very slight, *relative* differences of 0.01% to 0.02% were found for UF_6 test samples containing 0.2% to 0.72% ^{235}U. No statistically significant difference was found for samples with 3.3% ^{235}U [48]. The cause for the differences in the $^{235}U/^{238}U$ isotope ratios for the two sampling methods was not fully understood, although reasons like fractionation, contamination and memory effects were suggested [48].

2.4 Activated Carbon

Activated carbon as a sorbent for UF_6 has been known for a long time [46]. It offers fast reaction kinetics and large loading capacity. However, it has not been extensively used as a sorbent for UF_6 chemical analysis for unknown reasons (perhaps related to the complicated chemistry, or the difficulty to extract the adsorbed uranium into the form of a sample solution). The reactions are

complex and lead to many reaction products, including hydrolysis to uranyl fluoride (UO_2F_2), reduction to lower fluoride such as UF_4, UF_5, U_2F_9, and U_4F_{17}, and with formation of fluorocarbons ranging from CF_4 to wax-like material [46].

Compared to NaF and alumina, the reaction is very fast and equilibrium is almost reached in contact time of 10 minutes [44]. Also, the loading capacity is high, reaching a weight ratio of 1.98 to 3.14 [44].

2.5 Synthetic zeolite nanoparticles

In general, zeolites are aluminosilicates with micro-porous structure and usually have high degrees of entrained water in the lattice. A tailor-made synthetic zeolite nanocrystal, in the form of a thin-film coupon film, was developed as a sorbent for LAARS (to be discussed in Section 4.2.1) measurements. The film contains synthesized zeolite nanocrystals with pore sizes (radius) in the range of 2 to 10 nm [49, 50], which provides excellent gaseous UF_6 diffusion [51]. The specific zeolite in this developed sorbent coupon is of "Y zeolite" type [49], a designation typically refering to a zeolite with silica-to-alumina ratio higher than 3, with a Faujasite crystal structure [50]. With controlled H_2O content, uranyl fluoride (UO_2F_2) crystallization occurs in the nano-pores through the UF_6 hydrolysis reaction [51]. The reaction byproduct HF then seals the pore to trap the sample [51]. The collected sample remains stable and was claimed to do so indefinitely when stored in a sampler or in a low-humidity environment [49]. By controlling the film thickness, pore size and volume, the film can be tailored to capture a specific quantity of uranium mass [49] with ranges from 100 μg to 20 mg [52]. For LAARS measurements, sampled UF_6 mass per coupon (with diameter 12.7 mm) typically targets 100 μg of total U mass [50]. The zeolite nanocrystals offer a specific surface area of 600 m^2/g, which is significantly higher than that of activated alumina (typically < 250 m^2/g) [49]. Typical sample-loading time was listed as 5 minutes [52].

3. Analytical techniques and instrumentation options currently available for routine UF_6 enrichment assay

3.1 Introduction

In this section, the results of the comprehensive review of existing analytical techniques and instrumentation for routine UF_6 enrichment assay are summarized. The review covers their basic scientific operation principles, reported analytical characteristics and capabilities, and evaluations of their suitability to operate in-field for UF_6 enrichment assay. Many analytical techniques are currently available for UF_6 enrichment assay, and there are at least two different approaches to categorize them. One common way is to classify the techniques according to whether or not the analysis consumes (or destroys, all or part of) the samples. Under this classification scheme, the analytical techniques are broadly divided into two categories: non-destructive assay (NDA) and destructive assay (DA). An alternative categorization – and one that is more logical for comparing the capabilities and limitations of different techniques – is to divide the techniques based on their scientific principles. This approach is more logical due to the fact that analytical performance of a technique largely depends on its operating principle and its technological advance in that particular scientific discipline. Therefore, this review adopts the latter classification approach.

3.2 General overview of scientific principles for UF_6 enrichment assay

Although many analytical techniques are currently available for UF_6 enrichment assay, they are based on one of three scientific principles: radiometry, optical spectrometry, and mass spectrometry. Methods that use the radiometric principle measure the radioactive decay of the nuclei from the uranium decay chain, either directly or indirectly. Specific to UF_6 samples, direct measurement usually involves probing the intensity and energy of γ-rays emitted during radioactive decay, whereas the indirect approach probes neutrons emitted from the reaction between fluorine nuclei after capturing α-particles emitted from the decay of uranium [i.e., through the reaction $^{19}F + \alpha \rightarrow {}^{22}Na + n$, in short form $^{19}F(\alpha, n)^{22}Na$] .

Methods employing the optical-spectrometric principle are based on isotopic shifts in the optical transitions being measured. Briefly, the large uranium nucleus influences the electronic energy levels of the uranium atom through interactions between the nuclear charge and the field of the electrons [53, 54]. Because the shape and size of nuclear charge distributions are different in ^{235}U and ^{238}U nuclei, the corresponding interactions between the electrons and the nucleus are also slightly different for ^{235}U and ^{238}U atoms. As a result, optical transitions of ^{235}U and ^{238}U

atoms occur at slightly different wavelengths. Such shifts in absorption or emission wavelengths (optical transitions) are referred to as isotopic shifts. In addition, if the species being measured is in the form of a molecule (e.g., as a UF diatomic molecule), the vibrational and rotational motions of the atoms inside the molecule contribute additional isotopic shifts. As the masses of ^{235}U and ^{238}U atoms are different, the center of mass of a vibrational motion and the rotational moment of inertia of a chemical bond shift accordingly. Therefore, optical isotopic shifts appear in atomic absorption, atomic emission, vibrational/ro-vibrational spectroscopy (e.g., infra-red and Raman spectroscopy) and rovibronic spectroscopy (e.g., laser ablation molecular isotopic spectrometry – LAMIS).

Mass-spectrometric measurements assess the enrichment based on the different masses of ^{235}U and ^{238}U. All mass-spectrometric techniques comprise two essential components – an ionization source and a mass analyzer. The mass analyzer responds only to ions (charged particles) but not neutrals; thus, an ionization source is required to convert the neutral (uncharged) sample to charged ions. Although a large fraction of mass-spectrometric techniques operate in the positive-ion mode (i.e., measuring positively charged ions), the negative-ion mode is also possible [55]. Also, the ions being measured can be singly charged atomic ions (e.g., $^{235}U^+$ and $^{238}U^+$), singly charged molecular ions (e.g., $^{235}UO^+$ and $^{238}UO^+$, or $^{235}UO_2^+$ and $^{238}UO_2^+$ [56]), or doubly/multiple charged atomic or molecular ions (e.g., $^{235}U^{2+}$ and $^{238}U^{2+}$ [12]).

Nomenclature of mass-spectrometric techniques could appear confusing, and therefore, a brief introduction is included here for ease of later discussion. The name of a mass-spectrometric technique almost always contains information about the ionization source. For instance, techniques termed ICP-MS (inductively coupled plasma-mass spectrometry), TIMS (thermal ionization mass spectrometry), RIMS (resonance ionization mass spectrometry), and SIMS (secondary ion mass spectrometry) respectively refer to analyte ionization by means of an ICP, electrons generated from a heated (thermal) filament ionize the analyte, laser light tuned to the wavelengths that exactly match (i.e., resonance) the energy levels of the analyte, and focusing of a primary ion beam onto the sample surface that causes subsequent sputtering and ionization of the analyte in a sample in the form of a secondary ion. In general, each ionization source has its own analytical characteristics and the specific choice for a particular application depends on the purpose of the analysis. For instance, SIMS is capable of sputtering (thus analyzing) the composition of a sample surface to a depth of only 1 to 2 nm, and hence, is the technique of choice if such a spatial resolution of the sample is needed.

Different types of mass analyzers affect analytical performance through resolution, abundance sensitivity, and single *versus* multiple simultaneous measurement channels. In many cases, different types of mass spectrometers can be coupled to the same ionization source. For example, a mass spectrometer of quadrupole (Q) type, time-of-flight (TOF) type, or a multi-collector (MC) type are available in commercial ICP-MS instruments. The resulting instruments

in the above three examples are referred to as Q-ICP-MS, TOF-ICP-MS, and MC-ICP-MS, respectively.

3.3 Review of available radiometric techniques for UF_6 enrichment assay

3.3.1 Gamma-ray spectroscopy

The use of gamma-ray spectroscopy for UF_6 enrichment assay has been known for a long time [57, 58]. Handheld γ-ray spectrometers specifically designed for UF_6 cylinder verification is commercially available (e.g., ORTEC, model MICRO-UF6-PKG-1). The γ-ray at 185.7 keV is the most frequently used signature for ^{235}U [57-59], followed by the one at 143.7 keV. However, studies of γ-ray spectra for ^{238}U indicated that only two weak lines at 776.4 and 1001 keV are present for unique quantitative measurement of ^{238}U [58]. These two lines are not from ^{238}U, but from ^{234m}Pa – a decay daughter of ^{238}U. In other words, neither is a direct measurement for ^{238}U. The use of these two lines for ^{238}U measurements assumes an existence of equilibrium between ^{238}U and its decay daughters.

Gamma-ray spectroscopy has the advantages of portability [57] and non-intrusiveness for on-site measurements; however, the signal response is known to be heavily dependent on cylinder-related parameters such as variation in wall thickness and filling profile [60, 61]. For example, it has been stated that typical variation of the wall thickness ($\sim \pm 0.5$ mm) from the nominal value easily leads to an enrichment error of 6% [60]. Furthermore, the mean free path for the dominant γ-ray at 185.7 keV from ^{235}U is only ~ 2 mm [62] due to self-absorption, which makes this technique unfavorable for assaying the inner volume of the UF_6 cylinder and unable to detect certain diversion scenarios [63]. A recent report [61] studied γ-ray spectroscopy on UF_6 cylinders, with correction for attenuation of the ^{235}U γ-ray due to the cylinder wall. For a cylinder certified with 19.75% of ^{235}U, the reported enrichment was 18% (i.e., 9% relative bias) [61]. Another report [64] indicated measurement precision (as RSD) of 4.3% for a batch of UF_6 cylinders with ^{235}U enrichment ranging from 2.0% to 5.0%.

3.3.2 Neutron spectroscopy

Similar to gamma-ray spectroscopy, neutron spectroscopy offers non-destructive and on-site measurements for UF_6 cylinder assay. However, also similar to γ-ray spectroscopy, neutron spectroscopy is not a direct measurement for the fissile U-isotope, ^{235}U – of particular interest in nuclear material safeguards. Because very few neutrons are generated directly from ^{235}U in UF_6 [63], most neutron counting measurements are based on indirect passive neutron emissions

to determine the ^{235}U enrichment [62, 63, 65, 66]. The neutrons are primarily from ^{234}U and ^{238}U α-bombardment of fluorine through the $^{19}F(\alpha, n)^{22}Na$ reaction, as well as spontaneous fission in ^{238}U [63, 65]. The enrichment in ^{235}U is deduced from the measurement of ^{234}U because enrichment in ^{235}U is reported to be proportional to the ^{234}U in mass-based enrichment processes [63, 66]. One drawback of such an indirect measurement for ^{235}U is that the measurement accuracy relies on *a-priori* knowledge of the $^{235}U/^{234}U$ ratio [65]. Although this ratio is generally predictable, there may be cases where perturbations (e.g., reprocessed UF_6, re-enriched tails, and HEU downblending) in the minor uranium isotopes may affect the accuracy of the passive neutron measurement [65]. For instance, it has been reported that the $^{235}U/^{234}U$ ratio may vary by as much as a factor of four over the range of depleted-to-highly enriched uranium for gaseous diffusion enrichment process [67].

Compared to γ-ray spectroscopy, the advantage of neutron spectroscopy is the much longer mean free path of neutrons in UF_6 (~ 600 mm) [62] which, in turn, offer an assay that is sensitive to nearly the entire volume of the cylinder. Reported uncertainty in passive neutron-counting measurements was 5.2% RSD for a batch of UF_6 cylinders with ^{235}U enrichment ranging from 2.0% to 5.0% [64]. Although it seems that a commercial system is not readily available, field-deployable instruments have been reported [57, 64, 68].

3.3.3 COMbined Procedure for Uranium Concentration and Enrichment Assay (COMPUCEA)

The COMPUCEA technique, developed at the Institute for Transuranium Elements (ITU), is a transportable analytical system for on-site uranium concentration and enrichments assays [6]. Its application specifically for UF_6 enrichment assay is still under development by the IAEA [7], although its use on LEU-oxide samples is considered routine. In fact, IAEA has published an ITV for COMPUCEA – 0.4% *u(r)* and 0.2% *u(s)* for ^{235}U enrichment in LEU oxides [1]. ITVs for other enrichment levels (i.e., DU, NU and HEU oxides) are not published [1].

The COMPUCEA technique is based on energy-dispersive X-ray absorption edge spectrometry and gamma-ray spectrometry. Before presented to X-ray and gamma-ray measurements, the solid sample needs to undergo some laborious preparation steps. Briefly, the solid sample is quantitatively transformed into a uranyl nitrate solution, which involves sample digestion in 8 M nitric acid and subsequent dilution to 3 M acidity with a target U concentration about 190 g/L [6]. The solution is first characterized for its density and temperature [6]. During the process, standard laboratory tools (e.g., portable density meter, glass-ware, chemicals, hot plate, weighing balance) and operators' facilities (e.g., fume hood) are used [6].

The solution sample is then measured by X-ray and gamma-ray spectroscopy. Although ^{235}U and ^{238}U are not simultaneously measured, signal correlation for common-noise reduction does not apply in COMPUCEA because the isotopic assay is performed through radiometric counting (gamma ray), in which the dominated noise source is counting statistics. Typically, for an LEU sample, three replicates of each measurement type are performed; acquisition of each X-ray and gamma-ray spectrum takes about 1000 s and 2000 s, respectively [6]. For a natural U sample, the time is increased to 5000 s for each gamma-ray counting [69]. Data treatment is not very straightforward because the two measurements are interdependent. Specifically, the X-ray measurement needs the knowledge of the enrichment to accurately convert the measured uranium concentration into mass fraction, whereas the gamma measurement needs the uranium concentration as input to correct for self-attenuation effect [69]. Therefore, data evaluation is made in an iterative manner. Furthermore, the sample parameters (including solution density, sample volume, and bottom thickness of sample container) need to be taken in account [5]. Software has been developed for automatic data acquisition and analysis for the in-field COMPUCEA measurement system [6].

The analytical performance is impressive for an on-site measurement. For LEU samples, the achievable combined uncertainty (*u(r)* and *u(s)*) is typically around 0.25% relative [5, 6] (published ITV for combined uncertainty is 0.45% [1]). According to a recent IAEA report [7], the adaptation of the chemical preparation steps for COMPUCEA determination of UF_6 enrichment is currently being studied by IAEA and with the European Commission. As chemical transformation of UF_6 to uranyl nitrate solution is comparatively simple compared with its oxide counterpart, it is anticipated that the COMPUCEA method will be available for on-site UF_6 enrichment assay in the very near future. The drawback of the method is the relatively long counting time, especially for natural (3×5000 s) and depleted uranium, and its labor intensive sample preparation process.

3.4 Review of available optical spectrometric techniques for UF_6 enrichment assay

3.4.1 Tunable diode laser infrared (IR) absorption

The change of ^{235}U to ^{238}U in a UF_6 molecule causes a shift in the center of mass of some vibrational motions of the U–F chemical bond. Accordingly, some vibration frequencies of UF_6 depend on the specific uranium isotope in the UF_6 molecules. These vibrational frequencies appear in the mid-infra-red region in the electromagnetic spectrum, and several studies devoted to examining the isotopic shifts in molecular UF_6 have been published [70-72].

With isotopic shifts in the vibrational spectra of $^{235}UF_6$ and $^{238}UF_6$, UF_6 enrichment assay can be directly performed with infra-red absorption. Because the ν_3 fundamental band possesses the

largest isotopic shifts (~ 0.6 cm^{-1}) between $^{235}UF_6$ and $^{238}UF_6$ [73], a narrow-band tunable laser at around 16 μm matching the fundamental ν_3 vibrational band [74, 75], or the combination band ($\nu_1 + \nu_3$) at around 7.8 μm [28, 29, 76] is used. The availability of commercial quantum cascade laser technology favors the ~ 8 μm wavelength spectral region [76]. However, because the isotopic shift between $^{235}UF_6$ and $^{238}UF_6$ is only ~ 0.6 cm^{-1} in the ($\nu_1 + \nu_3$) combination band, whereas the absorption spectrum of UF_6 is broadened with abundant unresolved rotational-vibrational spectral features spanning > 5 cm^{-1} [28, 77], the isotopic shift is blended and difficult to resolve. As a result, extraction of isotopic information from the unresolved IR spectra can be achieved only with the use of chemometric or multivariate calibration techniques and with calibration standards.

The reported uncertainties (standard deviation) are 0.27% in absolute ^{235}U enrichment for short-term measurement (< 1 minute) and increased to 1% for longer (> 1 hour) measurements due to instrument drift [28]. Three UF_6 samples with ^{235}U abundances from 0.7% to 13.5% were studied [28]. Measurements for the two UF_6 isotopologues are typically achieved through rapid scanning of the laser wavelength; thus, the ^{235}U and ^{238}U measurements are sequential in nature. In addition, some mid-IR detectors (e.g., HgCdTe photodiode quoted in the work above [28, 77]) need to be cooled by liquid nitrogen to reduce the generation of electron carriers in the semiconductor from random thermal excitation (which otherwise would lead to increased dark current and noise). The need for liquid nitrogen cooling poses additional burden for continuous in-field measurements in an unattended mode (e.g., during process control). Recent advances in thermo-electric coolers have, to a large degree, mitigated this inconvenience [78]. For example, although not yet down to liquid-nitrogen temperature, a HgCdTe detector cooled by a three-stage Peltier cooler to a temperature of 205 K is commercially available [78]. A commercial system for gaseous UF_6 analysis is not readily available, but the sizes of the components can fit into a field-deployable instrument.

3.4.2 Gaseous Raman spectroscopy

Another spectroscopic technique commonly used to measure vibrational motions of chemical bonds is Raman spectroscopy. In many cases, Raman and infra-red spectroscopy give complementary information. Raman spectra of gaseous UF_6 have been reported in the literature [73, 79, 80]. However, for reasons that will be briefly stated below, Raman spectroscopy has not yet been applied specifically for UF_6 enrichment assay.

The UF_6 molecule is octahedral in shape and is a highly symmetrical. Therefore, of the six fundamental vibrational bands (denoted as ν_1, …, ν_6), only two (ν_3 and ν_4) of them express $^{235}UF_6$–$^{238}UF_6$ isotopic shifts [73, 81]. The lack of isotopic shifts for the other fundamental

bands can be understood from the viewpoint of molecular symmetry. For example, the symmetrical stretching of the bond F←U→F results in no change in the center of mass when the central uranium atom is switched from ^{235}U and ^{238}U (and hence no change in vibrational frequency for this symmetrical stretching). Out of the six fundamental vibrational bands, ν_3 and ν_4 bands are IR active whereas ν_1, ν_2 and ν_5 bands are Raman active [82]. It turns out that all fundamental Raman-active bands do not possess $^{235}UF_6$–$^{238}UF_6$ isotopic shifts. If Raman is to be utilized for UF_6 enrichment assay, then a combination band needs to be used. Raman signals from combination bands are orders of magnitudes weaker than the fundamental. For example, the Raman intensity of the (ν_3 + ν_6) combination band was reported to be 0.06 compared to a relative scale of 100 of the fundamental ν_1 band [73]. Very likely due to the fact that Raman-active fundamental bands do not possess isotopic shifts, Raman spectroscopy of gas-phase UF_6 has not been applied for UF_6 enrichment assay. Nonetheless, commercial Raman instruments that can handle gaseous samples (although they might not be sufficiently corrosion resistant for UF_6) are readily available in the market.

3.4.3 Atomic optical emission

The first work on isotopic analysis of uranium utilizing atomic optical emission spectrometry (OES) was published at least six decades ago [83]. In this particular context, the atom can be either charged (i.e., ionized) or neutral. Isotopic shifts for some uranium atomic lines can reach tens of picometers and are large enough to be readily measured with a medium-resolution optical spectrometer even under ambient pressure.

Particularly relevant to UF_6 enrichment assay is the study reported by Zamzow *et al.* [22], in which they introduced gaseous UF_6 directly into an atmospheric-pressure argon afterglow discharge source and measured the ^{235}U enrichment in the UF_6 sample. The discharge was operated with a power of only 40 W and sustained with argon at a flow rate ~ 100 mL/min. UF_6 was diluted in argon in a sampling cylinder to a concentration of 0.425% (weight percent) UF_6. The Ar-diluted sample was then introduced into the afterglow region of the discharge at a rate of 1 mL/min. A scanning spectrometer was used and the isotopic ratio was gauged from the emission lines U II 424.412 nm for ^{235}U and 424.437 nm for ^{238}U. Three UF_6 samples with 0.245%, 3.80% and 51.20% $^{235}UF_6$ were measured. The reported RSD for ten measurements were 30% and 6.4% for the two samples with lowest and highest ^{235}U, respectively. Because the two U isotopes were measured sequentially, the signals were not correlated. The authors also pointed out the use of simultaneous data acquisition [e.g., a charged coupled device (CCD) detector] could potentially improve the measurements.

Today, most atomic emission measurements are performed with an inductively coupled plasma (ICP). The capability of modern ICP-optical emission spectrometers for uranium isotopic analysis is documented in a series of recent publications by Krachler and co-workers [20, 21, 84]. In one study [20], Krachler and Carbol validated isotopic analysis of depleted, natural and enriched uranium with a commercial high-resolution ICP-OES instrument (Ultima2, Horiba Jobin-Yvon). The samples were in the form of solution at a total U concentration of 100 mg/L, with certified ^{235}U abundance from 0.32% to 4.52%. The reported precision (as RSD) varied between ~ 1% for the highest (4.5% ^{235}U) to ~ 5% for the lowest (0.3% ^{235}U) studied U-enrichment levels. For accuracy, the reported measurement values matched well the certified or reference values within experimental uncertainties [20]. Although the analysis was not in the form of gaseous UF_6, a solution sample can be readily prepared from UF_6 through a simple hydrolysis reaction. In fact, the European Commission's Joint Research Center, Institute for Reference Materials and Measurements (EC-JRC-IRMM) published a simple two-step procedure to hydrolyze gaseous UF_6 into a solution sample [9], which the EC-JRC-IRMM uses to certify the isotopic composition in UF_6 reference materials [9].

Depending on the atomic excitation source, atomic optical emission can be developed into a field-deployable instrument. Some atomic excitation sources operate under a modest power (< 100 W). Atomic emission is a mature technique and components are readily available in the market.

3.4.4 Glow discharge (GD) optogalvanic spectroscopy (OGS)

Optogalvanic spectroscopy (OGS), in principle, is a variant form of atomic absorption. In an electrical discharge (glow discharge in this specific example demonstrated by Shaw, Young, and Barshick *et al.* [23, 85, 86]), electrical energy is coupled to the discharge and an equilibrium between ionization and excitation levels of the atoms is then established. When the wavelength of a narrow-band tunable laser matches the transition wavelengths of an atom in the discharge, energy from the laser is coupled into the discharge *via* atomic absorption, which then shifts the equilibrium of the discharge. The impedance of the discharge then alters as a response to this change in ionization equilibrium, which results in a change of discharge current or voltage. If the bandwidth of the laser is narrower than the isotopic shift, isotopic analysis can be performed through monitoring the change of plasma impedance while scanning the laser wavelengths across the absorption profiles of the isotopes. Samples, in form of powder, are mixed with an electrical conducting binder to form hollow cathodes for the electrical discharge. For examples, samples in the form of metallic-U, UF_4 and U_3O_8 powders were mixed with high purity metallic silver and tantalum powder to form the hollow cathodes [23]. For UF_6 enrichment assay with GD-OGS, chemical conversion of gaseous UF_6 to a solid form is needed (for example, through simple hydrolysis reaction with water vapor to uranium oxyfluoride powder).

Eight pairs of atomic lines in the wavelength range from 776 to 836 nm were reported for U isotopic analysis [23, 86]. The studied range of ^{235}U abundances were from ~ 0.27% (depleted) to ~ 20% (highly enriched). Reported measurement precisions (as RSD) ranged from ~ 12% (0.3% ^{235}U abundance) to 1.8% (20% ^{235}U). The reported accuracy matched well with the values analyzed by TIMS for samples with ^{235}U abundances ≥ 10%, but some biases were observed for those samples with lower ^{235}U abundance. For example, the reported $^{235}U/(^{235}U + ^{238}U)$ ratios was 0.34% for a depleted U sample, whereas the cross-check value from TIMS was 0.490% [23].

Compared to atomic emission spectroscopy, GD-OGS does not require an optical spectrometer. Thus, the footprint of the instrument can be significantly reduced. In addition, power requirement is only modest. Similar to optical emission spectroscopy, GD-OGS does not require isotopic standards for calibration [86], but it is a scanning method and the two U isotopes are not measured simultaneously. A commercial GD-OGS system is not available. Based on the sizes of the components, development of a field-deployable instrument for this technique is likely feasible.

3.4.5 Laser ablation (LA) diode laser (DL) laser induced fluorescence (LIF)

Laser ablation-diode laser-laser induced fluorescence (LA-DL-LIF), again, measures isotopic ratios based on the isotopic shifts in the atomic transitions. The sample is typically in the form of a solid and it is sampled and converted to atom *via* laser ablation. A second, narrow-band, wavelength-tunable laser excites ^{235}U and ^{238}U atoms separately. Two excitation schemes were reported by Smith *et al.* [24]. In the first approach termed the wavelength scanning technique, the wavelengths of the diode laser are rapidly (within 2 ms) scanned across the absorption wavelengths of the ^{235}U and ^{238}U isotopes. As radiative lifetimes for allowed optical transitions are short (typically nanoseconds), these excited atoms almost immediately undergo fluorescence. The temporal fluorescence signal consists of two separate groups – one corresponds to ^{235}U and the other to ^{238}U. The advantage of this scheme is that both ^{235}U and ^{238}U signals are measured from the same laser-ablation sampling pulse; however, as laser ablation is a transient event, the atom population inside the laser plume actually changes during the scanning of the diode laser [24]. Thus, this temporal dependence of atomic population needs to be separately determined and corrected. In another scheme termed the fixed wavelength technique, the wavelength of the diode laser is tuned to the peak absorption profile of either isotope lines on alternating laser samplings [24]. In other words, ^{235}U is measured in one laser-ablation pulse and ^{238}U is measured in the next one. Analytical precision could suffer if there is variation in mass removal between two laser-sampling shots [24]. Reported precision for this method ranged from 27% RSD for samples with 0.204% ^{235}U to 7% RSD at 0.714% ^{235}U [24]. Reported analytical accuracy matched certified values within experimental uncertainties [24].

Because wavelength selectivity for the two isotopes comes from the narrow-band laser, the function of the optical spectrometer is to separate the fluorescence from the background. Thus, a compact spectrometer with low spectral resolution is sufficient, which in turn reduces the footprint of the instrument; development of a field-deployable instrument is likely feasible. Power requirement is modest. However, both excitation schemes are sequential [24] and the two U isotopes are not measured simultaneously. A commercial LA-DL-LIF system is not available, and the critical optical alignment of the two lasers (ablation laser and fluorescence-excitation laser) likely requires a high level of anti-vibration control.

3.5 Review of available mass spectrometric techniques for UF_6 enrichment assay

Overall, mass spectrometry offers very high accuracy and precision but the measurements are often performed off-site. In a mass-spectrometric measurement, the radionuclides actually enter the mass analyzer, which in turn increases the risk of radioactive contamination and memory effects. The chemical reactivity and corrosive nature of UF_6 not only place additional restrictions on the components of the mass analyzer, but also increase the likelihood of memory effects for isotopic analysis. To elaborate, many materials, even for those that are classified as UF_6-corrosion resistant, slowly react with UF_6. Such reactions sometimes are referred to as passivation. The reaction products are usually in the form of a thin layer of uranium-containing compound on the material surface, in equilibrium with the incoming corrosive UF_6. If the $^{235}U/^{238}U$ isotopic ratio of the incoming gaseous UF_6 is different from that of the surface-deposited U-containing compound, possible isotopic exchange of U then leads to memory effect *via* reaction ^{238}U–on surface + $^{235}UF_6 \leftrightarrow {}^{235}U$–on surface + $^{238}UF_6$.

3.5.1 Gas source mass spectrometry

Gas source mass spectrometry (GSMS) is currently the most sensitive and precise measurement technique for $^{235}U/^{238}U$ isotopic ratio analysis in gaseous UF_6 samples [87]. Several GSMS instruments, exclusively designed for UF_6 isotopic analysis, are commercially available (e.g., URANUS from Thermo Fisher, and IMU 200 from InProcess Instruments, Germany). In fact, GSMS is one of the two analytical techniques (the other one is thermal ionization mass spectrometry, TIMS) that the European Commission's Joint Research Center, Institute for Reference Materials and Measurements (EC-JRC-IRMM) uses to verify and certify the isotopic composition of UF_6 reference materials that EC-JRC-IRMM offers (the IRMM-019 to IRMM-029 series) [9, 87, 88].

Because of the homogeneity of gaseous samples, GSMS offers better measurement precisions by a factor of 5 than those attainable by TIMS [87], which is considered in many cases as the gold standard for isotope-ratio analysis. Although the reproducibility for $^{235}U/^{238}U$ ratio on a UF_6 GSMS measurement is at a level of 0.005% RSD, one measurement cycle consists of multiple measurements alternating between the sample and two calibration standards; the duration for one measurement cycle is about 5 hours [87]. The long measurement cycle is related to memory effects. To reach the ultimate uncertainty level, the equal-distance double-standard calibration approach, which is a standard-to-sample bracketing technique with two standards preferentially chosen with equal relative differences of their isotope ratios compared to that of the sample [87], needs to be used. This "equal distance" requirement, when fulfilled, will cancel out memory effects caused by the sequential introduction of gaseous UF_6 from the sample and the two standards with different isotopic compositions through the same inlet line into the same ion source [87].

The analytical performance of GSMS is remarkable; however, its long measurement time (several hours) for one sample, high power consumption (e.g., power requirement for the URANUS is 11 kW), its bulkiness in size (e.g., 4.5 m in length for the URANUS) and weight (~ 1500 pounds for IMU 200) are some of its drawbacks.

3.5.2 Thermal ionization mass spectrometry

As mentioned in the last section, thermal ionization mass spectrometry (TIMS) is another analytical technique employed by EC-JRC-IRMM to verify and certify the isotopic composition of UF_6 reference materials [9, 87, 88]. TIMS is known for its superior precisions in isotopic-ratio measurements. However, measurement precisions of TIMS are not as good as those of GSMS. The comparatively less reproducible measurement with TIMS is due to the fact that the solid sample on a TIMS filament becomes isotopically inhomogeneous due to fractionation during the measurement process [87].

In general, TIMS requires extensive sample preparation prior to measurement. For example, samples are laboriously purified with ion-exchange chromatography to maximize ionization of the analyte [89]. Samples are usually presented as a solution and deposited (sometimes, with the addition of modifiers) onto the TIMS filament for electrothermal vaporization. Both the sample preparation and sample-loading procedures control the overall detection efficiency and the presence of matrix interferences (spectral and non-spectral) in TIMS [90]; it was commented that only *extremely pure* samples yield sufficiently intense and stable ion beams [90]. Because UF_6 samples are usually presented in a very pure form, the usual stringent requirement for sample preparation could be slightly relaxed. A two-step reaction was suggested [9]: hydrolysis of UF_6 to UO_2F_2 ($UF_6 + 2\ H_2O \rightarrow UO_2F_2 + 4\ HF$), followed by conversion to nitrate salt with nitric acid

($UO_2F_2 + 2\ HNO_3 \rightarrow UO_2(NO_3)_2 + 2\ HF$). TIMS is not only able to measure isotopic ratios to a very precise level, but also isotopes that are present at very low levels of abundance. For example, it is capable of measuring the ^{234}U minor isotope at an abundance level of 0.0019755% with an uncertainty level of 0.0000022% [91]. Measurement time for TIMS is long (hours) for each sample [91], and the instrument is large in size.

3.5.3 Inductively coupled plasma mass spectrometry

The inductively coupled plasma (ICP) is a very efficient atomization and ionization source for most elements. Several different types of mass analyzers have been coupled to the ICP and are commercially available. As signal correlation has a determinative effect on the analytical performance of isotope-ratio measurement (Section 1.4), the multi-collector mass analyzer is utilized in almost all cases for those very demanding isotope-ratio measurements. As its name suggests, the multi-collector system allows the operator to position several detectors at different positions along the focal plane of the mass spectrometer [92]. The mass spectrometer is a double-focusing type consisting of an electrostatic sector and a magnetic sector. The double-focusing design compensates the relatively large spread of kinetic energy of the ions created by the ICP, and hence provides a mass resolution ($R = m/\Delta m$) reaching 10,000 that is needed to better differentiate isobaric interferences [92]. A modern MC-ICP-MS is equipped typically with about ten to fifteen detectors (combination of Faraday-cup and electron-multiplier detectors [92]).

An international inter-laboratory comparison research was recently published, in which four expert metrological institutes [Instituto de Pesquisas Energéticas e Nucleares (IPEN, from Brazil), Institute for Reference Materials and Measurements (IRMM, from Belgium), Institut Français de Recherche pour l'Exploitation de la Mer (IFREMER, from France) and National Institute of Standards and Technology (NIST, from USA)] compared the measurement results of U-isotope ratios, specifically for UF_6 samples, obtained by GSMS, TIMS and MC-ICP-MS [93]. Four UF_6 samples, with ^{235}U abundances ranging from 0.5 to 3.5% were used. Gaseous UF_6 were directly analyzed by GSMS whereas the samples were transformed to uranyl nitrate solution, with the two-step reaction discussed in the last section, for analyses with TIMS and MC-ICP-MS [93]. Through a detailed analysis of the sources of measurement uncertainty, it was concluded that the precision of isotope ratio measurements (as RSD) are 0.012%, 0.025% and 0.060% for GSMS, TIMS and MC-ICP-MS, respectively [93]. It was also concluded that the uncertainties in the certified values of the calibration standards are the dominant components in the uncertainty budget for GSMS [93]. The advantage of MC-ICP-MS is its higher sample throughput; the technique is able to process up to twenty samples per day compared to only five to ten for TIMS [93].

A new type of ICP-MS spectrometer, employing an array of ion detectors, which allows fully simultaneous measurements from ^{6}Li to ^{238}U was recently introduced into the market [11]. An array of semiconductor ion detector in complementary metal–oxide–semiconductor (CMOS) technology, consisting of 4,800 detector elements (pixels), allows simultaneous measurements of the full inorganic mass spectra [11]. The mass analyzer is still of a double-focusing type (electrostatic and magnetic) but with a different geometry (Mattauch-Herzog) than the MC-ICP-MS discussed above. A unique characteristic of the Mattauch-Herzog mass spectrograph is that the ions, after separation according to their mass-to-charge ratios, are focused along a *flat* focal plane where the semiconductor ion detector is placed. For a depleted U-sample ($^{235}U/^{238}U \sim 0.2\%$) solution at a concentration of 20 μg/L, the reported precision of the determined $^{235}U/^{238}U$ isotopic ratio was 0.052% RSD for ten replicates each with a 100-second read time (i.e., 1000 s total read time). Compared to MC-ICP-MS, the mass resolution of this array ICP-MS is low but its footprint is much reduced (although still unlikely to be field-deployable due to its power, cooling and argon-consumption requirements). For pure UF_6 samples, isobaric interference is likely predictable, comparatively minimal and reproducible. If its lower mass resolution is sufficient for UF_6 enrichment assay, the array detector ICP-MS could be a good alternative.

3.5.4 Multi-photon ionization mass spectrometry

There is a report on the use of multi-photon ionization (MPI) time-of-flight mass spectrometry for the measurements of $^{235}U/^{238}U$ isotopic ratios in UF_6 [12]. Gaseous UF_6 was diluted with argon to a UF_6/Ar ratio of 0.001 and then introduced directly into a TOF-MS. The UF_6 sample underwent photolysis and ionization from the 4^{th}- (266 nm) and the 2^{nd}-harmonic beams (532 nm) of a Nd:YAG laser ($UF_6 + h\nu$ (266 nm) $\rightarrow UF_5 + F$; $UF_5 + h\nu$ (532 nm) $\rightarrow U^+$ or U^{2+}) [12]. The dominant peak in the mass spectra were U^+ or U^{2+} ions, with minor peaks of UF^+, UF_2^+, and UF_3^+. UF_6 samples with ^{235}U abundance from 2% to 20% were measured, and it was reported that "excellent agreement was observed" [12]; however, quantitative details on analytical accuracy and precision were not given. Because of the measurements for ^{235}U and ^{238}U are not truly simultaneous for a TOF mass spectrometer, an estimation based on the published precision values from the more well-established ionization source ICP coupled with TOF-mass spectrometer would suggest that this MPI-TOF-MS technique is not capable in delivering the required analytical precision.

3.6 Assessment of currently available analytical techniques for in-field UF_6 enrichment assay

In this section, all the currently available analytical techniques covered in Sections 3.3 to 3.5 are assessed for their suitability to operate for in-field UF_6 enrichment assay. The evaluation will be based on a broad set of performance metrics in three categories: analytical performance, operation details, and ease of operation, as outlined in Section 1.3. Table 3.1 summarizes the results of performance evaluation. An "N/A" is used to indicate that performance characteristics are not applicable. Some remarks on the evaluation are given below.

For analytical accuracy and precision, only the four comparison benchmarks – COMPUCEA, GSMS, TIMS and ICP-MS – receive green (pass) or yellow (marginal) ratings; all other techniques fail (red). Only with the relaxed (10×) target values, the second-tier analytical techniques are revealed. With the relaxed criteria, two optical spectrometric techniques are identified as the second-tier techniques – atomic optical emission spectrometry is rated green (pass) under the relaxed requirement and glow discharge-optogalvanic spectroscopy (GD-OGS) scored yellow in precision.

For "direct measurements on both ^{235}U and ^{238}U", with the exception of the three radiometric techniques, all other analytical methods listed in Table 3.1 measure ^{235}U and ^{238}U directly (green). Measurement of ^{238}U by gamma-ray spectroscopy is through its decay daughter (^{234m}Pa). For neutron spectroscopy, ^{234}U is measured and enrichment in ^{235}U is deduced from the abundance of ^{234}U and relies on *a-prior* knowledge of the $^{235}U/^{234}U$ ratio. COMPUCEA is a special case and is somewhat between direct and indirect measurements. It measures total uranium ($^{235}U + ^{238}U$) by means of energy-dispersive X-ray absorption edge spectrometry and specifically ^{235}U with gamma-ray spectrometry. ^{238}U concentration is deduced back through iterative data processing.

Table 3.1 Assessment summaries of currently available analytical techniques for UF_6 enrichment assay. Color codes red, yellow and green indicate "pass", "marginal" and "fail", respectively. "N/A" indicates not applicable.

		Radiometric			Optical Spectrometric					Mass Spectrometric			
		Gamma-ray spectroscopy	Neutron spectroscopy	COMPUCEA	Tunable laser IR absorption	Gas-phase Raman spectroscopy	Atomic optical emission	GD optogalvanic spectroscopy	Laser ablation DL-LIF	Gas source MS	TIMS	ICP-MS	Multi-photon ionization TOF-MS
Analytical Performance	Analytical accuracy meets target ITV												
	Analytical precision meets target ITV												
	Analytical accuracy within 10× target ITV												
	Analytical precision within 10× target ITV												
	Direct measurements on both ^{235}U and ^{238}U												
	Simultaneous measurements on ^{235}U and ^{238}U			Note*									
	Portable or field-deployable instrumentation												
	Measurement time												
Operation Details	Non-destructive assay (NDA) or destructive assay (DA)	NDA	NDA	DA	NDA	NDA	DA	DA	DA	DA	DA	DA	DA
	Direct measurement on gaseous UF_6												
	No physical UF_6 sampling needed												
	Signal independent of cylinder parameter			N/A	N/A	N/A	N/A	N/A	N/A	N/A	N/A	N/A	N/A
	Relative ease to implement as an in-line technique												
	Comparatively free from memory effect												
	No repetitive on-site calibration required												
	Frequency of recalibration	N/A	N/A					N/A					
	No consumables or chemicals needed												
Ease of Operation	Overall maturity level of commercial instrument												
	Level of automation on instrument operation												
	Level of automation on data processing for isotopic analysis												
	Mechanical robustness of instrument												
	Electrical requirement												
	Sample preparation												
	Overall complexity of system												

*Signal correlation for measurement-noise reduction through simultaneous ^{235}U and ^{238}U measurement does not apply in COMPUCEA.

4. Emerging technologies for field-deployable UF_6 enrichment assay

4.1 Introduction

In this section, the results of a comprehensive review of emerging technologies that show potential to be further developed into field-deployable UF_6 enrichment-assay instruments are discussed. Similar to Section 3, the basic scientific operation principle and analytical characteristics of these techniques are summarized, and their current status or projected potential for in-field UF_6 enrichment assay are evaluated based on the same set of performance metrics as outlined in Section 1.3.

The identified emerging technologies can be classified, based on their scientific operating principles (Section 3.2), into two categories: optical spectrometry or mass spectrometry. The optical-spectrometric based emerging technologies include laser ablation absorbance ratio spectrometry (LAARS) developed at Pacific Northwest National Laboratory (PNNL) [25, 26], atomic beam tunable diode laser (DL) absorption under development at Los Alamos National Laboratory (LANL) [27], laser induced spectrochemical assay for uranium enrichment (LISA-UE) to be developed jointly by Lawrence Berkeley National Laboratory (LBNL) and Oak Ridge National Laboratory (ORNL), and high performance infrared (HPIR) spectroscopy with quantum cascade laser under development at Savannah River National Laboratory (SRNL) [30].

Almost all currently emerging technologies based on the mass-spectrometric principle focus on developments related to improving the ionization source which feeds the mass spectrometer. These efforts include: molecular UF_6 mass spectrometry with a portable/fieldable mass spectrometer developed at ORNL [14, 94], a laser ablation ionization mass spectrometer (LAI-MS) under development at LANL [15, 95], surface-enhanced laser desorption and ionization (SELDI) being developed at PNNL [3], liquid sampling-atmospheric pressure glow discharge (LS-APGD) mass spectrometry under development jointly at Clemson University and PNNL [16-18]. All the above technologies are targeted and have clear objectives towards uranium isotopic assay. An emerging technology, although currently not specifically focused on isotopic analysis, that shows potential for such use is the atmospheric-pressure solution-cathode glow-discharge (AP-SCGD) mass spectrometry under development jointly at Rensselaer Polytechnic Institute and Indiana University [19].

Research in national laboratories that focuses on the development of mass analyzers specifically targeting portable/fieldable mass spectrometry is also on-going, but less prevalent than the development on ionization sources. For example, ORNL developed a micro ion-trap mass spectrometer and built a battery-operated prototype [14, 96]. Perhaps because the ion capacity in

a miniaturized ion trap is limited for measurement of isotopic ratios to a high precision (counting statistics depends on the number of ion, which is restricted by the ion capacity), ORNL utilized a retrofitted commercial desktop ion-trap mass spectrometer (Thermo ITQ) for their portable UF_6 enrichment-assay system [94].

In an attempt to ensure that none of the developmental technologies were being misrepresented by the analysis and conclusions made in this study, the sections relevant to those technologies were sent to the developers for comment. Based on the ensuing correspondence, in a few cases, we have modified the text to more accurately reflect system performance and potential. In most cases, the developers agreed that the final version of this report accurately represented the current state of their technology and a reasonable prediction of its potential. However, it should not be assumed that this review of their material is an endorsement of the conclusions.

4.2 Review of emerging optical spectrometric techniques for UF_6 enrichment assay

4.2.1 Laser ablation absorbance ratio spectrometry (LAARS)

Laser ablation absorbance ratio spectrometry (LAARS), developed at PNNL, is an all-optical technique for uranium isotopic assay. Its working principle is based on the isotopic shifts in atomic transitions between ^{235}U and ^{238}U. Instead of probing the atoms with emission or fluorescence as outlined in Sections 3.4.3 and 3.4.5, respectively, LAARS employs atomic absorption as the measurement means. The root of LAARS can be traced back to earlier works by the Niemax group [97, 98] on measurements of uranium isotope ratios in solid samples through combination of laser ablation sampling and diode-laser atomic absorption spectrometry (LA-DL-AAS). Laser ablation creates free uranium atoms from the sample and these atoms are then probed by diode laser through atomic absorption. Measurements are conducted at a reduced-pressure environment and with a certain time delay (μs timescale) after the laser fires. Under these conditions, gas-kinetic temperatures, which determine Doppler line broadening, are typically in the range of 350 K to 400 K [26, 99]. The low-pressure and relatively low-temperature environment warrant a narrow spectral profile (compared to the magnitude of the isotopic shift) in the atomic transition, which in turn ensures that the ^{235}U and ^{238}U absorption profiles are baseline resolved and no further spectral deconvolution is needed. For instance, linewidths of 600 MHz [25] and 800 MHz [26] full width at half maximum (FWHM) were reported for LAARS measurements on U and Gd, respectively. The bandwidth of a diode laser is very narrow (typically < 5 MHz [26]) compared to the magnitude of isotopic shift (> 10 GHz for some U lines), and thus, at most, only one isotope is responsive to the light emitted from the diode laser at any time. The emitted wavelengths of the diode laser can be scanned to sequentially measure the two isotopes, or two separate diode lasers can be used for simultaneous isotopic measurements.

In the first published work by Quentmeier *et al.* [97], one diode laser was used and its wavelength was sequentially tuned to the absorption lines of the ^{235}U and ^{238}U isotopes. The sample was in the form of a solid, and laser ablation (with a pulsed Nd:YAG laser) was used for both solid sampling and atom generation. Diode laser absorption was measured on a pulse-to-pulse basis. This one-diode-laser-for-two-isotopes approach suffers the same shortcoming as that in laser ablation-diode laser-laser induced fluorescence (LA-DL-LIF) discussed in Section 3.4.5 – namely, the atom population inside the laser plume changes during the scanning of the diode laser, and a separate determination and correction for this temporal dependence of atomic population is needed [24]. With this one-diode-laser approach, the accuracy and precision were evaluated to be approximately 10% (relative) for depleted to natural uranium samples (0.204% to 0.714% ^{235}U) [97].

An improved version of the technique was reported by Liu *et al.* [98], in which two diode lasers were employed: one diode laser specifically for measurements of ^{235}U atomic absorption and the other for ^{238}U (i.e., altogether three lasers in the system – two diode lasers and one pulsed Nd:YAG laser for ablation). The two diode laser beams (682.6736 nm for ^{235}U and 682.0768 nm for ^{238}U) are spatially separated but formed an angle of approximately 4°, intersected each other on the axis of the ablating Nd:YAG laser beam at a well-defined (0.2 to 0.3 mm) distance above the sample surface [98]. The probed transitions for ^{235}U and ^{238}U are different atomic transitions, so as to increase the dynamic range of the enrichment assay [98]. To elaborate, as ^{238}U typically presents at a much higher abundance than ^{235}U (especially in natural or depleted samples), the ^{238}U absorbance signal will be comparatively easier to reach the optically thick regime of atomic absorption, in which the absorbance signal is no longer linear to the number of atoms present in the atomic reservoir (i.e., the laser plume in this case). To extend the dynamic range, a weaker atomic transition can be used for ^{238}U.

In this predecessor to LAARS, the two diode lasers need to be tightly aligned with each other so that the two laser beams are probing identical volumes of the laser plume generated by the ablation laser. The absorption of the two beams is directly related to the number density of ^{235}U and ^{238}U atoms along their optical path, which directly translates to $^{235}U/^{238}U$ ratio of the sample if an identical plasma volume is probed. Because the number densities of atoms inside laser induced plasma are spatially dependent, a slight misalignment of the two measurement beams (which then probe different volumes of the plasma) could lead to analytical bias on the measured $^{235}U/^{238}U$ ratios. After passing through the laser-plasma plume, the two diode laser beams are individually measured for their absorption by two photodiode detectors positioned offset to each other. This two-diode-lasers approach allows *simultaneous* measurements of the two U isotopes, and measurement precision was reported to be greatly improved to 1.1% RSD for a pure uranium-oxide sample with ^{235}U at natural abundance [98]. Reported accuracy for the $^{235}U/^{238}U$ ratio was within 5% (relative) for a uranium mineral sample at natural isotopic abundance.

The initial LAARS setup [25, 26] was somewhat similar to that reported by Liu *et al.* [98]. For instance, a three-laser system (one for ablation sampling and two for measurements of the relative abundances of ^{235}U and ^{238}U [25]) was initially reported for LAARS. Initially, two diode lasers operating at ~ 405 nm and ~ 415 nm [25] were used to probe the two U isotopes. The current LAARS system evolved in the last few years with several sophisticated advancements in place [51, 100]. First, the two probe laser beams are directed into a single-mode optical fiber, in which the two beams overlap and are directed to the laser plume with a single achromatic focusing lens. This single optical fiber approach largely reduces the difficulty of optical alignment and warrants that identical laser-plume volumes are probed by the two lasers. Second, the probing laser wavelengths are changed to 682.6776 nm for ^{235}U and 639.5458 nm for ^{238}U [51, 100]. These two wavelengths originate from the ground state but belong to different transitions. Because there is no apparent spatial offset for the two laser beams, they need to be spatially separated before directed onto their individual photo-detectors. Due to their comparatively large wavelength difference ($\Delta\lambda \approx 43$ nm), the two beams can be readily separated with a simple diffraction grating. Third, to minimize wavelength drifts, the wavelengths (optical frequencies) of these two diode lasers are stabilized and frequency locked. Instead of using a laser wavemeter (whose accuracy is insufficient [51]) to monitor and feedback control the wavelengths of the two diode lasers, a tailored laser frequency locking technique that provides frequency stabilization for both probe lasers to < 10 MHz (i.e., ~ 0.014 pm at 650 nm) was developed [51]. The frequency lock for the two probing lasers is sophisticated in design, but requires an additional wavelength tunable diode laser, which is termed the ^{238}U master laser and brings the total laser count in the system to four. The ^{238}U probe laser is frequency locked through a ^{238}U hollow cathode lamp, with the Zeeman splitting method [101]. In theory, the ^{235}U probe laser can also be similarly locked with a ^{235}U hollow cathode lamp; however, to avoid a lamp made with HEU, an offset locking method is used [51]. The additional (^{238}U master) laser is tuned to the ^{238}U counterpart of the ^{235}U probe wavelength [682.6736 nm, nominal isotopic shift about 17.7 pm (or 11.4 GHz) for this specific uranium transition] and is locked with another ^{238}U hollow cathode lamp. Both the ^{235}U probe laser and the ^{238}U master laser are coupled into a single mode fiber equipped with a fast optical detector. Due to the interferences from the two wavelengths, temporal beat patterns (beat frequency), which are related to the frequency (wavelength) difference of the two lasers, are registered by the detector. By comparing the monitored beat frequency to the frequency expected from the well-defined isotopic shift (i.e., ~ 11.4 GHz in this case), the ^{235}U probe laser can be tuned and frequency locked through the beat frequency.

Specific for UF_6 enrichment assay, LAARS employs a tailored solid thin-film sorbent to convert gaseous UF_6 to uranyl fluoride nanocrystals through a hydrolysis reaction [51]. More details about this sorbent can be found in Section 2.5. The thin-film sorbent loaded with converted UF_6 product is a solid sample, placed in a chamber under low pressure with an inert cover gas (argon at ~10 torr), and sampled by the ablation laser [25]. The ablation laser and the associated laser-

induced plasma convert the sample into gaseous uranium atoms, and the two uranium isotopes are then simultaneously probed by the two diode lasers.

Data from a presentation dated October 2014 [51] showed that accuracy and precision can achieve 0.1% in ^{235}U enrichment levels for natural U and LEU. Specifically, for three UF_6 samples with ^{235}U abundances at 0.725%, 3.982% and 5.119%, the reported *relative* bias with frequency-locked probe lasers were 10%, 0.8% and 0.3%, respectively [51]. Reported relative precisions for these three UF_6 samples were 8.3%, 1.5% and 1.5%, respectively [51]. The latest result [50, 102] demonstrated significant improvements in both accuracy and precision, especially for natural-U samples. For a sample with ^{235}U abundance at 5.119%, the relative bias and precision were about 0.1% and 0.6%, respectively. For a natural-U sample, the relative bias and precision were about 0.3% and 0.5%, respectively. Because the ITVs for relative random and systematic uncertainties [i.e., *u(r)* and *u(s)*] are both 0.1% for LEU and 0.2% for natural-U samples [1], the precision of LAARS is currently within 3× to 6× from the target as a replacement for laboratory-based mass spectrometry. Accuracies are close (within a factor of 2) to the target.

Measurement times for LAARS are fast and can be within 10 [25] to 30 minutes, depending on experimental parameters. A prototype LAARS instrument equipped with an ablation laser firing at 200 Hz has been built, and a 10-minute measurement consists of 120,000 discrete enrichment measurements. The overhead for sample preparation is also fast; the reaction time for the conversion of gaseous UF_6 onto the solid thin-film sorbent takes only several minutes [25]. Because the two probe wavelengths are about 40 nm apart and wavelength selectivity for the two isotopes comes from the narrow-bandwidth diode lasers, a small optical spectrometer/grating is sufficient to separate the two signals. The prototype instrument fits well into a standard instrument rack (~ 2 m × 1 m × 1 m) and requires < 10 amperes of electrical supply (110 VAC, single phase) [25]. The weight of the whole instrument is less than 400 pounds; the instrument cabinet weighs about 220 pounds whereas the LAARS modules together with the sample chamber, ablation laser, and pump weighs about 165 pounds [103]. Unintentional bumping is somewhat expected for an in-field instrument, and its requirement for mechanical robustness (e.g., vibration control) is currently unknown. The sophisticated design of the current LAARS system likely requires extensive expertise for troubleshooting.

4.2.2 Atomic beam tunable diode laser absorption

Atomic beam tunable diode laser absorption, currently under development at LANL [27, 104, 105], shares several features with LAARS described above. The scientific working principle is identical to LAARS and is based on ^{235}U and ^{238}U atomic absorption, in which the absorption occurs at slightly different wavelengths due to the isotopic shifts. Again, similar to LAARS, a

tunable narrow-band diode laser is employed as the absorption light source. Compared to LAARS, this atomic beam diode-laser absorption method differs in the way that atoms are generated. In this atomic-beam method, solid sample is placed in a micro oven inside a vacuum chamber [27, 104, 105]. The micro oven has a small nozzle/aperture opening. The sample is electro-thermally vaporized; the heating also causes atomization and generates free uranium atoms. These uranium atoms escape the oven through the small nozzle and expand into the vacuum chamber in the form of a collimated atomic beam [105], with a flux in the order of 10^{11} atoms/s [104, 105]. The diode-laser probe beam crosses with this atomic beam. Depending on the tuned wavelength of the diode laser (tuned to ^{235}U or ^{238}U), the absorbance is proportional to the number density of either ^{235}U or ^{238}U atoms in the atomic beam (and thus in the sample).

Despite a comparatively high micro-oven operating temperature (typically ≥ 1500°C [104]), because the nozzle forces the atoms to collimate and travel with the same directional motion with a small spread in their velocities, the gas-kinetic (i.e., Doppler) temperature of the atomic beam is low. As Doppler linewidth is proportional to the square-root of temperature, a lower temperature gives narrower absorption linewidth. For instance, for the U-atomic line at 861 nm, an absorption Doppler linewidth of < 170 MHz (~0.0004 nm at 861 nm) was reported for ^{238}U [104], which translates to a temperature of about 110 K (–163°C). In contrast, gas-kinetic temperatures under LAARS measurement conditions are typically in the range of 350 K to 400 K [26, 99]. Further lowering the temperature of the atomic beam is feasible through different combinations of the nozzle and oven configurations and their operating parameters, as already demonstrated by Schindler [106]. A lower temperature (hence narrower linewidth) will open up the possibility of probing other U atomic lines that have smaller isotopic shifts, or isotopes of other elements (e.g., Er [105, 106]) in which isotopic shifts are generally much smaller than those encountered in uranium. A narrower linewidth would also lead to a higher peak absorption signal.

Based on its operating principle, this method potentially could offer higher measurement duty cycle than LAARS. Measurement for this atomic beam method is continuous (i.e., always measuring data, 100% duty cycle) whereas lifetime of atomic species inside a laser induced plasma (e.g., in LAARS) is typically on the order of tens of microseconds [25, 98]; thus, measurement duty cycle is much lower for LAARS (maximum 2%, assuming 100 μs measurement time per laser shot and 200 laser shots per second). However, total signal strength depends not only on measurement duty cycle but also on the uranium atom density. Because uranium species are refractory (i.e., species that are difficult to vaporize and/or atomize) [107, 108] and the achievable temperature of the heating element inside the micro oven is quite limited (typical heating filament temperature is < 3500 K) compared to the temperature of a laser-induced plasma (> 10,000 K at the onset of the plasma), the efficiency to convert uranium in the sample to *free* uranium atoms could be lower in this atomic-beam method. One suggested solution [104] to ease the release of free U atoms is through reduction with another metal (M),

which has a greater affinity of oxygen than uranium through a generic reduction reaction: $UO_2 + M \rightarrow U + MO_2$. This reducing metal, M, is mixed with the U-sample inside the heating filament/crucible. Metals reported to show greater affinity for oxygen than uranium include erbium and dysprosium [104].

As this technique is still in its early stage of development, its analytical capabilities are not yet determined. Some preliminary figures quoted enrichment precision of < 10% [27]. Because this technique accepts sample only in solid form, chemical transformation is needed for gaseous UF_6 sample (e.g., chemical conversion to solid UO_2F_2 or adsorption onto a solid substrate). The single scanning diode-laser system is notably simpler in its setup than the frequency locked laser system developed for LAARS; however, the measurement mode is sequential in nature. Based on its working principle and the sizes of the components, development into a field-deployable instrument is likely feasible [105]. Power requirement is modest and claimed to be < 1500 W [27, 105].

4.2.3 Laser induced spectrochemical assay for uranium enrichment (LISA-UE)

Laser induced spectrochemical assay for uranium enrichment (LISA-UE) is in its very early stage of development (starting October 2016), and is a joint effort between LBNL and ORNL. It is an all-optical technique for uranium isotopic assay and is based, again, on the isotopic shifts in ^{235}U and ^{238}U atomic transitions. Instead of atomic absorption, LISA-UE employs atomic emission as the measurement means. Emission measurements require the atoms in their excited states and, thus, a higher temperature environment is needed. It is known that isotopic shifts for some uranium atomic lines can reach tens of picometers and are large enough to be readily measured with an optical spectrometer even under ambient pressure and comparatively high temperature (e.g., 5000 K) [109]. Specifically for UF_6 samples, a small gas chamber with optical access will be coupled directly to a UF_6 cylinder/pipeline valve for sampling. Through the optical port, a pulsed laser beam is focused into the UF_6 gas sample and the laser–gas interaction then creates a transient high temperature plasma excitation source. This high-temperature plasma is capable of breaking down the chemical bonds in the sample, converts it into its constituent atoms, and promotes a portion of these atoms into their excited states. These excited states, through radiative decay, emit photons that are characteristic of its elemental and isotopic identities. When this transient, laser-induced plasma starts to cool (typically after several microseconds), molecules then form through recombination, and the molecular emission carries isotopic information. The analytical technique through measurement of atomic emission inside the laser plasma is commonly referred to as Laser Induced Breakdown Spectroscopy (LIBS), whereas the measurement of molecular emission is termed Laser Ablation Molecular Isotopic Spectrometry (LAMIS). One potential advantage of employing emission over laser absorption is that a large collection of spectral lines (atomic) and bands (molecular) are emitted from the laser

induced plasma, which can be simultaneously measured with a multi-channel optical spectrometer. As many of these spectral features carry the isotopic information of the sample, multiple emission line/band measurement potentially improves analytical precision.

With the exception of two aspects, LISA-UE is largely different than LAARS reviewed in Section 4.2.1. The two similar aspects are that both techniques employ a pulsed ablation laser for sampling and exploit isotopic shifts in optical transitions as the scientific principle for U enrichment analysis. Other than these two features, the instrument setup and working methodology are different for the two techniques. The LISA-UE technique requires only one ablation laser whereas LAARS requires three (or four) lasers [25]. Plasma emissions in LISA-UE are collected by single set of light-collection optics and ^{235}U and ^{238}U emission are simultaneously measured, which inherently guarantee that an identical plasma emission volume is probed. In other words, a slight misalignment in the light-collection optics in LISA-UE would not induce bias in the measured $^{235}U/^{238}U$ ratios.

As LISA-UE is in its very initial stage of development, its analytical capabilities are not yet known at this point. However, it is anticipated that emission measurements on a collection of spectral features should offer advantage over single line-pair commonly employed in absorption measurements. For example, it has been shown through computer simulation that the use of a chemometric algorithm from a collection of spectral features provide several times improvement in the precision of ^{235}U abundance compared to those measurements utilizing only a single emission line [110]. The simulated ultimate precision was about 0.11% in absolute ^{235}U abundance for multiple line analysis [110], with signals accumulated from 10 laser pulses. Further improvement in precision can be achieved through more signal accumulation, although it is also anticipated that computer simulation probably offers the best-case scenario. The anticipated measurement time is within a few minutes for each UF_6 sample. A drawback of the chemometric calibration method is that it requires calibration with standards. An alternative approach, without the need to use calibration standards, is spectral decomposition by means of non-linear least-square fitting of the ^{235}U and ^{238}U atomic emission spectral peaks. This calibration-standard free approach has also been demonstrated for uranium isotopic analysis in soil [109].

Because the laser induced plasma breaks the chemical bonds of UF_6 molecules and this bond-dissociation process is irreversible, LISA-UE is a DA technique. The exact amount of UF_6 needed or destroyed in an analysis depends on the effective size of the laser plasma as well as the required number of laser shots for a measurement; both factors need to be thoroughly investigated with experimental means. A simple estimation, assuming a laser induced plasma with radius of 1 mm and length of 4 mm (i.e., volume ~ 12 mm^3), suggest that each laser pulse would dissociate around 18 μg of UF_6 [density of gaseous UF_6 at its saturated vapor pressure (~ 80 torr) at room temperature is about 1.5 g/L].

LISA-UE offers flexibility in sample preparation. In general, the laser can induce a plasma directly in a sample regardless of its physical form (i.e., solid, liquid, or gas). Thus, the laser can be focused directly into gaseous UF_6 samples and, hence, eliminate the need to perform any sample preparation, or the laser can be focused onto any solid sorbent (for example, to adapt to already defined sampling protocol). Commercial field-deployable LIBS instruments for direct solid-sample analysis are readily available. Although these commercial systems are not specifically designed for gaseous samples, modification for handling gaseous samples is practically feasible. The sizes, as well as power requirements, of the components can be readily fit into a field-deployable instrument.

4.2.4 High performance infrared (HPIR) spectroscopy with quantum cascade laser

High performance infrared (HPIR) spectroscopy with a quantum cascade laser, currently under development at SRNL [30, 111], shares the same scientific principle as in tunable diode laser (DL) infrared (IR) absorption reviewed in Section 3.4.1. In the initial setup, the HPIR approach combined the use of a quantum cascade laser (QCL) with a hollow core wave-guide (HCWG) as the optical cell [30, 111]. The gaseous UF_6 sample is introduced into the HCWG, which acts as the sample container as well as light guide for the laser. Because QCL power levels are high, generally 50 to 100 times that of common diode lasers [111], long waveguides with length extending to 100 meters and beyond can be used. As absorbance is directly proportional to path length, the use of a long waveguide improves sensitivity. Yet, because the internal diameter of the hollow waveguide is small, the total sample volume remains small (several milliliters) [30]. However, it was reported that there was a material incompatibility issue between the hollow core waveguide and UF_6; thus, the hollow waveguide is replaced with a multi-pass gas cell in the most recent experimental configuration [112]. The physical length of the multi-pass cell is short, about 10 cm [112]. As the laser beam reflects multiple times inside the cell, the optical path is magnified to about 2 m. The gas volume remains low and is reported to be 6 mL [112].

Isotopic spectral signatures from $^{235}UF_6$ and $^{238}UF_6$ have been demonstrated with the HPIR technique with the combination band ($\nu_1 + \nu_3$) at around 1290 cm^{-1} in wavenumbers (~ 7.8 μm in wavelength) [30, 111, 112]. The HPIR shares some of the shortcomings as those in the tunable diode laser IR absorption (reviewed in Section 3.4.1), namely: the isotopic measurement is sequential in nature; and the isotopic shift is blended and difficult to resolve due to the broad and complex rotational-vibrational (ro-vibrational) spectral features in UF_6.

High resolution ro-vibrational spectroscopy for UF_6 is moderately well studied [70, 73, 77, 113, 114] and the heavily blended ro-vibrational structures can be traced to two fundamental reasons, namely: wavelength shifts due to vibrational anharmonicity [77], and spectral-line broadening

[70, 115]. To elaborate, vibrational anharmonicity causes the vibrational frequencies ($\nu_1 + \nu_3$ in this specific case) to slightly shift depending on the vibrational quantum numbers of other vibrational modes [77], and for UF_6 at room temperature, many vibrational modes are thermally excited. Because some vibrational frequencies of the UF_6 molecule are low, for example the fundamental ν_4 , ν_5 and ν_6 frequencies are only 186, 200 and 143 cm^{-1} [73], respectively, room temperature is sufficient to promote and set the UF_6 molecule into one (or even more) of its vibrational excited states. For instance, the vibrational partition function of UF_6 at 295K (22°C) is 241 [70], which means that only 1 in 241 (or about 0.4%) UF_6 molecules are not vibrationally excited (i.e., in the ground state). Even at a temperature of 95K (–178°C), already half of the population of UF_6 molecules are vibrationally excited [114]. These vibrationally excited states (the so-called hot-bands), each slightly shifts the ($\nu_1 + \nu_3$) frequencies, complicate the ($\nu_1 + \nu_3$) spectrum. As a result, although the typical spacing of UF_6 ro-vibrational lines is approximately 0.13 cm^{-1}, the averaged line spacing is greatly reduced to the order of 0.0006 cm^{-1} [115] due to the superimposition of many hot-bands, each with a slightly shifted vibrational frequency. Spectral line broadening is another important contributor to the blended spectral structure. For instance, each ro-vibrational line is pressure broadened. If there is no temperature and pressure control, for UF_6 at a pressure of 80 torr (i.e., its vapor pressure at 20°C), the linewidth (full width at half maximum, FWHM) is approximately 0.013 cm^{-1} [115]. In other words, the linewidth is of the order of 20 averaged line spacing and leads to blended and overlapping ro-vibrational structures of UF_6 at its vapor pressure at room temperature.

It follows from the foregoing discussion that the spectrum can be simplified through sample cooling (either conventional or through supersonic beam expansion [114]) and reduced pressure [77]; however, the experimental setup will become more elaborate, in particular, for an in-line measurement system. As demonstrated by Nabiev *et al.* [77], UF_6 isotopic analysis with IR absorption is typically performed under reduced pressure (defined as lower than the vapor pressure of UF_6 at room temperature, i.e., < 80 torr). The lowest pressure reported by Nabiev *et al.* [77] was 10 torr. It is anticipated that HPIR measurements would also be performed under reduced pressure to minimize the effect of pressure broadening. Another possibility is to perform the isotopic measurements at the so-called *P*- and *R*-branches of the vibrational bands, which are more spread-out in structure. The *Q*-branch is more crowded (and hence, offers higher overall peak absorptivity) than the *P*- and *R*-branches, but the far wings of these open-structured *P*- and *R*-branches may show better performance for isotopic analysis through some of the reported "peak-hole" structures [70].

The analytical capabilities of the HPIR method are not yet fully characterized, but it is listed under "anticipated final capabilities" that the uncertainty for $^{235}U/^{238}U$ ratio would be ±0.5% [30, 112]. A capability to measure $^{235}U/^{238}U$ ratio with ±0.5% uncertainty is similar to those figures reported from conventional tunable diode laser IR absorption (±0.27% to ±1% in absolute ^{235}U enrichment [28], Section 3.4.1).

Both the hollow core waveguide and the multi-pass gas cell are compact in size [30, 112]. Although the total length of the hollow waveguide is long, the waveguide can be coiled [30]. The sizes of other components (e.g., QCL and IR detector) are also compact. Therefore, instrument size is no doubt field-deployable, and it is quite likely that a handheld instrument can be developed. In fact, the footprints for the two instrument versions (HCWG or multi-pass cell) were reported to be $3 \times 1.5 \times 2$ cubic foot in size [30, 112]. Also, the measurements are non-invasive; the UF_6 molecules remain intact and are not dissociated or destroyed after the measurement. Furthermore, the techniques can be relatively easily coupled to a processing pipe and applicable for both online and offline measurements.

4.3 Review of emerging mass spectrometric techniques for UF_6 enrichment assay

4.3.1 Molecular mass spectrometry with portable/fieldable mass spectrometer

Molecular mass spectrometry with portable/fieldable mass spectrometer, developed at ORNL [14], measures ions generated directly from gaseous UF_6. This technique can be viewed as a miniaturized version of gas source mass spectrometry (GSMS, Section 3.5.1) in principle.

Conceptually relevant to this ORNL molecular mass spectrometry approach, Kahr, Abney and Olivares at LANL [116] reported a method to analyze solid uranium samples using a small mass spectrometer. Kahr *et al.* employed the fluorinating agent chlorine trifluoride (ClF_3) to convert solid uranium samples into volatile UF_6, and the UF_6 gas was then introduced into a mass spectrometer with electron-impact ionization [116]. The employed mass spectrometer was a quadrupole, and was small and transportable [116]. The doubly charged uranium atomic ion (U^{2+}) was used to determine the $^{235}U/^{238}U$ ratio and several uranium standard reference materials were studied including U950a (with 0.72% ^{235}U), U030 (3.05% ^{235}U) and U500 (49.7% ^{235}U) [116]. Relative analytical biases were 12.3%, 6.1% and 6.6% for the three uranium SRMs U950a, U030 and U500, respectively [116]. Analytical precisions, expressed in RSD, were 7.3% and 4.6% for U030 and U500 (precision not reported for U950a) [116]. These reported analytical figures of merit were ~ 60× to 130× from the ITVs.

ORNL's molecular mass spectrometry with portable/fieldable mass spectrometer approach differs in several ways from that employed by Kahr *et al.* [116]. First, instead of the more common positive ion mode, negative ion mode is used [96]. Second, at least two ionization modes are described; one involves negative electron impact [117] and the other utilizes charge transfer from SF_6^- ions generated by an external glow discharge [96]. It is claimed that, for UF_6, negative ion MS is preferred because the reaction products of the positive ions with residual water in the vacuum system cause substantial interference [96]. Third, instead of employing a mass spectrometer of sequential scanning type (like a quadrupole), an ion trap mass

spectrometer, which allows *partially* simultaneous measurement of different *m/z* ions, is used. In brief, in an ion-trap mass spectrometer, packets of ions with a range of *m/z* ratios are introduced, trapped and stored in a potential well. By varying the potentials of this potential well, ions with different *m/z* ratios are then sequentially ejected from the well (the trap) and detected [118]. Several ion trap mass spectrometers including a miniature toroidal mass analyzer, as well as commercial units from Torion Technologies (model Guardion) and Thermo Fisher Scientific (model ITQ), are mentioned [96, 117].

According to the latest report published in February 2017 [94], precisions of 0.5% or 0.8% were reported for UF_6 samples with 3% ^{235}U; it is also noted that some slightly larger RSDs were observed for measurements performed at similar experimental conditions. As such, typical routine measurement precision likely lies in the neighborhood at or above 1%.

Although the report [94] contains no dedicated study towards signal correlations between ^{235}U and ^{238}U, the presented temporal profiles could possibly provide some hints. For example, in the sample manifold carry-over experiment (Figure 8 of the report [94]), in which periodic cyclic injections of UF_6 were performed, the temporal profiles of ^{235}U and ^{238}U signals were overall not well correlated. The cause for this lack of signal correlation was not further evaluated.

Isotopic analyses of gaseous samples with portable/fieldable mass spectrometer were also investigated by other research groups and their results likely can provide some useful insights and guidelines on the general analytical characteristics of this technology for in-field isotopic analysis. Particularly relevant is the study by Madzunkov and Nikolić at the Jet Propulsion Laboratory (JPL) [119], in which they reported isotopic measurements of xenon with portable/fieldable ion-trap mass spectrometer. Pure xenon gases, with various certified combinations of isotopic compositions, were introduced directly into the mass spectrometer with electron-impact ionization. For xenon samples with wide ranges of isotopic abundances, the reported accuracy (i.e., bias) was better than 0.07% in absolute abundance (which transforms to 10% relative bias if the isotopic abundance is only 0.7%) [119]. Analytical precisions were better, decreasing from ~10% RSD for some readings with isotopic abundance at ~ 0.1%, to ~ 1% RSD and ~ 0.3% RSD for isotopic abundances at ~ 0.7% and ~ 3%, respectively [119]. As it is very likely that xenon is an easier sample to be analyzed by gaseous mass spectrometer due to the fact that it is an inert and monoatomic gas (thus almost no side reaction and no molecular fragments, that would otherwise spread the total signals into several components, are present), it is logical to predict that, unless there is a major breakthrough in fieldable/portable ion-trap technology, those figures of analytical accuracy and precision reported for xenon are likely the approximate upper achievable limit for this technique.

As gaseous UF_6 samples are directly introduced into the mass spectrometer, memory effects similar to those encountered in GSMS (isotope exchange at the passivated surface through

reaction: ^{238}U–on surface + $^{235}UF_6 \leftrightarrow {}^{235}$U–on surface + $^{238}UF_6$, Section 3.5.1) could be a potential problem and needs to be thoroughly investigated. This isotope-exchange memory effect is of a different nature as the more common "sample washout" type of memory effect, which is defined as non-zero baseline due to slow, spontaneous release of trapped analyte in the system. Sample-washout memory effect in this fieldable molecular MS technology was evaluated [94]; the U-signals return to baseline and become undetectable when a UF_6 sample is removed from the sample-introduction manifold.

Compared to GSMS, the mass spectrometer and other components are greatly miniaturized, and thus, development of a field-deployable instrument is highly feasible. In fact, a field-deployable system with sampling manifold was already developed [94], which greatly facilities ease of operation.

4.3.2 Laser ablation ionization mass spectrometry (LAI-MS)

Laser ablation ionization mass spectrometry (LAI-MS), currently under development at LANL [15, 95], is conceptually similar to ICP-MS through replacement of the bulky and energy-demanding ICP with laser ablation as the ionization source. Solid sample (in case of gaseous UF_6, transformation to solid with a sorbent is necessary) is placed very close to the inlet (sampler) of the mass spectrometer in ambient environment, laser ablation is used to atomize and ionize a portion of the sample, and the ablated sample is subsequently measured by the mass spectrometer [95]. Preliminary data showed that when uranyl fluoride (UO_2F_2, the hydrolysis reaction product between UF_6 and H_2O) powder was deposited onto a solid substrate and ablated, uranium-containing molecular ions can be detected directly, without the need for an additional ionization source [95]. However, it was also reported that the identities of the dominant ion changed quite dramatically with the laser power. For instance, the dominant ions in LAI-MS were $UO_2F_2^+$ and its water adduct $UO_2F(H_2O)^+$ at laser pulse energy of 15 mJ, but switched to UO_2^+ when the pulse energy was nominally increased to 17 mJ [95].

As this technique is still under development, its analytical capabilities specifically for UF_6 enrichment assay are not yet disclosed. However, a 2011 report from research teams at JPL, University of Wisconsin-Madison, and National Aeronautics and Space Administration (NASA) [120], in which a laser ablation-miniature mass spectrometer for elemental and isotopic analysis, similar in principle to LAI-MS, could provide some reference and estimation on the overall magnitude of analytical performance of direct laser ablation-MS. Different from LAI-MS, the work by Sinha *et al.* [120] employed an IonCCD, which is capable of performing simultaneous parallel ion detection, and laser ablation of the sample was implemented in a separate low-pressure chamber (instead of in open air as in LAI-MS) connected to the mass spectrometer through an aperture [120]. In addition, as laser ablation produces two to six orders

of magnitude more neutrals than ions, an electron-impact ionization source was used to ionize the neutrals that resulted from laser ablation [120]. The samples were potassium- and silicon-rich minerals and the reported $^{41}K/^{39}K$ and $^{29}Si/^{30}Si$ ratios were (0.077±0.004) and (0.052±0.006) [120]. In other words, for isotopes with abundance at ~ 5% to 7%, measurement precisions were roughly 5% to 12% RSD. A recent similar study from University of Bern [121] on laser ablation–mass spectrometry also reported roughly 10% relative accuracy on the minor isotope of lead with a 1.63% isotopic abundance (NIST SRM 981, pure metallic lead sample).

As prototypes for miniaturized laser ablation–mass spectrometers have been discussed in the literature [120, 121], development of a field-deployable LAI-MS instrument is highly probable.

4.3.3 Surface-Enhanced Laser Desorption and Ionization (SELDI)

Surface-enhanced laser desorption and ionization (SELDI), currently under development at PNNL [122], is similar in principle to the more well-known matrix-assisted laser desorption/ionization (MALDI) technique, which can be viewed as a variant of laser ablation ionization mass spectrometry (LAI-MS) discussed in the previous section. In MALDI, the sample is mixed with a matrix (e.g., organic acids with chromophoric property), which usually absorbs strongly at the laser wavelength. The sample and matrix mixture is dried and then irradiated with a pulsed laser, resulting in desorption of the sample and matrix material. A fraction of the desorbed matrix is also ionized, which in turn facilitates the ionization of the analyte through chemical ionization (e.g., proton transfer) mechanism. Compared to direct laser ablation ionization, MALDI offers higher sensitivity in particular for analytes that do not have a strong absorption band at the laser wavelength.

In the SELDI approach, the surface where the analyte is deposited is modified to further increase the efficiency of analyte laser desorption/ionization [123]. Most reported MALDI and SELDI applications are for large molecules (e.g., proteins and biomolecules) [123-125], and the techniques are comparatively seldom utilized for inorganic species or elemental/isotopic analysis. Thus, comparatively little has been presented in the open literature on their analytical performance for elemental isotopic analysis. Specifically for U-analysis, there were at least two open reports on the use of C_{60}-fullerene [126] and graphite [127] as substrates; the reported precisions were far from the ITVs [126, 127]. For instance, in the 2013 report published by Walton and Mitchell, in which the performance of MALDI with graphite substrate was documented, they concluded that “discrimination between depleted, natural and 1% enrichment was not readily achievable” [127].

In the SELDI approach under development at PNNL, the researchers deposited colloidal graphite (commercial available lubricant – Neolube) suspended in isopropanol onto the sample plate,

followed by pipetting a uranium-containing solution onto the dried colloidal graphite [122]. Other modifiers, for example C_{60} fullerene, have also been used [122]. Two different commercial instruments were tested by the PNNL researchers [122]; one is a commercial MALDI-TOF-MS system (Bruker Autoflex II) and the other instrument involved coupling a commercial off-the-shelf (COTS) MALDI system with an Orbitrap mass spectrometer (Thermo Exactive). It should be pointed out that, whilst the samples were placed in vacuum in earlier measurements, the samples are positioned in front of the inlet of the MS-sampler in ambient environment under atmospheric pressure (AP) [122] in the latest development. The AP-configuration eases sample changing and handling. The best precision reported for AP-SELDI was 0.54% for a U-sample with 3.13% ^{235}U (with colloidal graphite as the substrate) [122], although poorer precision (e.g., 5.31%) also was reported depending on the experimental conditions and substrate [122]. Analytical accuracy was not yet determined. In addition, analytical precision with the AP-SELDI system under development at PNNL was not yet reported for lower ^{235}U isotopic abundance. Analysis is fast and can be achieved within 10 minutes. Specific to UF_6 enrichment assay, a chemical transformation of gaseous UF_6 to uranyl nitrate solution, through the well-defined hydrolysis reaction, is needed.

4.3.4 Liquid sampling-atmospheric pressure glow discharge (LS-APGD) mass spectrometry

Liquid sampling-atmospheric pressure glow discharge mass spectrometry (LS-APGD-MS), under joint development from Clemson University and PNNL [16-18], is the most well characterized emerging mass-spectrometric technique, especially for determination of isotopic ratio of uranium. The LS-APGD is a microplasma (volume ~ 1 mm^3) formed by imposing a low direct-current potential (typically several hundred volts) between the surface of an electrolyte solution (e.g., 2% nitric acid) and a metallic counter electrode [128, 129]. The supporting electrolyte solution flows out of a small (~ 100 μm) glass capillary housed within a slightly larger metal capillary, between which cooling gas is passed [129]. The normal operating parameters include liquid electrolyte flow rates of 5–100 μL/min, cooling gas (typically helium or argon) flow rate of < 1 L/min, and power consumption of < 40 W [17]. The LS-APGD typically operates under the total consumption mode, in which all the electrolyte solution is consumed [16]. An advantage of the total consumption LS-APGD is that no chemical waste solution is generated. Several physical characteristics (e.g., temperature, electron density) of this microplasma discharge have also been characterized; temperatures of 1000 K to 3000 K were reported [130].

Currently, the researchers coupled this LS-APGD ionization source to the inlet of a high-resolution mass spectrometer (the Orbitrap). The Orbitrap mass spectrometer is of Fourier-transform type and is capable of delivering a mass resolution ($m/\Delta m$) > 100,000. Hoegg *et al.* [16, 17] recently discussed various aspects of the LS-APGD and Orbitrap combination for

uranium isotopic analyses, including optimization of various operating parameters (both for the discharge and the Orbitrap), preliminary analytical figures of merit, and known limitations. The U-containing sample was introduced in a solution form and mixed with the supporting electrolyte. The researchers reported that the dominant U-species in the mass spectra was UO_2^+, and little U^+ or UO^+ were detected [16]. The estimated detection limits for the LS-APGD were greater than 25 μg/mL for U^+ and less than 1 μg/mL for UO_2^+ [18].

The researchers reported an important glitch in the Orbitrap software that could seriously impact the overall accuracy of isotopic analysis. Specifically, they found that the background/baseline-correction function of the Orbitrap software overcorrects the background [17]. As a result, isotopic accuracy suffers because, if a constant overcorrected baseline offset is applied to both the major and minor isotopes, the proportion of the minor isotope that is overcorrected is greater. For instance, the determined $^{235}U/^{238}U$ ratio from solutions of natural uranium was found to increase from ~ 0.0059 to ~ 0.0070 when the total uranium concentrations were increased from 100 to 800 ng/mL [17]. The large bias in the determined $^{235}U/^{238}U$ ratio at lower U total concentration was attributed to the lower ion signals; in this case, an overcorrected background affected the isotope ratio most [17].

Because of the aforementioned software glitch, the reported accuracy in $^{235}U/^{238}U$ ratio measurements should not be taken as representative and significant improvement is anticipated once the software bug is fixed. At present, the researchers evaluated the analytical accuracy through a correction scaling factor [16, 131]. In their latest report [131], the researchers determined this scaling factor through a certified reference material of natural U, and measured the $^{235}U/^{238}U$ ratios of three unknown natural-U samples. With cross validation with multi-collector-ICP-MS, it was reported that there was no statistical difference in the determined $^{235}U/^{238}U$ ratios from the two instruments (i.e., LS-APGD-MS and MC-ICP-MS) [131]. However, it has been stated that this correction scaling factor depends on the $^{235}U/^{238}U$ ratio, as well as a change every time that the system is restarted [131]. At this point, it would be difficult to estimate or project the accuracy of the LS-APGD-MS technique in the field for a sample with unknown ^{235}U abundance.

The reported analytical precision is encouraging, and so far is the best in all the emerging techniques reviewed. The researchers [17] investigated repetitive precisions of the technique. Each analytical session contained ten sets of data acquisitions and RSD from these ten acquisitions were calculated. The sessions were then repeated ten times (i.e., a total of ten RSD values). For a U-sample (with natural isotopic abundance) solution at a total U-concentration of 5 μg/mL, precisions in the $^{235}U/^{238}U$ ratio ranged from 0.41% to 1.67% RSD [17]. In their most recent work [131], which the effort was primarily focused on factors affecting the precision of isotope ratio measurements, reported precisions (in terms of RSD of measured $^{235}U/^{238}U$ ratios from 1 μg/mL natural-U solutions, before correction of scaling factor) were in the range

of 0.05% to 0.13% and met the ITV target for precision (i.e., 0.2% RSD for ^{235}U at natural abundance).

There are two potential shortcomings of this technique as presented. First, the current technology of the Orbitrap mass spectrometer makes it inappropriate to serve as a field-deployable instrument [3]. A comment from the LS-APGD-MS research team [3] is that "*Although a conveniently available instrument for this work* (the LS-APGD-MS)*, it* (the Orbitrap) *is not one that would be appropriate for the type of in-field work envisioned by the potential user."* To elaborate, although the Orbitrap is a benchtop instrument, it is rather large and heavy (490 pounds [132]). Also, the requirement for environmental conditions for the Orbitrap mass spectrometer is quite demanding. For instance, according to the pre-installation manual of the Orbitrap [132], the optimum operation temperature is between 18°C to 21°C and temperature fluctuations of 1°C or more over a 10 minute period can affect performance. There are also rather strict requirements for humidity and vibration controls [132].

It should also be noted that the high resolution offered by the Orbitrap likely contributes to the impressive analytical figures of merit reported for the LS-APGD-MS, as it is documented that several low-intensity, non-uranium ions remain after collision-induced dissociation (CID, a process to dissociate and reduce background ions in the mass spectrometer) and require the high-resolution capability of the Orbitrap to resolve them [18]. If the Orbitrap is replaced by a more fieldable (and very likely lower resolution) mass spectrometer, it is currently unknown how such replacement would affect the analytical accuracy and precision. Two ways were discussed to minimize the background ions in the LS-APGD-MS [131]. In the first approach, the anode is repositioned so that the plasma, anode and the sampling capillary are not collinear. Background ions (mainly water clusters at low masses) are significantly reduced and it is believed that the anode provides a surface where water molecules and ions can be absorbed, form clusters and then be desorbed; anode repositioning removes this active surface [131]. In the second approach, an upgrade version of the Orbitrap spectrometer, Q-Exactive, was used, in which a quadrupole (Q) serves as a mass filter to allow the user to define what mass range enters the Orbitrap to be analyzed [131]. However, at present, it is not clear the efficacy of these two means to those specific, aforementioned background ions in the close proximity of the analyte ion.

Second, memory effects in LS-APGD-MS have been documented in several reports [3, 17, 133]. The cause(s) for the memory effect is not well characterized but it was suggested that material deposited on the capillary counter-electrode and/or the mass spectrometer capillary interface could be the source [3, 133].

Specific for UF_6 enrichment assay and for the current configurations of LS-APGD-MS, a chemical transformation is needed either through the well-known hydrolysis reaction to a uranyl

nitrate solution or through the various solid sorbents already reviewed in Section 2. Although not demonstrated with those specific uranium solid sorbents, laser ablation has been utilized as a means for sample introduction to the LS-APGD for elemental mass spectrometry [133]. Apart from coupling to the Orbitrap, the LS-APGD ionization source has been coupled to other types of mass spectrometers – for example, an ion trap mass spectrometer (Thermo Scientific, model LTQ Advantage Max) [134]. Compared to the Orbitrap, an ion-trap would be more transportable although currently no work has been reported specifically on U isotopic analysis under such a configuration.

4.3.5 Atmospheric-pressure solution-cathode glow-discharge (AP-SCGD) mass spectrometry

Atmospheric-pressure solution-cathode glow-discharge mass spectrometry (AP-SCGD-MS), currently under development jointly at Rensselaer Polytechnic Institute and Indiana University [19], is identical in scientific principle to the LS-APGD-MS reviewed in the last section but different in design for the generation of the microplasma discharge. The AP-SCGD is a direct-current plasma sustained directly on the surface of a flowing liquid electrode (typically at a rate of 1–2 mL/min), supported in ambient air without the need for any compressed or other gas supply [19]. Power of AP-SCGD is ~ 70 W (normally < 100 W) [135], and is generally slightly higher than that of the LS-APGD. A distinct difference between AP-SCGD and LS-APGD is that AP-SCGD is sustained on a flowing liquid cathode, with the liquid in excess and thus overflows from the liquid capillary, whereas LS-APGD operates in a total-consumption [16] mode without generation of chemical waste solution. Although the excessive flow of electrolyte generates chemical waste for AP-SCGD, the continuously self-renewing liquid surface of the flowing solution cathode potentially minimizes memory effects. In addition, the AP-SCGD does not require a careful balance between total solution consumption and incoming solution flow.

Although not yet characterized for its performance on isotopic analysis, the AP-SCGD is reported [19] to offer significantly better detection limits than the LS-APGD as an ionization source for atomic mass spectrometry; the reported detection limit in AP-SCGD for uranium was 0.8 ng/mL (ppb, parts per billion) with UO_2^+ as the measured ion [19]. As detection limit is related directly to sensitivity and/or background noise, the significantly better detection limit for the AP-SCGD suggests that either it offers higher sensitivity and/or lower background noise than the LS-APGD. As both factors are important for isotopic ratio measurements, the AP-SCGD should be considered as a candidate and further evaluation of its full potential for uranium isotopic assay is merited.

In terms of instrument setup, footprint and operation requirements, the AP-SCGD shares many similarities with LS-APGD. Likewise, the AP-SCGD–Orbitrap combination is not appropriate

for a field-deployable instrument [3] for reasons discussed in the last section. The AP-SCGD ionization source has been coupled to other mass-spectrometric platforms [for example, a linear ion-trap MS (Thermo Scientific, model LTQ XL)], although to date no work has been reported specifically on U isotopic analysis with such a configuration. For on-site UF_6 enrichment assay, chemical transformation of UF_6 into a solution, for example through the well-established simple direct hydrolysis reaction or chemisorption with alumina followed by hydrolysis (i.e., Cristallini method, Section 2.3), is needed.

4.4 Assessment of emerging analytical techniques for in-field UF_6 enrichment assay

In this section, all the emerging analytical techniques reviewed in Sections 4.2 and 4.3 are assessed for their suitability to operate for in-field UF_6 enrichment assay. Similar to the evaluation of currently available analytical techniques presented in Section 3.6, the assessment will be based on the same set of broad performance metrics in three categories: analytical performance, operation details, and ease of operation. Because all these techniques are emerging and active research is on-going, it is very difficult to obtain up-to-date information. In addition, information on some areas is not yet available or disclosed. Although the evaluation presented below is based largely on data presented in literature, some extrapolation and even guesswork based on known scientific principles are unavoidably necessary in some cases. Those assessments involve extrapolation, inferences from data of other elements, or guestimates based on known scientific principles are marked with diagonal hatches.

Table 4.1 summarizes the results of performance evaluation of the reviewed emerging techniques; performances are color coded in green, yellow or red. Overall, a “green” rating indicates meeting the criteria, a “yellow” rating represents not meeting the criteria but fails only marginally, and a “red” rating denotes not meeting the criteria. The definitions and details of the performance criteria were outlined in Section 1.3. Because all the emerging techniques are still under development, evaluations on “overall maturity of commercial instrument”, “level of automation on instrument operation” and “level of automation on data processing for isotopic analysis” are premature at this stage. Accordingly, these three performance parameters are removed from the evaluation.

Table 4.1 **Assessment summaries of emerging analytical techniques for UF_6 enrichment assay. A question mark indicates that information is either not yet available or sufficient for estimation, and "N/A" indicates not applicable. Box with diagonal hatch indicates extrapolation from very limited relevant (i.e., U) data, or estimation from either other elements or the scientific principle. Color codes red, yellow and green indicate "pass", "marginal" and "fail", respectively.**

		Optical Spectrometric				Mass Spectrometric				
		LAARS	Atomic beam diode laser absorption	LISA-UE	HPIR Spectroscopy	Molecular MS with fieldable mass spectrometer	LAI-MS	AP-SELDI (Orbitrap MS)	LS-APGD-MS (Orbitrap MS)	AP-SCGD-MS (Orbitrap MS)
Analytical Performance	Analytical accuracy meets target ITV							?	?	?
	Analytical precision meets target ITV									
	Analytical accuracy within 10× target ITV			?				?	?	?
	Analytical precision within 10× target ITV									
	Direct measurements on both ^{235}U and ^{238}U									
	Simultaneous measurements on ^{235}U and ^{238}U									
	Portable or field-deployable instrumentation									
	Measurement time									
Operation Details	Non-destructive assay (NDA) or destructive assay (DA)	DA	DA	DA	NDA	DA	DA	DA	DA	DA
	Direct measurement on gaseous UF_6									
	No physical UF_6 sampling needed									
	Signal independent of cylinder parameter	N/A	N/A	N/A	N/A	N/A	N/A	N/A	N/A	N/A
	Relative ease to implement as an in-line technique									
	Comparatively free from memory effect					?				?
	No repetitive on-site calibration required									
	Frequency of recalibration	N/A	N/A	N/A		?	N/A	?	?	?
	No consumables or chemicals needed									
Ease of Operation	Mechanical robustness of instrument									
	Electrical requirement									
	Sample preparation									
	Overall complexity of system									

5. Identification of technological gaps and any SOA/COTS components that can be modified to expedite developing fieldable/portable capability

5.1 Introduction

In this section, based on the review results presented in Sections 3 and 4, the technological gaps between needs and capabilities of current portable/field-deployable UF_6 enrichment-assay instrumentation with overall analytical performance at a level comparable to laboratory-based mass spectrometry are analyzed and identified. Based on the identified technological gaps, an assessment of state-of-the-art (SOA) and commercial off-the-shelf (COTS) components that could be modified to expedite the development of a portable/field-deployable instrument is conducted.

From the review results presented in the last two sections, it is clear that for mass-spectrometric methods, the current focus is on the development of various in-field ionization sources. In almost all cases, the ionization sources under development are coupled to commercially available mass analyzers. For those methods operated on optical-spectroscopic principles, research efforts are focused on combining various approaches (e.g., atomic absorption, atomic emission and laser ablation) already in use in other analyses in a new way that has not yet been reported specifically for uranium/UF_6 enrichment assay. As in the case in mass-spectrometric methods, commercially available optical detectors are used in almost all cases. Before looking into COTS components, it is important to identify the key features of the systems that are important for isotopic assay.

5.2 Important key features of the systems that are important for isotopic assay

Important key features of an isotopic assay system include those common attributes like wide linear dynamic range, adequate spectral resolution, stable response, and negligible noise. A feature particularly important for isotopic assay is the capability to perform simultaneous measurements on the isotopes of interest, as already discussed in detail in Section 1.4. In an idealized situation, in which all other noise sources are eliminated, measurement precision should be governed only by counting statistics.

Furthermore, an ideal detector should not have any amplification of noise due to gain fluctuations. To elaborate, with only a few exceptions, most mass or optical spectrometric detectors include amplifications of the primary ions (for mass spectrometric) or photons (for optical) through electron multipliers. In the classical operation of an electron multiplier, high voltage is applied between a series of cathodes and an anode. Primary ions or photons refer to

those ions/photons that hit the first (starting) cathode. A series of cathodes (referred to as dynodes) are arranged in a fashion such that each one is biased at a slightly less negative potential (i.e., relatively more positive), with the first one at the most negative potential. The anode is typically held at ground potential and is where the signal is measured. The bombardment of primary ions/photons generates some secondary electrons, which are then accelerated to the next dynode and induce even more secondary electrons. This electron-multiplication process can be repeated a number of times, resulting in a large shower of electrons at the anode. The advantage of multiplication is that it multiplies incident charges or photons. The disadvantage is that the amplification process is not exactly reproducible but stochastic. As a result, the size of electron burst gathered at the anode from a single ion/photon varies, and hence increases the overall noise level of the measurement.

This electron multiplication noise, which is due to the statistical distribution of the number of secondary photoelectrons, is typically represented by the excess noise factor defined as

$$\sigma_{RSD,output} = F\sigma_{RSD,input} \tag{5.1}$$

where F is the excess noise factor, and $\sigma_{RSD,input}$ and $\sigma_{RSD,output}$ represent the noise levels, expressed in RSD, at the input and output terminals, respectively, of the multiplier. It should be noted that, because the amplification acts on each incoming ions/photons in a stochastic fashion, the amplification noise is not correlated and therefore cannot be reduced even when the two isotopic signals are simultaneously measured. In fact, precision in isotopic ratio is further degraded because ratioing involves addition of two uncorrelated noise sources. For an ideal detector designed for isotopic assay, F should be equal to 1.

One way to eliminate the amplification noise is to perform the measurement in ion-counting or photon-counting mode. In the counting mode, the signal is not the exact intensity of the ion/photon spikes, but is the occurrences of spikes above a preset threshold value. An alternative way to eliminate the amplification noise is to avoid using a stochastic amplifier. For example, the signals (ions or photons) can be integrated and the accumulated charges (ion charges or photoelectrons) are then measured. Multi-collector mass spectrometers with Faraday cup detectors and CCDs (charge coupled devices) are two examples that do not employ electron-multiplying amplifications and both have unity excess noise factor (i.e., the ideal case with $F = 1$).

Because of the prime importance of measurement precision in UF_6 enrichment assay, the search direction for COTS system components will focus on two criteria: (i) simultaneous, either truly or pseudo, measurements of the two uranium isotopes; and (ii) a unity excess noise factor.

5.3 Identification of SOA or COTS components for mass-spectrometric systems

Several surveys on portable and fieldable COTS mass spectrometers were independently produced by different research groups [31, 136-138] in the last four years. For example, an extensive market research survey of COTS mass spectrometers that are deemed pertinent to IAEA needs and strategic objectives was performed by PNNL, LANL and SRNL in 2013 [31]; the market survey was further updated in 2015 by LANL researchers [136]. In 2015, a review was published by the research groups of Ouyang and Cooks [137] at Purdue University, in which portable and fieldable mass-spectrometer systems from both academic and commercial sectors were emphasized. In 2016, a review on mass spectrometers based on micro-electro-mechanical systems (MEMS) technology was published [138]. In addition, a section of a 2015 report on fieldable mass spectrometers [3] was dedicated to survey and evaluate available, small MS instruments that might have the potential for in-field use for safeguards applications.

The conclusion of the market surveys indicated that available COTS MS instruments that were relatively small (<400 pounds), capable of atomic ion generation and isotope ratio analysis, were essentially limited to bench-top ICP-MS [31, 136]. Although bench-top in size, ICP-MS instruments are generally not ideal for fieldable applications due to their power and consumable (gaseous argon consumption) requirements. Because the two market surveys [31, 136] were already specifically targeted for IAEA needs and were recent, an extensive complete market survey is not performed in the present study. Instead, based on the literature review presented in Sections 3.5 and 4.3, the types of mass spectrometers that are considered to be exceptional for isotopic analysis were first identified. A market survey was then performed to identify the availability of that specific type of mass spectrometer in a COTS and fieldable format.

Not all types of mass analyzer can be miniaturized and be available in a fieldable version. The extensive review by the research group of Ouyang and Cooks [137] summarized the SOA and COTS miniaturized and fieldable mass spectrometers that are being developed or have been developed at universities or commercial sectors since 2009 (developments up to 2009 were covered in an earlier review [139]). The characteristics (types of mass analyzer, power requirement, system weight, mass range, mass resolution, capability to perform tandem MS/MS) of thirty-six mass spectrometers were tabulated; only those that are operated on principles of ion trap, quadrupole, time of flight, and sector field are available in a miniaturized fieldable version.

Literature reviews reveal that the most precise mass spectrometer for isotopic analysis is of multi-collector type, followed by flat focal plane ion-detector array. This is reasonable as both detectors offer the capability of truly simultaneous measurements and are without amplification noise (i.e., unity excess noise factor). The second tier of mass spectrometer for isotopic analysis belong to those that offer pseudo simultaneous measurements, such as the ion-trap mass spectrometer followed by the time-of-flight mass spectrometer. As discussed in detail in

Section 1.4, Meija and Mester [36] compared the correlation coefficients (ρ) between isotopes of three types of mass analyzers coupled to ICP, and found that the ρ values were 0.066, 0.276 and >0.999 for quadrupole, time-of-flight, and multi-collector ICP-mass spectrometers, respectively [36]. Clearly, the ρ value of time-of-flight significantly deviates from the $\rho = 1$ ideal case. For isotopic analysis, the quadrupole-based mass spectrometer is non-optimal due to its sequential scanning nature. Mass analyzers based on Fourier transform (e.g., the Orbitrap) offer superior mass resolution but are not available in a fieldable form, and therefore, are not further considered in this study.

Based on the above ranking, fieldable multi-collector and ion-detector array mass spectrometers should be the primary target of this study. It was found that an ion-detector array coupled to a Mattauch-Herzog geometry mass spectrometer, in a fieldable form, is commercially available. The array detector is offered by OI Analytical (Pelham, Alabama) and is termed IonCCD. The IonCCD operates in virtually the same fashion as common photo-sensitive CCDs, with the exception that the semiconductor oxide layer responsible for the electron hole-pair formation upon photon bombardment is replaced by a conductor electrode (TiN) for charge collection through ion neutralization upon impact [140]. The IonCCD comprises 2126 active pixels with a 24-μm pitch (pixel width of 21 μm and pixel-to-pixel gap of 3 μm) [140]. The reported linearity of the detector response was over three orders of magnitude and can be easily be extended to $10^{5–6}$ when using different integration times [140]. Other features of the IonCCD include: it acts as a charge counter, production of up to 360 mass spectra (frames) per second; and detection efficiency is virtually independent from the particle energy (250 eV, 1250 eV), impact angle (45°, 90°) and flux [140].

A field transportable mass spectrometer named IonCam, also offered by OI Analytical, couples the IonCCD detector to the focal plane of a miniaturized Mattauch-Herzog geometry mass spectrometer [137]. The mass spectrometer employs a 1 Tesla NdFeB permanent magnet, measures 25 cm × 42 cm × 43 cm, weighs 44 pounds, consumes an average of 50 W power, and can be battery operated [141]. Analytical performance of the IonCam spectrometer for uranium isotopic analysis was not published, but isotopic analyses on krypton and xenon were reported [141]. The data [141] showed spectral peaks from xenon isotopes 124 and 126 (both with natural abundances ~ 0.09%) can be readily distinguished from the baseline and other xenon isotopes present at much higher abundances. Furthermore, according to the review published in 2016 [137], the IonCam instrument is in the process of being updated. The IonCCD and IonCam are the only currently commercially available MS component (detector) or standalone mass spectrometer that utilizes ion-detector array technology.

5.4 Identification of SOA or COTS components for optical-spectrometric systems

For pulsed or weak emission-based (including fluorescence) optical measurements, a gated ICCD (intensified-CCD) optical detector is usually used. ICCDs are powerful, especially for their multichannel proficiency to register emission intensities simultaneously at an array of wavelengths, and its low-light amplification and gating capabilities. However, ICCDs also pose two drawbacks that are particularly important in isotopic analysis. First, it has been reported that when an ICCD is coupled to an optical spectrometer, the attainable spectral resolution is reduced by factors of 2 to 3 [142]. This resolution reduction is caused by the intensifier due to electron spreading to adjacent microchannels in the image intensifier tubes [143]. Because the magnitude of optical isotopic shift is minute (on the order of 10 pm), it is crucial to have the highest spectral resolution possible, and a 2-3× degradation by the ICCD is certainly detrimental for isotopic analysis. Second, the amplification noise is comparatively high for ICCDs; depending on the specific photocathode, the intensifier assembly and the operating conditions, the excess noise factor (F) of ICCDs typically range from 1.6 to 4.2 [144]. Because the amplification noise is uncorrelated, precision in isotope ratio is further degraded due to propagation of measurement uncertainties.

A relatively new class of optical detector, named EMCCD (electron multiplying CCD), amplifies the signal with an approach that does not use a standard image intensifier (the component which degrades the attainable resolution, as discussed above). Instead, a series of semiconductor structures, called a gain register, is inserted between the end of the shift register of the CCD and the readout circuitry. In this on-chip amplification approach, a charge is accelerated with sufficient energy to create another electron-hole pair through 'impact ionization' inside the semiconductor. The amplification process is still stochastic, but the noise factor is reduced to 1.4 [145] for a wide range of operating conditions. The reduced noise factor is a result of the EMCCD gain register, which behaves like an ideal staircase avalanche photodiode [145]. Noise factors in EMCCDs can be further eliminated by photon counting.

The most important feature for EMCCDs is that there is no spread of electrons during the amplification process, and thus, there is no excessive degradation in spectral resolution. Although EMCCDs cannot be gated, gating as short as nanosecond (key features of ICCD) is not necessary for a measurement; typical optical measurements are performed with integration times of hundreds of microseconds or longer. Most modern EMCCDs can be externally triggered and used with a pre-set exposure time, which suffices for most analytical applications.

The newest generation of EMCCD offers amplification factors high enough, and the data can be read fast enough, to allow photon counting [146, 147]. In photon counting mode, the exposure time is set to a very short interval to make sure that the probability of two photons falling onto any single detector pixel is negligibly small. Although most pixels on the detector receive no

photons, those that receive a single photon will generate a spike (after amplification) in the readout. With photon counting mode, precision is then limited only by counting statistics. Several EMCCDs, which offers photon counting capability, are commercially available. For example, the iXon EMCCD Camera Series (Models iXon Ultra 897 and 888) from Andor Technology Ltd. and ProEM Series from Princeton Instruments. The choice depends on other requirements, for example, the physical size and pixel dimensions of the detector.

To summarize, based on the key features that are important for isotopic assay systems, namely simultaneous measurements of the two uranium isotopes with a unity excess noise factor, we have identified two SOA and COTS components that could be modified to expedite the development of portable/field-deployable instruments. The IonCCD multichannel ion-detector array and a miniaturized Mattauch-Herzog transportable mass spectrometer named IonCam, both offered by OI Analytical (Pelham, Alabama) have the potential to become a key component in the next generation mass-spectrometric based portable/field-deployable instruments. For the next-generation optical-spectrometric instruments, EMCCDs with photon counting capability, commercially available from several vendors, are potential detectors and their analytical characteristics specifically for optical isotopic analysis of uranium should be thoughtfully investigated.

6. Recommendations of reliable technologies for the next-generation portable/field-deployable UF_6 enrichment-assay instrument

6.1 Methodology for ranking different analytical techniques

In this section, technologies for the next-generation portable/field-deployable UF_6 enrichment-assay instrument are recommended. In previous sections (cf. Tables 3.1 and 4.1), both established and emerging techniques were evaluated against a long list of performance metrics. Although all the considered metrics have their own significance, it is also obvious that the metrics are not equally important in assessing the potential of an analytical method.

In the present study, the ranking of different techniques are based on a simplified evaluation focused on two main areas – analytical performance and operation. The most essential features for the next-generation portable/field-deployable UF_6 enrichment-assay instrument are its abilities to deliver *accurate*, *precise* and *timely* *on-site* analyses. As such, recommendations are made based on seven assessment criteria: meeting predefined targets for analytical accuracy and precision (two separate criteria), meeting relaxed targets for accuracy and precision (two criteria), simultaneous ^{235}U and ^{238}U measurements, measurement time, and overall ease of operation and system complexity. Similar to Tables 3.1 and 4.1, there are three grades for each assessment metric – pass (color coded green), marginal (color coded yellow) and fail (color coded red). A total score is computed based on the evaluation – each passed, marginal and failed criterion carries 3, 1, and 0 points, respectively. Because analytical performance of some emerging techniques is not yet characterized, extrapolation and estimation based on known scientific principles are needed in these cases, and such assessments are noted with diagonal hatches in the assessment table. For those metrics that there is insufficient information even for a reliable estimation, a question mark is indicated in the table. Because no score for that metric can be assigned in this case, the denominator in the calculation of the percentage total score is adjusted accordingly.

The definitions of the seven assessment metrics are identical to those presented in Section 1.3, and are briefly summarized below. The first two metrics are analytical accuracy and precision. For analytical accuracy and precision, a "green" rating indicates meeting the stated criterion, a "yellow" rating represents not meeting the criterion but is within 3× the target (i.e., marginally fail), and a "red" rating denotes not meeting the criterion even if the target is relaxed by a factor of 3. The ITVs of TIMS and MC-ICP-MS [1] published by the IAEA are used as comparison references (cf. Table 1.1).

Because the IAEA ITVs are intended for more established techniques, to better gauge the potential of emerging techniques that are still under active development, an additional set of performance criteria is set by relaxing the target values by 10×. In case the emerging technique is so new that experimental data are not yet available specifically for uranium, projected or extrapolated values from very similar techniques sharing the same scientific principle are used. As the prime quality of a chemical analysis is accuracy and precision, it is justifiable to increase its weighing by setting two standards.

The metric "Simultaneous ^{235}U & ^{238}U measurements" summarizes if the ^{235}U and ^{238}U measurements are performed in truly simultaneous (green), quasi-simultaneous (yellow) or sequential (red) fashions. The metric "Measurement time" refers to typical measurement time for each sample. Techniques rated "green" typically require less than 10 minutes, those that need typically more than 10 minutes but less than one hour are rated "yellow", and those requiring more than one hour are rated "red".

The metric "Overall ease of operation" reflects the overall complexity of the measurement procedures and instrument hardware operation, and is based on several factors including: general robustness of the instrument and the technique, skills required (e.g., turn-key *versus* complicated systems), sample preparation procedures, and overall complexity of operating procedures. A green rating is awarded to robust simple system that can be easily mastered. A yellow rating refers to system that is comparatively more complex and more difficult to master. A red rating means that the system is overall complex and requires the operator to have more expertise.

It should also be noted that the evaluations are based solely on results that can be found in the open literature, for example: journal articles, conference proceedings, open reports, traceable presentations in scientific meetings or conferences, and IAEA or NNSA factsheets. Although we have included the latest open literature results to the best of our knowledge, because active research is still on-going on many emerging techniques, the most updated performance of a technique could be better than what was published in the open literature.

6.2 Recommendations

6.2.1 Overviews

Table 6.1 summarizes the performance of the benchmark laboratory-based techniques (GSMS, TIMS, and MC-ICP-MS), the benchmark field technique (COMPUCEA), and all candidate existing and emerging techniques covered in the present study for in-field UF_6 enrichment assay. The column on "Field deployability of technique" refers to the overall ease and feasibility to

develop a field-deployable instrument for that particular analytical technique, and does not necessarily agree with the field-deployability associated with the current version of the instrument as described in the literature. For instance, the LS-APGD-MS and AP-SCGD-MS technologies, reported thus far, utilized an Orbitrap mass spectrometer, which is considered as not field deployable. However, if a field-deployable mass spectrometer is coupled to the LS-APGD or the AP-SCGD ionization source, the techniques will then become field deployable. Thus, the boxes for "Field deployability of technique" are checked for both LS-APGD-MS and AP-SCGD-MS, because it is practically feasible to transform both techniques to fieldable versions. Because of this ambiguity, field deployability is listed for reference only and does not count towards the total score for ranking. In contrast, if it is already known that a candidate technique (e.g., ICP based techniques) is practically infeasible to be operated in-field due to the required infrastructure (e.g., ventilation) or consumables (e.g., argon gas), the technique will not be recommended even if its score is high. In other words, a prerequisite for a technique to be recommended as the next generation field-deployable instrument for UF_6 enrichment assay is that the box on "Field deployability of technique" must be checked.

All reviewed techniques are classified into one of the three categories – recommended, promising and not recommended. Loosely speaking, the classification also ties to the years of further development to implement the technology for in-field UF_6 enrichment assay. For a recommended technique, it is projected that in-field use could be realized within a development time of 5 years. For a promising technique, the estimated development time is roughly between 5 to 10 years. For a not-recommended technique, either the estimated development time is more than 10 years or it is not likely that the technique could offer in-field analysis capability close to the targeted analytical accuracy or precision. It should be stressed that each technique is evaluated solely for its suitability to provide on-site enrichment assay specifically for UF_6. Accordingly, a technique not recommended for on-site measurement of UF_6 samples should not be viewed negative as a whole because it is possible that the candidate technique could be promising for other applications (e.g., for other types of U samples, as an in-laboratory analytical method, or its ability to perform quick screening measurement that does not require the stated high accuracy or precision).

In short, a total of five techniques are recommended – two belong to mass spectrometric and three operate with optical spectrometric principles. The five recommended techniques are: liquid sampling-atmospheric pressure glow discharge-mass spectrometry (LS-APGD-MS) and its variant atmospheric pressure-solution cathode glow discharge-mass spectrometry (AP-SCGD-MS); laser ablation-diode laser-atomic absorption spectrometry (LA-DL-AAS) and its variant laser ablation absorbance ratio spectrometry (LAARS); and laser induced spectrochemical assay for uranium enrichment (LISA-UE). These recommended and other (benchmark, promising, and not recommended) techniques will be briefly summarized and compared in the following paragraphs and subsequent sub-sections.

All three MS-based benchmark techniques (GSMS, TIMS and MC-ICP-MS) offer outstanding analytical performance but demanding operation in terms of measurement time as well as expertise in instrument operation. Miniaturized GSMS for improved field deployability has already been developed by ORNL, which will be separately discussed under the technique coined "molecular MS with fieldable mass spectrometer". The other benchmark technique, COMPUCEA, is a transportable analytical system for on-site uranium concentration and enrichments assays [6]. Its application specifically for UF_6 enrichment assay is still under development by the IAEA [7], although its use on LEU-oxide samples is considered routine. The analytical performance is impressive for an on-site measurement. The drawback of the method is the relatively long counting time, especially for natural uranium (3×5000 s) [69] and depleted uranium, and its labor intensive sample preparation process.

6.2.2 Recommendations for mass spectrometric techniques

For mass spectrometric methods, the recommended techniques are LS-APGD-MS and its variant AP-SCGD-MS. Currently, the LS-APGD-MS [16-18] is the most well characterized emerging mass-spectrometric technique, especially for the determination of uranium isotopic ratios. The reported analytical precision is encouraging, and is, so far, the best in all the emerging techniques reviewed. In the most recent published work [131], the reported precisions (in terms of RSD of measured $^{235}U/^{238}U$ ratios from 1 μg/mL natural-U solutions, before correction of scaling factor) were in the range of 0.05% to 0.13% and met the ITV target (i.e., 0.2% RSD for ^{235}U at natural abundance) for precision. A similar technique, also based on microplasma as an ionization source, is the AP-SCGD-MS. Although not yet characterized for its performance on isotopic analysis, the AP-SCGD demonstrated a significantly better detection limit than the LS-APGD as an ionization source for atomic mass spectrometry [19]. As detection limit is related directly to sensitivity and/or background noise, the significantly better (lower) detection limit for the AP-SCGD implies that it offers higher sensitivity and/or lower background noise than the LS-APGD. As both factors are important for isotopic ratio measurements, and consider the fact that both AP-SCGD and LS-APGD share the same scientific principle, the AP-SCGD is thus recommended to be further developed and evaluated for its full potential for uranium isotopic assay, along with LS-APGD.

Three other MS-techniques are listed as promising: atmospheric pressure-surface enhanced laser desorption and ionization (AP-SELDI), molecular MS with fieldable mass spectrometer, and laser ablation ionization (LAI)-MS. AP-SELDI and LAI-MS are rather new techniques and very little of their analytical performance has been presented in open literature. The best precision reported for AP-SELDI was 0.54% for a U-sample with 3.13% ^{235}U (with colloidal graphite as substrate) [122], although poorer precision (e.g., 5.31%) also was reported depending on the experimental conditions and substrate [122]. The SELDI technique is not entirely new [126,

127], but earlier measurements were performed in vacuum whereas the latest development is to place the samples in front of the inlet of the MS-sampler in ambient environment under atmospheric pressure [122]. The molecular fieldable MS can be viewed as a miniaturized version of GSMS in principle. According to the latest report published in February 2017 [94], although precision as good as 1% RSD or below were reported for some measurements, typical routine measurement precision likely lies in the neighborhood at or above 1%. The reported precisions are notably lower than those reported for LS-APGD-MS. A field-deployable system with sampling manifold was already developed [94], which greatly facilities ease of operation. For LAI-MS, its analytical capabilities specifically for U enrichment assay are not yet disclosed. However, it was reported that the identities of the dominant ion changed quite dramatically with the laser power. For instance, the dominant ions in LAI-MS were $UO_2F_2^+$ and its water adduct $UO_2F(H_2O)^+$ at laser pulse energy of 15 mJ, but switched to UO_2^+ when the pulse energy was nominally increased to 17 mJ [95]. The assessment in Table 6.1 is based on extrapolation from other LAI-MS work [120, 121] reported for isotopes of other elements. Furthermore, it should be stressed that LS-APGD-MS, SELDI and LAI-MS are undergoing an NA-24-funded test campaign; more information on their analytical performance is expected to be available from the campaign. As such, their rankings and classifications could change.

The two not recommended mass-spectrometric techniques are ICP-Array (Mattauch-Herzog)-MS and multi-photon ionization TOF-MS. Although the analytical performance of ICP-Array (Mattauch-Herzog)-MS ranks high on the list, it is not recommended because the ICP ionization source is unlikely to be field deployable in the foreseeable future due to its power and argon consumption (roughly at a rate of 15 L/min) requirements. The multi-photon ionization TOF-MS technique directly analyzes gaseous UF_6 after dilution with a buffer gas (e.g., Ar) through photolysis of UF_6 molecule and subsequent ionization with a pulsed laser. The first report was published in 1996 but quantitative details on accuracy and precision for UF_6 enrichment assay are not yet available.

6.2.3 Recommendations for optical spectrometric techniques

From a total of nine reviewed optical spectrometric methods, three are recommended, two are listed as promising and the remaining four are not recommended. The recommended ones are LAARS, LA-DL-AAS, and LISA-UE. The working principles of these three techniques are all based on the isotopic shifts in atomic transitions between ^{235}U and ^{238}U atoms. LAARS and LA-DL-AAS are identical in scientific principle and are very similar in experimental setup, and both offers simultaneous measurements of the relative abundances of ^{235}U and ^{238}U [25]. Briefly, laser ablation creates free uranium atoms from a solid sample, and these atoms are then probed by two diode lasers through atomic absorption. Measurements are conducted in a reduced-pressure environment to reduce spectral-line broadening. Measurement precision

of 1.1% RSD for a pure uranium-oxide sample with ^{235}U at natural abundance was reported for LA-DL-AAS [98]. A tailored solid thin-film sorbent to convert gaseous UF_6 to uranyl fluoride through a hydrolysis reaction is used in LAARS [51]. The latest LAARS results [50, 102] demonstrated precisions within 3× to 6× and accuracies within a factor of 2 from the target as a replacement for laboratory-based mass spectrometry for natural-U and LEU samples.

LISA-UE is in a very early stage of development, but its working principle is based on an extension of the well-known laser induced breakdown spectroscopy technique to low-pressure gaseous UF_6 samples. LISA-UE utilizes only one laser (non-resonant) in its setup and uses atomic emission as the measurement means. The LISA-UE system is targeted for direct analysis of gaseous UF_6 samples (in both online and offline fashions), although a solid sample (e.g., UF_6 absorbed on a solid substrate) also can be used. As a new method, its analytical capabilities are not yet characterized. However, it is anticipated that emission measurements on a collection of spectral features offers advantage over single line-pairs commonly employed in absorption measurements. For example, it has been shown through computer simulation that the use of a chemometric algorithm from a collection of spectral features provides several times improvement in the precision of ^{235}U abundance compared to those measurements utilizing only a single pair of emission lines [110]. In simulation, the ultimate precision was about 0.11% in absolute ^{235}U abundance for multiple line analysis [110], with signals accumulated from 10 laser pulses. Further improvement in precision can be achieved through more signal accumulation (i.e., accumulating signal from more than 10 laser pulses), although it is also anticipated that computer simulation probably offers the best-case scenario. While it is extremely early in the development cycle, the LISA-UE instrumentation set up – with a single laser excitation source and a single set of light-collection optics – is likely to be the simplest among all the techniques discussed above, which is advantageous as an in-field instrument.

The two promising optical spectrometric methods are tunable laser IR absorption and its upgraded version termed high performance infrared (HPIR) spectrometry. Both techniques directly probe UF_6 molecules with wavelength-tunable IR lasers. The measurements are non-invasive in the sense that the UF_6 molecules remain intact and are not dissociated or destroyed after the measurement. Moreover, the techniques can be easily coupled to a processing pipe and applicable for both online and offline measurements. The shortcomings are its sequential measurement nature and the measurement uncertainties. One source of the uncertainty is the strongly blended rotational-vibrational spectral features of UF_6 infrared absorption spanning several cm^{-1}, whereas the isotopic shift between $^{235}UF_6$ and $^{238}UF_6$ is only ~ 0.6 cm^{-1} [76].

The four not recommended optical techniques are inductively coupled plasma-atomic emission spectrometry (ICP-AES), laser ablation-diode laser-atomic fluorescence spectrometry (LA-DL-AFS), atomic beam tunable diode laser absorption, and glow discharge optogalvanic spectroscopy (GD-OGS). Because of the power and consumable requirements for operation of

the ICP, even though the overall performance of ICP-AES is outstanding and scores high on the list, it cannot be recommended as an in-field instrument. The remaining three techniques – LA-DL-AFS, atomic beam tunable diode laser absorption, and GD-OGS – are ranked low in the list for this specific application because their analytical accuracy and precision are on the short side compared to other evaluated techniques, their measurement mode being sequential, and overall ease of operation is at best marginal.

The atomic beam tunable diode laser absorption technique is worthy of some additional comments. This atomic beam method offers a unique feature that is superior to other reviewed optical techniques, namely its immunity to spectral interference from other co-existing elements present in the sample. Spectral interference refers to atomic lines from other elements that absorb at the exact wavelengths, and hence produce atomic absorption signals, as the U isotopes. Among other factors, the likelihood of spectral interference depends on the overlaps between the laser wavelength and the line width of the interfering spectral line from other elements. As the bandwidth of the laser is very narrow, the likelihood is already relatively low. This narrow laser bandwidth advantage also applies to other laser-spectrometric techniques (e.g., LAARS), but line widths of the atomic lines are generally narrower in this atomic beam than in other atom reservoirs (e.g., the laser plume for LAARS), due to the directional expansion of the atomic beam. Therefore, the likelihood of spectral interference is further reduced for this atomic beam method than in LAARS. The immunity to spectral interference from other elements is very important for the analysis of complex samples (e.g., soil, spent nuclear fuel), in which lots of different elements could be present. However, specific for UF_6 enrichment assay, the sample is likely to be in a very pure form. Therefore, spectral interference from other elements is not likely a problem to be encountered in UF_6 enrichment assay with atomic absorption; and thus, this unique feature of the atomic beam becomes inconsequential for this particular application. Clearly, the fieldable atomic beam laser spectrometer is a valuable and promising tool for other applications, but its current version is on the short side compared to other evaluated techniques specifically for UF_6 enrichment assay. One possible reason for its comparatively low precision is the fact that the current version of the technique utilizes only one diode laser. Thus, its measurement mode is sequential in nature and any fluctuations in the number density of the atomic beam during the wavelength scanning of the laser degrade isotopic precision. If precision is limited by fluctuation in the number density of the atomic beam, a dual laser-beam approach (i.e., one laser for ^{235}U and one for ^{238}U, as already demonstrated in LAARS) would be a solution to greatly minimize this noise and provide improvements.

6.3 Conclusion and Outlook

To summarize, a comprehensive and in-depth review was conducted on existing state-of-the-art and emerging technologies for field enrichment analysis of UF_6. All technologies that we were

aware of (through literature research and word of mouth from funding agencies) were included in this study. However, there is always a possibility that other technologies are being developed and may be superior to those included here. All techniques were assessed for their potential to serve as an alternative for laboratory-based mass spectrometry. The LS-APGD-MS is currently the most promising, in terms of published analytical capabilities, in all the emerging techniques reviewed. A similar technique, AP-SCGD-MS, also shows its potential through offering better detection limits. Unlike the ICP, these glow-discharge ion sources use microplasmas which allow operation under low power and low gas flow (if a plasma gas is ever needed) — and, thus, are highly field deployable. Given the impressive isotopic-ratio precisions and detection limits achievable by the two techniques, one might think that the problem of looking for the next generation of field-deployable instrument for UF_6 enrichment assay is already solved. However, both technologies to date have employed an Orbitrap mass spectrometer, which is considered inappropriate as an in-field mass spectrometer due to its demanding requirements for environmental conditions (e.g., temperature, humidity and vibration controls) [132]. Thus, the current technical challenge is to identify and couple these microplasma ionization sources to field-deployable mass spectrometers that can maintain the analytical figures of merit offered by the Orbitrap MS.

Some emerging techniques based on optical spectrometric techniques are also promising. For instance, LAARS shows its promise with a relative bias of 0.1% for LEU (5.119% ^{235}U) and 0.3% for NU samples, and relative precisions around 0.6% for both LEU and NU samples. LISA-UE is a new development and is based on well-established atomic emissions (LIBS). These emerging mass- and optical-spectrometric technologies show potentials to serve as alternatives for off-site MS techniques and be developed into the next-generation instrument for in-field UF_6 enrichment assay.

Finally, it is appropriate to stress again that this work is based on analytical performance as presented in the open literature, and active research is on-going with many of these emerging techniques. For instance, a test campaign is currently planned for LS-APGD-MS, AP-SELDI and LAI-MS. Thus, the ranking of the different analytical techniques presented here could change.

Table 6.1 **Recommendation summaries of existing and emerging techniques for in-field UF_6 enrichment assay. Color codes red, yellow and green indicate "pass", "marginal" and "fail", respectively. Box with diagonal hatch indicates estimation from scientific principle. A question mark indicates that information either is not yet available or is insufficient for estimation.**

		Analytical Performance					Operation				
		Accuracy meets target	Precision meets target	Accuracy within 10× target	Precision within 10× target	Simultaneous ^{235}U & ^{238}U measurements	Measurement time	Overall ease of operation	Total Score	Field deployability of technique	Remark
Comparison Benchmark	Gas source mass spectrometry	3	3	3	3	3	0	0	**15**/21 (71%)		Benchmark reference
	Thermal ionization mass spectrometry	3	3	3	3	3	0	0	**15**/21 (71%)		Benchmark reference
	MC-ICP-MS	3	3	3	3	3	1	0	**16**/21 (76%)		Benchmark reference
	COMPUCEA	1	1	3	3	3*	0	0	**11**/21 (52%)	✓	Benchmark reference
Mass Spectrometric Methods	ICP-Array (Mattauch-Herzog)-MS	3	3	3	3	3	1	1	**17**/21 (81%)		**Not recommended**
	LS-APGD-MS (currently w/ Orbitrap MS)	?	3	?	3	3	3	1	**13**/15 (87%)	✓	**Recommended**
	AP-SCGD-MS (currently w/ Orbitrap MS)	?	3	?	3	3	3	1	**13**/15 (87%)	✓	**Recommended**
	AP-SELDI (currently w/ Orbitrap MS)	?	0	?	3	3	3	1	**10**/15 (67%)	✓	**Promising**
	Molecular MS w/ fieldable mass spectrometer	0	0	1	1	1	3	3	**9**/21 (43%)	✓	**Promising**
	Laser ablation ionization (LAI)-MS	0	0	1	1	1	3	1	**7**/21 (33%)	✓	**Promising**
	Multi-photon ionization TOF-MS	0	0	0	0	1	3	1	**5**/21 (24%)	✓	**Not recommended**
Optical Spectrometric Methods	Atomic emission with ICP	0	0	3	3	3	3	3	**15**/21 (71%)		**Not recommended**
	LAARS	1	1	3	3	3	3	1	**15**/21 (71%)	✓	**Recommended**
	Laser ablation – diode laser AAS	0	0	1	3	3	3	1	**11**/21 (52%)	✓	**Recommended**
	LISA-UE	0	0	?	1	3	3	3	**10**/18 (56%)	✓	**Recommended**
	Tunable laser IR absorption	0	0	0	0	0	3	3	**6**/21 (29%)	✓	**Promising**
	HPIR spectroscopy	0	0	0	0	0	3	3	**6**/21 (29%)	✓	**Promising**
	Laser ablation – diode laser AFS	0	0	1	0	0	3	1	**5**/21 (24%)	✓	**Not recommended**
	Atomic beam tunable diode laser absorption	0	0	0	0	0	3	1	**4**/21 (19%)	✓	**Not recommended**
	GD optogalvanic spectroscopy	0	0	0	1	0	3	0	**4**/21 (19%)	✓	**Not recommended**

*Signal correlation for measurement-noise reduction through simultaneous ^{235}U and ^{238}U measurement does not apply in COMPUCEA because the isotopic assay is performed through radiometric counting (gamma ray), in which the dominated noise source is counting statistics.

References

1. International Atomic Energy Agency, International target values 2010 for measurement uncertainties in safeguarding nuclear materials, STR-368, International Atomic Energy Agency (IAEA), (2010).
2. N. Anheier, B. Cannon, A. Martinez, C. Barrett, M. Taubman, K. Anderson, L.E. Smith, A new approach to enrichment plant UF_6 destructive assay sample collection and analysis, PNNL-SA-112353, Pacific Northwest National Laboratory, (2015).
3. C.J. Barinaga, G.J. Hager, E.D. Hoegg, A.J. Carman, G.L. Hart, Feasibility of a fieldable mass spectrometer FY 2015 year-end report, PNNL-24842, Pacific Northwest National Laboratory, (2015).
4. L.E. Smith, A.R. Lebrun, Design, modeling and viability analysis of an online uranium enrichment monitor, in 2011 IEEE Nuclear Science Symposium Conference Record, (2011), 1030-1037.
5. N. Erdmann, P. Amador, P. Arboré, H. Eberle, K. Lutzenkirchen, H. Ottmar, H. Schorlé, P. van Belle, F. Lipcsei, P. Schwalbach, COMPUCEA: A high performance analysis procedure for timely on-site uranium accountancy verification in leu fuel fabrication plants, ESARDA Bulletin 43 (2009) 30-39.
6. A. Berlizov, A. Schachinger, K. Roetsch, N. Erdmann, H. Schorlé, M. Vargas, J. Zsigrai, A. Kulko, M. Keselica, F. Caillou, V. Unsal, A. Walczak-Typke, Feedback from operational experience of on-site deployment of bias defect analysis with COMPUCEA, J. Radioanal. Nucl. Chem. 307 (2016) 1901-1909.
7. International Atomic Energy Agency, Development and implementation support programme for nuclear verification 2016-2017, STR-382, International Atomic Energy Agency (IAEA), (2016).
8. G.M. Hieftje, The future of plasma spectrochemical instrumentation. Plenary lecture, J. Anal. At. Spectrom. 11 (1996) 613-621.
9. S. Mialle, S. Richter, C. Hennessy, J. Truyens, U. Jacobsson, Y. Aregbe, Certification of uranium hexafluoride reference materials for isotopic composition, J. Radioanal. Nucl. Chem. 305 (2015) 255-266.
10. S. Boulyga, S. Konegger-Kappel, S. Richter, L. Sangely, Mass spectrometric analysis for nuclear safeguards, J. Anal. At. Spectrom. 30 (2015) 1469-1489.
11. D. Ardelt, A. Polatajko, O. Primm, M. Reijnen, Isotope ratio measurements with a fully simultaneous Mattauch-Herzog ICP-MS, Anal. Bioanal. Chem. 405 (2013) 2987-2994.
12. Y. Okada, S. Kato, S. Satooka, K. Takeuchi, Measurements of U-235/U-238 isotopic ratio in the photoproduct UF_5 by multiphoton ionization and time-of-flight mass spectrometry, Appl. Phys. B 62 (1996) 515-519.
13. D.P. Armstrong, D.A. Harkins, R.N. Compton, D. Ding, Multiphoton ionization of uranium hexafluoride, J. Chem. Phys. 100 (1994) 28-43.
14. W.B. Whitten, P.T.A. Reilly, G. Verbeck, J.M. Ramsey, Mass spectrometry of UF_6 in a micro ion trap, in 7th International Conference on Facility Operations: Safeguards Interface, Charleston, SC, (2004), 345-349.
15. NNSA Office of Nonproliferation and Arm Control, Safeguards technology factsheet - portable mass spectrometry working group (MSWG), (2016).
16. E.D. Hoegg, C.J. Barinaga, G.J. Hager, G.L. Hart, D.W. Koppenaal, R.K. Marcus, Preliminary figures of merit for isotope ratio measurements: The liquid sampling-atmospheric pressure glow discharge microplasma ionization source coupled to an Orbitrap mass analyzer, J. Am. Soc. Mass Spectrom. 27 (2016) 1393-1403.
17. E.D. Hoegg, C.J. Barinaga, G.J. Hager, G.L. Hart, D.W. Koppenaal, R.K. Marcus, Isotope ratio characteristics and sensitivity for uranium determinations using a liquid sampling-atmospheric pressure glow discharge ion source coupled to an Orbitrap mass analyzer, J. Anal. At. Spectrom. 31 (2016) 2355-2362.

18. C.J. Barinaga, G.J. Hager, G.L. Hart, D.W. Koppenaal, R.K. Marcus, S.M. Jones, B.T. Manard, Toward a fieldable atomic mass spectrometer for safeguards applications: Sample preparation and ionization, in 12th Symposium on International Safeguards: Linking Strategy, Implementation and People (IAEA-CN-220), Vienna, Austria, (2014), S08-08.
19. A.J. Schwartz, K.L. Williams, G.M. Hieftje, J.T. Shelley, Atmospheric-pressure solution-cathode glow discharge: A versatile ion source for atomic and molecular mass spectrometry, Anal. Chim. Acta 950 (2017) 119-128.
20. M. Krachler, P. Carbol, Validation of isotopic analysis of depleted, natural and enriched uranium using high resolution ICP-OES, J. Anal. At. Spectrom. 26 (2011) 293-299.
21. M. Krachler, D.H. Wegen, Promises and pitfalls in the reliable determination of U-233 using high resolution ICP-OES, J. Anal. At. Spectrom. 27 (2012) 335-339.
22. D. Zamzow, G.M. Murray, A.P. Dsilva, M.C. Edelson, High-resolution optical-emission spectroscopy of uranium hexafluoride in the argon afterglow discharge, Appl. Spectrosc. 45 (1991) 1318-1321.
23. C.M. Barshick, R.W. Shaw, J.P. Young, J.M. Ramsey, Evaluation of the precision and accuracy of a uranium isotopic analysis using glow-discharge optogalvanic spectroscopy, Anal. Chem. 67 (1995) 3814-3818.
24. B.W. Smith, A. Quentmeier, M. Bolshov, K. Niemax, Measurement of uranium isotope ratios in solid samples using laser ablation and diode laser-excited atomic fluorescence spectrometry, Spectrochim. Acta Part B 54 (1999) 943-958.
25. B.D. Boyer, N. Anheier, P. Cable-Dunlop, L. Sexton, Incorporation of new, automated environmental sampling systems into safeguards approaches, LA-UR-13-28412, Los Alamos National Laboratory, (2013).
26. B.A. Bushaw, N.C. Anheier Jr, Isotope ratio analysis on micron-sized particles in complex matrices by laser ablation-absorption ratio spectrometry, Spectrochim. Acta Part B 64 (2009) 1259-1265.
27. NNSA Safeguards Technology Factsheet, Fieldable atomic beam laser spectrometer for isotopic analysis, LA-UR-16-20890, (2016).
28. A.G. Berezin, S.L. Malyugin, A.I. Nadezhdinskii, D.Y. Namestnikov, Y.Y. Ponurovskii, D.B. Stavrovskii, Y.P. Shapovalov, I.E. Vyazov, V.Y. Zaslavskii, Y.G. Selivanov, N.M. Gorshunov, G.Y. Grigoriev, S.S. Nabiev, UF_6 enrichment measurements using TDLS techniques, Spectrochim. Acta Part A 66 (2007) 796-802.
29. G.Y. Grigor'ev, A.S. Lebedeva, S.L. Malyugin, S.S. Nabiev, A.I. Nadezhdinskii, Y.Y. Ponurovskii, Investigation of $^{235}UF_6$ and $^{238}UF_6$ spectra in the mid-IR range, Atomic Energy 104 (2008) 398-403.
30. NNSA Fact Sheet, Spectroscopic methods for ultra-low isotopic analysis of proliferant material, SRNL-STI-2016-00217, (2016).
31. G.L. Hart, C.J. Barinaga, G.J. Hager, D.C. Duckworth, Market research survey of commercial off-the-shelf (COTS) portable MS systems for IAEA safeguards applications, PNNL-22237, Pacific Northwest National Laboratory, (2013).
32. NNSA Office of Nonproliferation and International Security (NIS), Implementing safeguards-by-design at natural uranium conversion plants, NGSI-SBD-002, (2012).
33. G.M. Hieftje, Signal-to-noise enhancement through instrumental techniques. 1. Signals, noise, and S/N enhancement in the frequency domain, Anal. Chem. 44 (1972) 81A-88A.
34. E.P.P.A. Derks, B.A. Pauly, J. Jonkers, E.A.H. Timmermans, L.M.C. Buydens, Adaptive noise cancellation on inductively coupled plasma spectroscopy, Chemometrics and Intelligent Laboratory Systems 39 (1997) 143-159.
35. G.M. Hieftje, Emergence and impact of alternative sources and mass analyzers in plasma source mass spectrometry, J. Anal. At. Spectrom. 23 (2008) 661-672.
36. J. Meija, Z. Mester, Signal correlation in isotope ratio measurements with mass spectrometry: Effects on uncertainty propagation, Spectrochim. Acta Part B 62 (2007) 1278-1284.

37. M. Grotti, J.L. Todoli, J.M. Mermet, Influence of the operating parameters and of the sample introduction system on time correlation of line intensities using an axially viewed CCD-based ICP-AES system, Spectrochim. Acta Part B 65 (2010) 137-146.
38. J.M. Mermet, Potential of time correlation to improve limits of detection in inductively coupled plasma-atomic emission spectrometry, Can. J. Anal. Sci. Spectros. 49 (2004) 414-422.
39. G.D. Schilling, S.J. Ray, R.P. Sperline, M.B. Denton, C.J. Barinaga, D.W. Koppenaal, G.M. Hieftje, Optimization of Ag isotope-ratio precision with a 128-channel array detector coupled to a Mattauch-Herzog mass spectrograph, J. Anal. At. Spectrom. 25 (2010) 322-327.
40. I. Peka, Kinetics of reaction between sodium fluoride and uranium hexafluoride, Collect. Czech. Chem. Commun. 30 (1965) 217-222.
41. A. Esteban, O. Cristallini, J.A. Perrotta, UF_6 sampling method using alumina, in 49th INMM Annual Meeting, Nashville, TN, USA, (2008), 1-9.
42. G. Vanschalkwyk, P.J. Hendra, Hydrolysis of uranium hexafluoride over alumina catalysts, J. Inorg. Nucl. Chem. 39 (1977) 894-895.
43. J. Binenboym, H. Selig, S. Sarig, Intercalation of uranium hexafluoride into A graphite lattice, J. Inorg. Nucl. Chem. 38 (1976) 2313-2314.
44. M. Afsari, J. Safdari, J. Towfighi, M.H. Mallah, The adsorption characteristics of uranium hexafluoride onto activated carbon in vacuum conditions, Annals of Nuclear Energy 46 (2012) 144-151.
45. R.M. Schultz, W.E. Hobbs, J.L. Norton, M.J. Stephenson, Sorbent selection and design considerations for uranium trapping, K/ET-5025, Oak Ridge Gaseous Diffusion Plant, Union Carbide Corporation, (1981).
46. S.H. Smiley, D.C. Brater, C.C. Littlefield, J.H. Pashley, Quantitative recovery of uranium hexafluoride from a process gas stream, Industrial and Engineering Chemistry 51 (1959) 191-196.
47. F.E. Massoth, W.E. Hensel, Kinetics of the reaction between sodium fluoride and uranium hexafluoride .1. Sodium fluoride powder, J. Phys. Chem. 62 (1958) 479-481.
48. S. Richter, J. Hiess, U. Jacobsson, Validation of Cristallini sampling method for UF_6 by high precision double-spike measurements EUR 28211 EN, EU Joint Research Centre, (2016).
49. C.A. Barrett, A. Martinez, B.K. McNamara, B.D. Cannon, N.C. Anheier Jr, Adsorptive films in support of in-field UF_6 destructive assay sample collection and analysis, in 55th Annual Meeting of the Institute of Nuclear Materials Management (INMM 2014), Atlanta, Georgia, USA, (2014), pp. 3303-3312.
50. C.A. Barrett, B.D. Cannon, A. Martinez, C.S. Chen, R. Guerrero, N.C. Anheier Jr, Destructive assay safeguards technology for sample collection and assay (presentation), in STM Workshop on Analytical Developments, Reference Materials, and Statistical Applications in the Nuclear Fuel Cycle, Vienna, Austria (2016), PNNL-SA-118821.
51. N. Anheier, B. Cannon, A. Martinez, C. Barrett, M. Taubman, K. Anderson, L.E. Smith, A laser-based method for onsite analysis of UF_6 at enrichment plant, PNNL-SA-105776, Pacific Northwest National Laboratory, (2014).
52. NNSA Safeguards Technology Factsheet, UF_6 single use destructive assay (SUDA) sampler, PNNL-SA-116597, NNSA, (2016).
53. W.H. King, Isotopic shifts in atomic spectra, 1st ed., Plenum Press, New York (1984).
54. I.V. Hertel, C.-P. Schulz, Hyperfine structure, in Atoms, molecules and optical physics 1: Atoms and spectroscopy, 1st. ed., Springer Berlin Heidelberg, Berlin, Heidelberg (2015) pp. 447-493.
55. T. Walczyk, Iron isotope ratio measurements by negative thermal ionisation mass spectrometry using FeF_4^- molecular ions, Int. J. Mass Spectrom. Ion Processes 161 (1997) 217-227.
56. D. Willingham, M.R. Savina, K.B. Knight, M.J. Pellin, I.D. Hutcheon, RIMS analysis of ion induced fragmentation of molecules sputtered from an enriched U_3O_8 matrix, J. Radioanal. Nucl. Chem. 296 (2013) 407-412.
57. R.B. Walton, T.D. Reilly, J.L. Parker, J.H. Menzel, E.D. Marshall, L.W. Fields, Measurements of UF_6 cylinders with portable instruments, Nucl. Technol. 21 (1974) 133-148.

58. J.W. Rowson, S.A. Hontzeas, Uranium isotopic ratio determination by gamma-ray spectroscopy, Nucl. Instr. and Meth. 154 (1978) 541-548.
59. R.B. Strittmatter, A gas-phase UF_6 enrichment monitor, Nucl. Technol. 59 (1982) 355-362.
60. R. Berndt, E. Franke, P. Mortreau, ^{235}U enrichment or UF_6 mass determination on UF_6 cylinders with non-destructive analysis methods, Nucl. Instr. Meth. Phys. Res. A 612 (2010) 309-319.
61. S. El-Mongy, K.A. Allam, O. Farid, Non-destructive assay and computational model for enrichment verification of UF_6 cylinders, Radiat. Meas. 43 (2008) 62-65.
62. K.A. Miller, M.T. Swinhoe, S. Croft, T. Tamura, S. Aiuchi, A. Kawai, T. Iwamoto, Measured F(α, n) yield from ^{234}U in uranium hexafluoride, Nucl. Sci. Eng. 176 (2014) 98-105.
63. W. Mengesha, S.D. Kiff, Neutron spectrometry for UF_6 enrichment verification in storage cylinders, IEEE Trans. Nucl. Sci. 62 (2015) 272-280.
64. L.E. Smith, E.K. Mace, A.C. Misner, M.W. Shaver, Signatures and methods for the automated nondestructive assay of UF_6 cylinders at uranium enrichment plants, IEEE Trans. Nucl. Sci. 57 (2010) 2247-2253.
65. K.A. Miller, H.O. Menlove, M.T. Swinhoe, J.B. Marlow, Monte Carlo feasibility study of an active neutron assay technique for full-volume UF_6 cylinder assay using a correlated interrogation source, Nucl. Instr. Meth. Phys. Res. A 703 (2013) 152-157.
66. S. Kiff, M. Gerling, P. Marleau, S. Mrowka, M. Streicher, Experimental measurement of uranium hexafluoride enrichment using fast neutron spectroscopy, Trans. Am. Nucl. Soc. 109 (2013) 1013-1016.
67. H.A. Smith Jr., The measurement of uranium enrichment, in D. Reilly, N. Ensslin, H. Smith Jr., S. Kreiner (eds), Passive nondestructive assay of nuclear materials (NUREG/CR-5550), 1st. ed., Los Alamos National Laboratory, Los Alamos, NM, USA (1991) pp. 195-219.
68. T.D. Reilly, E.R. Martin, J.L. Parker, L.G. Speir, R.B. Walton, Continuous in-line monitor for UF_6 enrichment, Nucl. Technol. 23 (1974) 318-327.
69. N. Erdmann, N. Albert, P. Amador, P. Arboré, H. Eberle, K. Lutzenkirchen, H. Ottmar, H. Schorlé, P. van Belle, F. Lipcsei, P. Schwalbach, S. Jung, R. Lafolie, COMPUCEA 2nd generation performance evaluation, IAEA-CN-184/316, International Atomic Energy Agency, (2010).
70. J.W. Eerkens, Spectral considerations in laser isotope-separation of uranium hexafluoride, Appl. Phys. 10 (1976) 15-31.
71. D.M. Cox, J. Elliott, IR spectroscopy of UF_6, Spectrosc. Lett. 12 (1979) 275-280.
72. J. Bron, R. Wallace, Vibrational theory of polyatomic-molecules - fundamental frequencies, overtone and combination bands of $^{235}UF_6$ and $^{235}UF_6$, J. Chem. Soc., Faraday Trans. 2 74 (1978) 611-617.
73. R.S. McDowell, L.B. Asprey, R.T. Paine, Vibrational-spectrum and force-field of uranium hexafluoride, J. Chem. Phys. 61 (1974) 3571-3580.
74. K.C. Kim, M.J. Reisfeld, High-resolution infrared-spectroscopy using a temperature-controlled long-path absorption cell - the ν_3-band of uranium hexafluoride at 16 μm, Appl. Spectrosc. 39 (1985) 1056-1062.
75. G. Baldacchini, R. Fantoni, S. Marchetti, V. Montelatici, A. Giardiniguidoni, P. Morales, F. Catoni, Diode-laser absorption of UF_6 at room-temperature around 16 μm, Nuovo Cimento Soc. Ital. Fis., D 8 (1986) 203-210.
76. R. Lewicki, A.A. Kosterev, F. Toor, Y. Yao, C. Gmachl, T. Tsai, G. Wysocki, X. Wang, M. Troccoli, M. Fong, F.K. Tittel, Quantum cascade laser absorption spectroscopy of UF_6 at 7.74 μm for analytical uranium enrichment measurements, Proc. SPIE 7608, Quantum Sensing and Nanophotonic Devices VII, 7608 (2010) 76080E.
77. S.S. Nabiev, V.M. Semenov, D.B. Stavrovskii, P.L. Men'shikov, L.I. Men'shikov, G.Y. Grigor'ev, Measurements of the isotopic composition of UF_6 according to the fine structure of the IR absorption spectrum in the $\nu 1 + \nu 3$ band, Russ. J. Phys. Chem. B 11 (2017) 61-76.

78. W. Spencer, P. O'Rourke, N. DeRoller, S. Serkiz, System characterization and modification report, SRNL-STI-2016-00279, Savannah River National Laboratory, (2016).
79. J.C. Devillardi, M. Clerc, P. Isnard, J.M. Weulersse, Coherent stokes and anti-Stokes Raman-spectra of the $\nu_1(A_1)$ and $\nu_2(E)$ bands of SF_6 and UF_6, J. Mol. Spectrosc. 84 (1980) 319-333.
80. H.H. Claassen, B. Weinstock, J.G. Malm, Raman spectrum of UF_6, J. Chem. Phys. 25 (1956) 426-427.
81. S. Manzhos, T. Carrington, L. Laverdure, N. Mosey, Computing the anharmonic vibrational spectrum of UF_6 in 15 dimensions with an optimized basis set and rectangular collocation, J. Phys. Chem. A 119 (2015) 9557-9567.
82. A.J. Ceulemans, Representations, in Group theory applied to chemistry, 1st. ed., Springer Netherlands, Dordrecht (2013) pp. 51-102.
83. L.E. Burkhart, G. Stukenbroeker, S. Adams, Isotope shifts in uranium spectra, Phys. Rev. 75 (1949) 83-85.
84. M. Krachler, R. Alvarez-Sarandes, S. Van Winckel, Challenges in the quality assurance of elemental and isotopic analyses in the nuclear domain benefitting from high resolution ICP-OES and sector field ICP-MS, J. Radioanal. Nucl. Chem. 304 (2015) 1201-1209.
85. R.W. Shaw, C.M. Barshick, L.W. Jennings, J.P. Young, J.M. Ramsey, Discharge conditioning for isotope ratio measurements by glow discharge optogalvanic spectroscopy, Rapid Commun. Mass Spectrom. 10 (1996) 316-320.
86. J.P. Young, R.W. Shaw, C.M. Barshick, J.M. Ramsey, Determination of actinide isotope ratios using glow discharge optogalvanic spectroscopy, J. Alloys Compd. 271 (1998) 62-65.
87. S. Richter, H. Kuhn, J. Truyens, M. Kraiem, Y. Aregbe, Uranium hexafluoride (UF_6) gas source mass spectrometry for certification of reference materials and nuclear safeguard measurements at IRMM, J. Anal. At. Spectrom. 28 (2013) 536-548.
88. S. Mialle, S. Richter, J. Truyens, C. Hennessy, U. Jacobsson, Y. Aregbe, Certification of the uranium hexafluoride (UF_6) isotopic composition: The IRMM-019 to IRMM-029 series, JRC91461, European Commission Joint Research Centre, Institute for Reference Materials and Measurements, (2014).
89. F. Albarede, B. Beard, Analytical methods for non-traditional isotopes, Rev. Mineral. Geochem. 55 (2004) 113-152.
90. S.F. Boulyga, Calcium isotope analysis by mass spectrometry, Mass Spectrom. Rev. 29 (2010) 685-716.
91. S. Richter, H. Kuhn, Y. Aregbe, M. Hedberg, J. Horta-Domenech, K. Mayer, E. Zuleger, S. Burger, S. Boulyga, A. Kopf, J. Poths, K. Mathew, Improvements in routine uranium isotope ratio measurements using the modified total evaporation method for multi-collector thermal ionization mass spectrometry, J. Anal. At. Spectrom. 26 (2011) 550-564.
92. M. Wieser, J. Schwieters, C. Douthitt, Multi-collector inductively coupled plasma mass spectrometry, in Isotopic analysis - fundamentals and applications using ICP-MS, 1st ed., Wiley-VCH Verlag, (2012) pp. 77-91.
93. O.P. de Oliveira, W. de Bolle, A. Alonso, S. Richter, R. Wellum, E. Ponzevera, J.E.S. Sarkis, R. Kessel, Demonstrating the metrological compatibility of uranium isotope amount ratio measurement results obtained by GSMS, TIMS and MC-ICPMS techniques, Int. J. Mass Spectrom. 291 (2010) 48-54.
94. C.V. Thompson, W.B. Whitten, FY16 safeguard technology cart-portable mass spectrometer project final report, ORNL/TM-2017/70, Oak Ridge National Laboratory, (2017).
95. M. Dirmyer, B. Judge, Merging sample preparation with field portable instrumentation: UF_6 chemical stabilization & laser ablation ionization-MS (presentation), LA-UR-16-25370, LANL, (2016).
96. W. Whitten, C. Thompson, ORNL hand-portable mass spectrometer for isotope ratio measurements on uranium hexafluoride (presentation), Oak Ridge National Laboratory, (2016).

97. A. Quentmeier, M. Bolshov, K. Niemax, Measurement of uranium isotope ratios in solid samples using laser ablation and diode laser-atomic absorption spectrometry, Spectrochim. Acta Part B 56 (2001) 45-55.
98. H. Liu, A. Quentmeier, K. Niemax, Diode laser absorption measurement of uranium isotope ratios in solid samples using laser ablation, Spectrochim. Acta Part B 57 (2002) 1611-1623.
99. M. Miyabe, M. Oba, K. Jung, H. Iimura, K. Akaoka, M. Kato, H. Otobe, A. Khumaeni, I. Wakaida, Laser ablation absorption spectroscopy for isotopic analysis of plutonium: Spectroscopic properties and analytical performance, Spectrochim. Acta Part B 134 (2017) 42-51.
100. A. Martinez, B. Cannon, C. Chen, C. Barrett, M. Taubman, N.C. Anheier, High precision uranium isotope analysis by diode laser absorption spectroscopy, (2017) manuscript in preparation.
101. K.L. Corwin, Z.-T. Lu, C.F. Hand, R.J. Epstein, C.E. Wieman, Frequency-stabilized diode laser with the zeeman shift in an atomic vapor, Appl. Opt. 37 (1998) 3295-3298.
102. NNSA Safeguards Technology Factsheet, Laser ablation absorption ratio spectroscopy (LAARS), PNNL-SA-123926, (2017).
103. NNSA Safeguards Technology Factsheet, Laser ablation absorption ratio spectroscopy (LAARS), PNNL-SA-116387, (2016).
104. A. Castro, Fieldable atomic beam laser spectrometer for isotopic analysis (presentation), in Nuclear Security Applications Research & Development Program Review Meeting (NSARD 2017), North Las Vagas, NV, USA, (2017),
105. A. Castro, Atomic beam laser spectrometer for in-field isotopic analysis, LA-UR-16-24170, Los Alamos National Laboratory, (2016).
106. J. Schindler, Characterization of an erbium atomic beam, University of Innsbruck, M.S. Thesis (2011).
107. A.G. Page, S.V. Godbole, K.H. Madraswala, M.J. Kulkarni, V.S. Mallapurkar, B.D. Joshi, Selective volatilization of trace-metals from refractory solids into an inductively coupled plasma, Spectrochim. Acta Part B 39 (1984) 551-557.
108. D.M. Goltz, D.C. Gregoire, J.P. Byrne, C.L. Chakrabarti, Vaporization and atomization of uranium in a graphite tube electrothermal vaporizer - A mechanistic study using electrothermal vaporization inductively-coupled plasma-mass spectrometry and graphite-furnace atomic-absorption spectrometry, Spectrochim. Acta Part B 50 (1995) 803-814.
109. G.C.Y. Chan, I. Choi, X. Mao, V. Zorba, O.P. Lam, D.K. Shuh, R.E. Russo, Isotopic determination of uranium in soil by laser induced breakdown spectroscopy, Spectrochim. Acta Part B 122 (2016) 31-39.
110. G.C.Y. Chan, X. Mao, I. Choi, A. Sarkar, O.P. Lam, D.K. Shuh, R.E. Russo, Multiple emission line analysis for improved isotopic determination of uranium – a computer simulation study, Spectrochim. Acta Part B 89 (2013) 40-49.
111. J. Gray, S. Serkiz, P. O'Rourke, T. White, H. Colon-Mercado, B. Garcia-Diaz, R. Poland, N. DeRoller, Laser-based methods for ultra-low isotopic analysis of proliferant materials, in 2014 Savannah River National Laboratory (SRNL) laboratory directed research and development (LDRD) program annual report, SRNL-STI-2015-00165, Savannah River National Laboratory, (2015).
112. NNSA Fact Sheet, Spectroscopic methods for ultra-low isotopic analysis of proliferant material, SRNL-STI-2017-00207, (2017).
113. R.N. Mulford, The Fourier transform spectrum of the infrared combination band ($\nu_1 + \nu_3$) of UF_6, J. Mol. Spectrosc. 147 (1991) 260-266.
114. V.S. Letokhov, C.B. Moore, Laser isotope separation, in Chemical and biochemical applications of lasers - volume 3, 1st ed., Academic Press, (1977) pp. 1-165.
115. J.W. Eerkens, High mass isotope separation arrangement, UK Patent 1573508 (1975).
116. M.S. Kahr, K.D. Abney, J.A. Olivares, Analysis of solid uranium samples using a small mass spectrometer, Spectrochim. Acta Part B 56 (2001) 1127-1132.

117. NNSA Safeguards Technology Factsheet, Forward-deployable, cart-portable mass spectrometry system, NNSA, (2016).
118. A. Westman-Brinkmalm, G. Brinkmalm, A mass spectrometer's building blocks, in R. Ekman, J. Silberring, A. Westman-Brinkmalm, A. Kraj (eds), Mass spectrometry, 1st ed., John Wiley & Sons, Inc., (2008) pp. 15-87.
119. S.M. Madzunkov, D. Nikolić, Accurate Xe isotope measurement using JPL ion trap, J. Am. Soc. Mass Spectrom. 25 (2014) 1841-1852.
120. M.P. Sinha, E.L. Neidholdt, J. Hurowitz, W. Sturhahn, B. Beard, M.H. Hecht, Laser ablation-miniature mass spectrometer for elemental and isotopic analysis of rocks, Rev. Sci. Instrum. 82 (2011) 094102.
121. A. Riedo, S. Meyer, B. Heredia, M.B. Neuland, A. Bieler, M. Tulej, I. Leya, M. Iakovleva, K. Mezger, P. Wurz, Highly accurate isotope composition measurements by a miniature laser ablation mass spectrometer designed for in situ investigations on planetary surfaces, Planetary and Space Science 87 (2013) 1-13.
122. G.H. Hager, E.D. Hoegg, G.L. Hart, R.K. Marcus, Towards a fieldable, atomic mass spectrometer for safeguards applications, in DOE NNSA MS Working Group Meeting 2016, (2016), Presentation.
123. P.A. Kuzema, Small-molecule analysis by surface-assisted laser desorption/ionization mass spectrometry, J. Anal. Chem. 66 (2011) 1227-1242.
124. C.Y. Shi, C.H. Deng, Recent advances in inorganic materials for LDI-MS analysis of small molecules, Analyst 141 (2016) 2816-2826.
125. K.P. Law, J.R. Larkin, Recent advances in SALDI-MS techniques and their chemical and bioanalytical applications, Anal. Bioanal. Chem. 399 (2011) 2597-2622.
126. J. Havel, J. Soto-Guerrero, Matrix assisted laser desorption ionization (MALDI) and laser desorption ionization (LDI) mass spectrometry for trace uranium determination: The use of C_{60}-fullerene as a matrix, J. Radioanal. Nucl. Chem. 263 (2005) 489-492.
127. S.L. Walton, D.J. Mitchell, A novel rapid detection approach for the analysis of radionuclides in environmental samples using graphite MALDI mass spectrometry, J. Radioanal. Nucl. Chem. 296 (2013) 1113-1118.
128. C.D. Quarles, A.J. Carado, C.J. Barinaga, D.W. Koppenaal, R.K. Marcus, Liquid sampling-atmospheric pressure glow discharge (LS-APGD) ionization source for elemental mass spectrometry: Preliminary parametric evaluation and figures of merit, Anal. Bioanal. Chem. 402 (2012) 261-268.
129. R.K. Marcus, C.D. Quarles, C.J. Barinaga, A.J. Carado, D.W. Koppenaal, Liquid sampling-atmospheric pressure glow discharge ionization source for elemental mass spectrometry, Anal. Chem. 83 (2011) 2425-2429.
130. B.T. Manard, J.J. Gonzalez, A. Sarkar, M.R. Dong, J. Chirinos, X.L. Mao, R.E. Russo, R.K. Marcus, Liquid sampling-atmospheric pressure glow discharge as a secondary excitation source: Assessment of plasma characteristics, Spectrochim. Acta Part B 94-95 (2014) 39-47.
131. E.D. Hoegg, R.K. Marcus, D.W. Koppenaal, J. Irvahn, G.J. Hager, G.L. Hart, Determination of uranium isotope ratios using a liquid sampling-atmospheric pressure glow discharge - Orbitrap mass spectrometer system, Rapid Commun. Mass Spectrom. 31 (2017) 1534-1540.
132. Thermo Fisher Scientific, Exactive™ series: Exactive™ and Q Exactive™ preinstallation requirements guide, Revision A - 1288110, (2011).
133. A.J. Carado, C.D. Quarles, A.M. Duffin, C.J. Barinaga, R.E. Russo, R.K. Marcus, G.C. Eiden, D.W. Koppenaal, Femtosecond laser ablation particle introduction to a liquid sampling-atmospheric pressure glow discharge ionization source, J. Anal. At. Spectrom. 27 (2012) 385-389.
134. L.X. Zhang, B.T. Manard, S.K. Kappel, R.K. Marcus, Evaluation of the operating parameters of the liquid sampling-atmospheric pressure glow discharge (LS-APGD) ionization source for elemental mass spectrometry, Anal. Bioanal. Chem. 406 (2014) 7497-7509.

135. A.J. Schwartz, S.J. Ray, G.M. Hieftje, Evaluation of interference filters for spectral discrimination in solution-cathode glow discharge optical emission spectrometry, J. Anal. At. Spectrom. 31 (2016) 1278-1286.
136. T.M. Yoshida, C.P. Leibman, P.C. Stark, Market research survey of commercial off-the-shelf mass spectrometers for in-field analysis: FY 15 update, LA-UR-15-28831, Los Alamos National Laboratory, (2015).
137. D.T. Snyder, C.J. Pulliam, Z. Ouyang, R.G. Cooks, Miniature and fieldable mass spectrometers: Recent advances, Anal. Chem. 88 (2016) 2-29.
138. R.A.S. Richard, W. Steven, Mems mass spectrometers: The next wave of miniaturization, Journal of Micromechanics and Microengineering 26 (2016) 023001.
139. Z. Ouyang, R.G. Cooks, Miniature mass spectrometers, Annual Review of Analytical Chemistry 2 (2009) 187-214.
140. O. Hadjar, G. Johnson, J. Laskin, G. Kibelka, S. Shill, K. Kuhn, C. Cameron, S. Kassan, IonCCD™ for direct position-sensitive charged-particle detection: From electrons and kev ions to hyperthermal biomolecular ions, J. Am. Soc. Mass Spectrom. 22 (2011) 612-623.
141. G. Kibelka, S. Kassan, O. Hadjar, C. Cameron, S. Shill, A transportable double-focusing mass spectrometer (presentation), in 7th HEMS Workshop, Santa Barbara, CA, USA, (2009),
142. P. Robert, C. Fabre, J. Dubessy, M. Flin, M.-C. Boiron, Optimization of micro-laser induced breakdown spectroscopy analysis and signal processing, Spectrochim. Acta Part B 63 (2008) 1109-1116.
143. C. Pasquini, J. Cortez, L.M.C. Silva, F.B. Gonzaga, Laser induced breakdown spectroscopy, J. Braz. Chem. Soc. 18 (2007) 463-512.
144. S.E. Moran, B.L. Ulich, W.P. Elkins, R.J. Strittmatter, M.J. DeWeert, Intensified CCD (ICCD) dynamic range and noise performance, Proc. SPIE 3173, Ultrahigh- and High-Speed Photography and Image-based Motion Measurement (1997) 430-457.
145. M.S. Robbins, B.J. Hadwen, The noise performance of electron multiplying charge-coupled devices, IEEE Trans. Electron Devices 50 (2003) 1227-1232.
146. A. Padeganeh, E. Lareau, O. Daigle, A.M. Ladouceur, P. Maddox, Improved single-molecule imaging based on photon counting with an EMCCD camera, Biophys. J. 102 (2012) 480A.
147. K.B.W. Harpsoe, M.I. Andersen, P. Kjaegaard, Bayesian photon counting with electron-multiplying charge coupled devices (EMCCDs), Astronomy & Astrophysics 537 (2012) A50.